Università degli Studi del Piemonte Orientale

Dipartimento di Scienze e Innovazione Tecnologica

Dottorato di Ricerca in Chemistry & Biology

Curriculum: Energy, Environmental and Food Sciences

XXXV ciclo a.a. 2019-2023

SSD: BIO/19

Microbiota of *Vitis vinifera* cv. Barbera grapes: a focus on the mycobiota and a look at the culturable indigenous *Saccharomyces* spp. strains under three different experimental conditions in vineyard

Laura Pulcini

Supervised by Prof.ssa Elisa Gamalero and Dott.ssa Antonella Costantini

PhD program co-ordinator Prof. Gian Cesare Tron

Università degli Studi del Piemonte Orientale

Dipartimento di Scienze e Innovazione Tecnologica

Dottorato di Ricerca in Chemistry & Biology

Curriculum: Energy, Environmental and Food Sciences

XXXV ciclo a.a. 2019-2023

SSD: BIO/19

Microbiota of *Vitis vinifera* cv. Barbera grapes: a focus on the mycobiota and a look at the culturable indigenous *Saccharomyces* spp. strains under three different experimental conditions in vineyard

Laura Pulcini

Supervised by Prof.ssa Elisa Gamalero and Dott.ssa Antonella Costantini

PhD program co-ordinator Prof. Gian Cesare Tron

Contents

Chapter I

Introduction

1.Introduction

1.1Grapevine (*Vitis vinifera* L., 1753*)*

Vitis vinifera L. (1753), commonly known as grapevine, is a dicotyledonous plant belonging to the *Vitaceae* family (Table 1.1). The *Euvitis* subgenus (*Vitis* Genus) includes several species, classified according to the geographical and climates areas. Among the American species adapted at temperate climate, the species *V. riparia*, *V. berlandieri* and *V. rupestris*, represent the main types used for the creation of hybrid rootstocks resistant to phylloxera and other ampelopathies (1).

Table 1.1 Systematic classification of Vitis vinifera L., 1753

Domain	*Eukaryota*
Kingdom	*Plantae*
Underkingdom	*Tracheobionta* (vascular plant)
Superdivision	*Spermatophyta* (seed plant)
Division	*Magnoliophyta* (flowering plant)
Class	*Magnoliopsida* (dicotyledons)
Order	*Rhamnales*
Family	*Vitaceae* o *Ampelidaceae*
Subfamily	*Ampelideae*
Genus	*Vitis* L.
Subgenus	*Euvitis* o *Vitis (2n = 38)*
Species	*Vitis vinifera* L.
Subspecies	*Vitis vinifera* L. ssp. *sativa* (cultivated grape)

V. vinifera, the European-Asiatic species, adapted at temperate climate, includes the cultivated varieties classified as *sativa* subspecies and the wild form classified as *silvestris* subspecies (1-4, 6).

V. vinifera spp. *sativa* encompasses, in turn, three ecological and geographical groups, distinguished for their origin, domestication and historical uses:

- *proles occidentalis*: wine grapes lineage (e.g., Pinot Noir, Cabernet, Reisling). These grapes have been cultivated and used for winemaking for thousands of years, particularly in regions like France, Italy, and Spain;

- *proles pontica*: descendants of wine (e.g., Muscat, Malmsey) and table (Pearl of Csaba) grapes;

- *proles orientalis*: table grapes lineage (e.g., Regina). These ones originated in the Middle East and were primarily domesticated for consumption as table grapes.

1.1.1 Botany of the grapevine

Grapevine is a woody perennial climbing plant, consisting of a root system (hypogeal part) and a cauline apparatus (cauline apparatus) (Fig.1.1). Cultivated rooted cuttings typically consists of two bionts: the rootstock (hypogeal), and the productive portion (epigeal), which indicates the cultivar (cv). The latter comprises a woody stem and a foliar apparatus.

V. vinifera seeds typically develop a primary taproot that grows downwards into the soil. Lateral roots branch from the taproot, forming

a complex root system. Adventitious roots from cuttings appear very brunched (fasciculate root system). The extent of root development depends on the rootstock hybrids and soil type (1,2). The root system serves performs several functions, including anchoring the plant, absorbing nutrients and water, storing carbohydrates for winter, and producing phytohormones to regulate vine growth.

The vine stem serves as both a support and a conduit for sap transport. It consists of a primary axis, the trunk, which gives rise to secondary woody branches. Vegetative shoots develop from these branches annually, exhibiting an acrotonic pattern. These one-year shoots support buds, leaves, tendrils, inflorescences, and bunches (clusters). The trunk and the branches display lignification and possess a characteristic external bark called rhytidome (3).

The trunk is the permanent structure that support the vegetative (leaves and sprout) and reproductive (flowers and fruits) organs. The trunk of an adult vine has short branches, so called arms or spur, which are in different positions depending on the training system. To ensure the fructification, some systems use one-year-old branches, known as cordons. The branch includes nodes and internodes (canes).

Grapevine leaves have long stalks and have an alternate phyllotaxy (couplets) at the nodes. They are typically simple, large and webbed, often divided into 3-5 lobes with either entire or dentate margins, depending on the variety. The underside is covered with hair. During the vegetative phase they are green due to chlorophyll, while in autumn, they can turn yellow or red, reflecting the berry colour of the cultivar, whether white or red. Bunches or tendrils (cirrus) are inserted from the second or third node in the opposite position to the leaves. The tendrils serve for plant anchoring and climbing by rolling up. As the fruit ripens,

the vines harden and become woody (1,3,11). Two types of buds are found in the leaf axils: dormant (or latent) buds and lateral buds. Lateral buds develop beneath the basal bract in the current season and give rise to a summer lateral shoot of varying length. Dormant buds typically germinate the following year and contain cluster primordia, representing the potential for grape production in the next season (Fig.1.2).

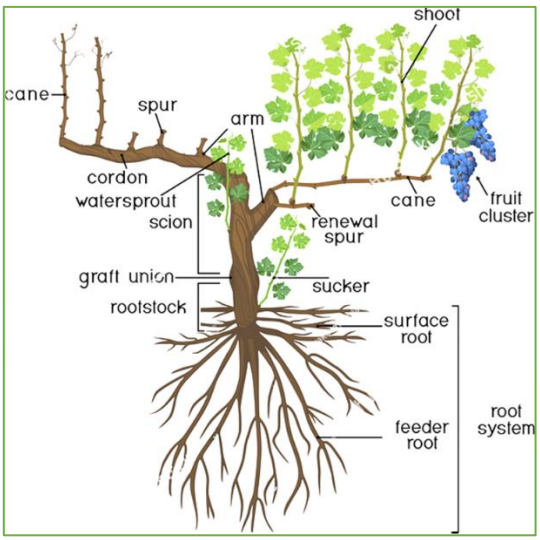

Figure 1.1. Parts of vine. Morphology of the grapevine plant, including itsroot system and the structure of its epigeal part. (Modified from www.shutterstock.com (5)).

The number and placement of fruiting buds vary depending on the cultivar and are connected to the training system. The quantity of fruiting buds per vine has a direct impact on grape productivity and, consequently, quality.

The grape inflorescence, also known as a cluster or raceme, is composed of 100-2000 small flowers (4-5 mm) and is positioned opposite the leaves on the shoot. It produces 1-3 clusters as shown in Figure 3. The raceme initially erect and later becomes pendulous. The

inflorescence consists of a central axis called the rachis, which holds numerous pedicels bearing the flowers. These flower clusters emerge on new shoots at nodes opposite the leaves, in the same position as the tendrils (Fig. 1.3).

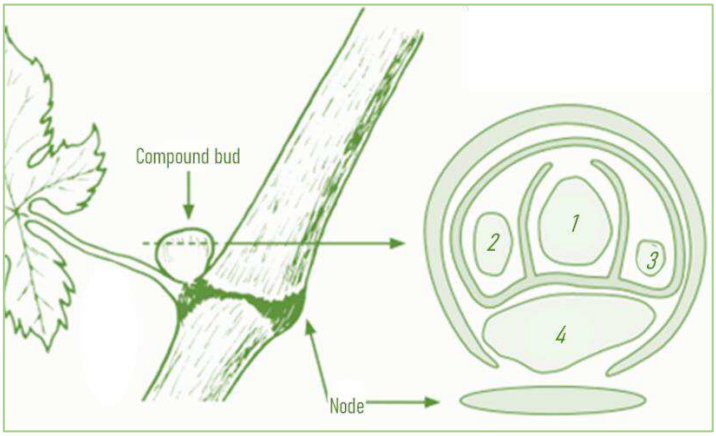

Figure 1.2. Dormant (compound) bud in V. vinifera including its morphology its cross section. Where 1 is the primary axis (or bud, fruitfulness), 2 and 3 are the secondary axes (sketches of the secondary and tertiary buds), 4 represent the lateral bud (producing summer lateral shoot). (Modified from: Fregoni M., 2013 Viticoltura di qualità (Italian Edition) (p.61). Tecniche Nuove. Kindle Ed.).

In *V. vinifera* varieties the flower is typically pentamerous and hermaphroditic (perfect flower). The five petals fuse into a green structure known as the calyptra or 'cap,' which encloses both the pistil (female organ) and five stamens (male organs). The calyptra falls off after blooming when the stamens mature (Fig. 1.4). Self-pollination occurs in most cultivars.

The grapevine fruit, berry, is composed two primary components: the exocarp and the sarcocarp (Fig. 1.5). The exocarp is the cutinized epidermis, which may be covered by a bloom layer, depending on the variety, that retains yeasts on the surface. The epidermis is rich in enzymes, phenolic compounds, including anthocyanins, flavones,

tannins and aromatic compounds such as linalool and geraniol. The sarcocarp comprises the flesh (or pulp), which includes the mesocarp and the endocarp with four lodges that contain grape seeds.

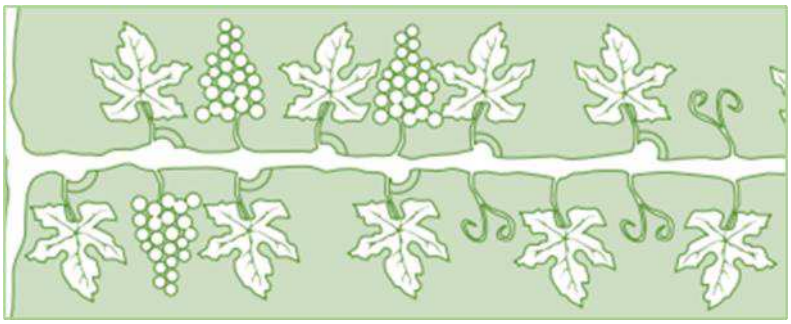

Figure 1.3. Shoot morphology of V. vinifera. Annual shoot with nodes and canes, alternate leaves, with lateral and dormant buds at the leaf axil. The shoot also has clusters or tendrils (cluster homologous organs). (Modified from Fregoni M., 2013 Viticoltura di qualità (Italian Edition) (p.63). Tecniche Nuove. Kindle Ed.).

The grape flesh contains sugars (glucose and fructose), organic acids (tartaric, malic, citric, etc.), nitrogen compounds, pectin, and minerals. The berries are connected to pedicels, which merge into a single structure called the stalk. The grape or bunch can vary in colour (from green to yellow, pink to purplish-red), shape (round, oblate, ellipsoidal, ovoid, etc.), weight, and size, influenced by factors such as grape variety (cultivar), plant age, climate, and cultivation type (3, 13). Bunches or clusters can also differ in size, shape (cylindrical, conical, winged, etc.), and thickness (scattered, compact, etc.) depending on the grape variety (3, 13).

Ampelography has emerged as a discipline due to the extensive botanical diversity among *V. vinifera* varieties. It involves the precise description of the botanical characteristics of each vine organ, including leaf shape, size, and hairiness, leaf margin, cluster colour, shape, size, and compactness, seed number, shape, and size, among others. This

scientific branch aims to study, identify, and classify vines by creating descriptive profiles of various plant organs, considering different growth stages such as the sprouting, flowering, and ripening periods.

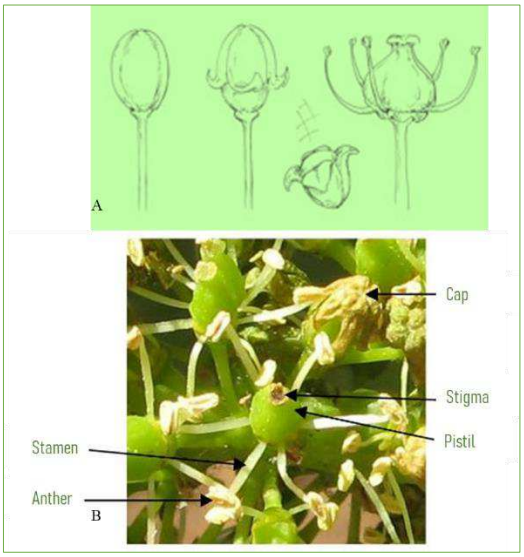

Figure 1.4. Flower morphology of V. vinifera. Anthesis *(A), male and female organs of the hermaphroditic flower (B) (Modified from https://grapes.extension.org/parts-of-the-grape-vine-flowers-and-fruit/#Recommended_Links)* (10).

The traditional ampelographic method, which relies on describing varietal morphological features, is still in use. In addition to the traditional approach, ampelography also benefits from modern strategies such as i) chemotaxonomy, which classifies organisms based on similarities and differences in the structure of specific compounds produced, ii) DNA analysis methods like RFLP (Restriction Fragment Length Polymorphism) for identifying species within the Vitis genus, and iii) microsatellite PCR for assessing grapevine varieties.

Specific microsatellite loci are used to identify grapevine varieties and clones (1, 13, 14). The sequencing of grapevine genome in 2007,

has led to numerous genomics studies (21, 31, 32), Which strongly supports genetic improvement in grapevines, particularly in addressing biotic and abiotic challenges (1,15).

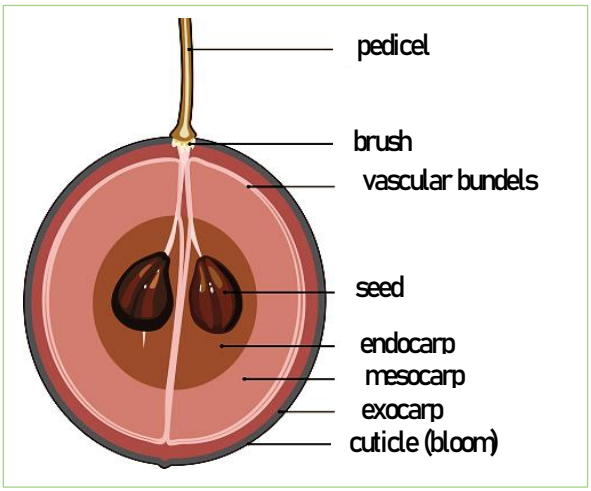

Figure 1.5. Grapevine berry morphology. Longitudinal section (Modified from: https://it.depositphotos.com/) (12).

1.1.2 Grapevine physiology

The grape's life cycle begins with the birth (germination of the seed or rooting of the cutting) and ends with the death of the plant. The life cycle of a grapevine varies in duration depending on factors such as rootstock, grape variety, vineyard management, productivity, etc. Grapevines undergo changes in organic carbon concentration (sugars from photosynthesis, proteins, fats, etc.), as well as alterations in the elaborated sap, and the uptake of nitrogen and other mineral substances from the roots (raw sap), throughout its life. The Carbon (organic compound produced from the foliage) and Nitrogen (mineral and organic substances absorbed at the root level) ratio determines different physiological phases. The vine's growth

and development in response to seasonal changes and environmental stimuli are subject to phytohormone control. Auxins, gibberellins (GAs), and cytokinins promote fructification, whereas abscisic acid (ABA) inhibits productive differentiation in compound buds. The grape's life cycle aligns with that of the vineyard and can be categorized into four growth stages (Fig.1.6):

- Unproductive period (young vine): 1-3 years old, from planting;
- Increasing Productivity period: 4th-7th year from planting;
- Constant Productivity period (adult vine): 7th-25th (30th) year from planting;
- Decreasing Productivity period (senescence stage): after the 30th year from planting.

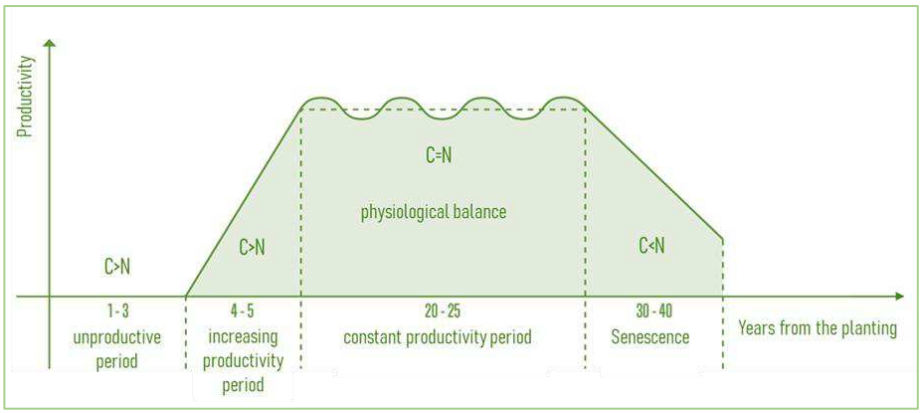

Figure 1.6. Grapevine and vineyard life cycle. (Modified from Fregoni, M. 2013 Viticoltura di qualità (Italian Edition) (p.214). Tecniche Nuove. Kindle Ed.).

The life cycle of the grapevine can be divided into different annual cycles, each with specific physiological phases that characterize the vine phenological stages. (Figure 1.7). The annual growth cycle of the grapevine begins with bud burst in spring, followed by inflorescence development, flowering (anthesis), fruit

setting, and veraison during summer. Most cultivated varieties complete bunch maturation in autumn (harvest), followed by leaves fall and dormancy in winter.

The timing and duration of these stages vary depending on factors such as: grape cultivar (e.g. early budding of Chardonnay and Merlot or late budding of Cabernet Franc and Reisling), geographical location (e.g. northern or southern hemisphere, or equator), environmental conditions (e.g. soil composition, nitrogen fertilisation, pruning time, etc.), climate and seasonal weather (e.g. altitude, exposure, temperature, solar radiation, etc.). However, the sequence of events remains constant (7).

Both a vegetative and a reproductive sub-cycle occur on the same one-year shoot, together forming an annual cycle (1).

The vegetative sub-cycle covers the development of all parts of the crown except the flowering and fruiting phases. It begins with bud burst, corresponding to the start of a new annual cycle, and ends in late autumn with leaf fall, followed by shoots maturation and lignification. The dormant phase of the vegetative cycle coincides with the end of the annual cycle (Figure 7). It begins in spring when the temperature remains around 10°C for 7-10 consecutive days, resulting into the growth of dormant buds and the production of shoots. The timing of each phase is influenced by factors such as pruning time, climate, and soil composition (3, 7).

Physiologically, bud break is initiated by an increase in cytokinin production in the roots, which promotes cell division in dormant buds. At the same time there is a decrease in ABA due to changing environmental conditions. Shoot growth and elongation are facilitated by gibberellins. The vegetative cycle promotes crown development

through chlorophyll photosynthesis and the biosynthesis of carbohydrates from inorganic molecules in the raw sap within the leaves (1).

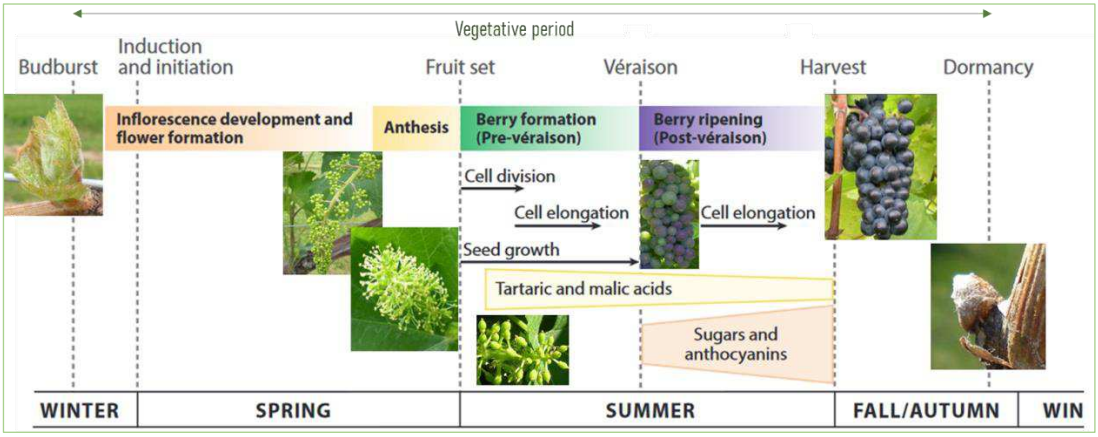

Figure 1.7. Grapevine annual cycle and main phenological stages. (Modified from Rayapati *et al*., 2015 (16))

The reproductive sub-cycle begins with the differentiation of annual and compound buds in spring during the bud breaks phase. It then proceeds to flowering. The compound buds, which were initiated in the previous spring, remain dormant over the winter. Their differentiation results in three types of embryonic axis, namely primary, secondary, and tertiary buds (Fig. 2). The primary axis has the potential to develop into fruiting shoot, producing flowers and fruit. The secondary and tertiary axis can develop in the same year as their formation, and they constitute the annual buds. (1,3). The bloom phase, also known as flowering phase, is a complex process that is highly regulated by genetic factors, environmental conditions, and viticultural practices (e.g., pruning and harvesting times, etc.), as well as phytohormones such as auxin and cytokinin. This phase involves the differentiation of flower organs. From a phenological point of view, it includes the appearance of small flower clusters, the formation of grape flowers, their growth and opening

(1).

After flowering the fertilized flower develop into berries with seeds, fruit set. Achieving a favourable fruit set requires a delicate balance influenced by factors such as plant health, gibberellin, temperature, humidity, and water stress. Only a portion of the flowers will develop into berries, making this stage crucial for grape yield and wine production (1).

Berry growth is influenced by auxins, cytokinins, and gibberellins, and occurs in three phases: rapid initial growth, a lag phase, and veraison. During the first phase seeds and berries expand rapidly, causing the berries to double in size and appear dark green. The subsequent lag phase is a brief period of slower growth. The final phase of fruit maturation is characterized by a decrease in acidity, an increased in sugar content (glucose and fructose), pulp softening due to pectolytic enzymes, synthesis of polyphenols (e.g., anthocyanins and flavonols), and the development of varietal aromas (e.g., rose for Gewürztraminer, banana for Chardonnay, green pepper for Cabernet Sauvignon, etc.) (1). During veraison, the maturation stage, the berries undergo a colour change from green to yellow-golden or black, depending on the grapevine variety. This is due to the degradation of chlorophyll and the prevalence of cultivar-specific pigments. Additionally, various metabolic pathways occur during this stage, leading to the degradation of organic acids, which raise the pH level and the accumulation of sugars and other compounds. Maturation is influenced by environmental and climatic conditions, plant nutrition, hormonal factors, and closely tied to the genotype, including grapevine cultivar and rootstock type. During this phase, the skin and flesh undergo changes, with a peak in glucose and fructose, polyphenols

(anthocyanins, catechins, flavonoids, etc.), as well as volatile compounds (methoxypyrazines, terpenes, esters, thiols, etc.). Meanwhile the levels of malic, citric, tartaric acids, and tannins are typically lower (1,17).

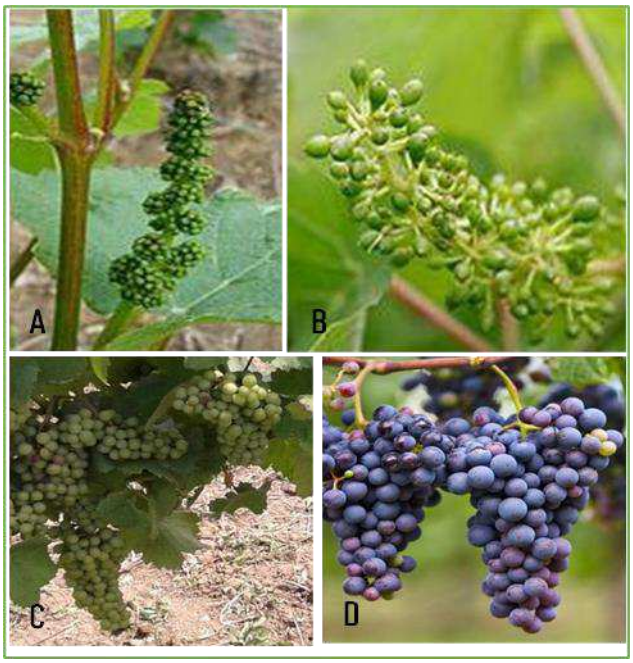

Figure 1.8. Pictures of phenological stage of V. vinifera. A) Inflorescence development during flowering; B) Formation of young grapes during fruit set; C) Fruit development; and D) Maturation of grapes during veraison.

Maturation takes place at this stage. (Figure 1.8).

The harvest stage consists in removing the grape bunches from the plant. Ripeness of the grapes is determined by chemical analysis of the berry compounds (sugars, acids, tannins). This assessment helps to determine the optimal time for harvest. Harvest is a critical step that significantly impacts the winemaking process and the ultimate quality of the wine.

After the harvest, the vine begins to store reserves in its trunk and roots while continuing photosynthesis. As temperatures drop in late

autumn, the vine produces more abscisic acid (ABA), leading to the cessation of photosynthesis. This causes the chlorophyll in the leaves to break down, Revealing the varietal pigments and resulting in a change of colour to either yellow or red, depending on the variety. As winter approaches, the grapevine enters a period of dormancy (1). In viticulture, understanding the interaction among phytohormones, environmental factors, and management practices is crucial for optimizing grape yield and quality (physiology), especially for winemaking purposes.

1.1.3 Grapevine genetics

Without going into details, this paragraph briefly discusses genetics and genetic improvement of the vine (Figure 1.9).

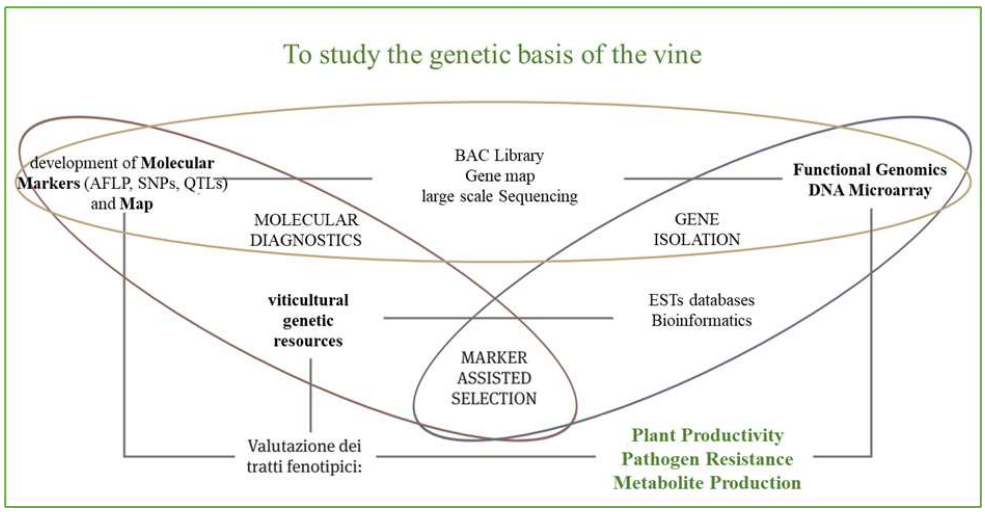

Figure 1.9. Representation of some knowledge that science has made available to viticulture, to study the grapevine from a genetic point of view, and some strategies available for genetic improvement. (Kindly provided by R. Velasco and Modified from Grando S., Velasco R.,2004) (23).

The vine species spread from their zone of origin to temperate and equatorial regions of the Earth through natural selection and

domestication. Domestication is estimated to have occurred 5,000 years ago in Asia Minor or Armenia. Grapevine ancestors have undergone significant changes in both phenotype and adaptation to the environment due to selective pressure from nature and humans. The Vitis genus comprises over 70 species that can be grouped geographically. (18, 19).

The grapevine species, *V. vinifera*, exhibit macroscopic differences between its subspecies *silvestris* and *sativa. Silvestris* is dioecious and more rustic, while *sativa*, hermaphroditic (sometimes having atrophic male or female sexual organs in the flower) and sensitive to diseases (1).

Due to its their phylogenesis and reproductive traits, the grapevine species is characterized by heterozygosis and a huge genetic variability, making it an excellent candidate for the genetic improvement (1,18). Therefore, the ease asexual propagation has led to an estimated number of over 10,000 cultivated varieties (18).

The intraspecific genetic diversity in *V. vinifera* is attributed to the presence of transposons in its genome. The presence of microsatellites in the genome leads to phenotypic differences between cultivar, which explains the diverse morphological and metabolic features of varieties and clones (1, 19).

V. vinifera L. spp. *sativa* has 38 chromosomes. Numerous scientific studies have been conducted since the advent of the molecular biology to explain its variability and to accurately identify varieties. In grapevines, more over 30,000 genes have been discovered, their function has been ascertained; and a gene map has been created (20, 21).

Like other agricultural species, genetic improvement can be achieved through sexual reproduction (from the seed), asexual reproduction (vegetative propagation), or through the new genetic engineering technologies (trans-genesis, cis-genesis) which require the support of

cell culture and *in vitro* cultivation (1).

Table 1.2 Characters of Vitis resistance to certain biotic and abiotic adversities (Modified from Fregoni, M. 2013 Viticoltura di qualità (Italian Edition) (p.168). Tecniche Nuove. Kindle Ed.).

BIOTIC AND ABIOTIC RESISTANCE IN *VITIS* GENUS (polygenic characters)					
PHYLLOXERA	**NEMATODES**	**WINTER COLD**	**DOUGHT**	**SALINITY**	**CHLOROSIS**
high resistance					
V. rotundifolia	*V. champini (Meloidogynae)*	*V. amurensis* (-40°C)	*V. monticola*	*V. champini*	*V. vinifera*
V. riparia	*V. rufotomentosa*	*V. riparia* (-30°C)	*V. berlandieri*	*V. vinifera*	*V. berlandieri*
V. rupestris	*V. rotundifolia*	*V. rupestris* (-30°C)	*V. vinifera*		
V. cordifolia	*V. doaniana (Xiphinema)*	*V. labrusca* (-25°C)			
V. berlandieri					
V. monticola					
V. arizonica					
V. lincecumii					
medium resistance					
V. cinerea	*V. riparia*	*V. berlandieri* (-20°C)	*V. rupestris*	*V. berlandieri*	*V. rupestris*
V. aestivalis	*V. rubra*	*V. rotundifolia* (-18°C)		*V. solonis*	
V. candicans	*V. solonis*	*V. vinifera* (-17°C)			
V. solonis					
low resistance					
V. vinifera	*V. vinifera*	several Asian and American tropical species	*V. riparia*	*V. riparia*	*V. riparia*
V. champini					
V. labrusca					
V. californica					

The knowledge gained in grapevine genetics has enabled us to understand the origin of natural or induced mutations at the gene level, such as deletions or additions of nucleotides in the DNA sequence. This

understanding has also shed light on the mechanisms of bud mutation, which form the basis of clonal and mass selection (18-20). The traditional breeding program has focused on improving grape quality. Following the emergence of phylloxera, the selection of rootstocks with genetic resistance to pathogens, drought, water stagnation, or calcareous soil became crucial. This was done to enhance the symbiote (rootstock + cultivar) and its resistance traits. Table 1.2 displays some of the most studied resistance traits in the *Vitis* genus.

Much research effort has been directed at introducing disease resistance genes, from wild species into cultivars, with limited success due to the resulting loss of grape quality. For example, the use of *Vitis labrusca* to confer resistance to downy mildew has resulted in undesirable wine characteristics, such as a 'foxy' flavour (1, 19). Through the use of molecular markers within a back-cross improvement schedule new cultivars expressing resistance genes, while maintaining the original quality of the cultivar, have been realized. This procedure, called pyramiding, involves many years of trials to evaluate the effect of the genetic improvement aimed at the introgression of the resistance genes, also in refer to polygenic systems (19, 20, 22).

Recently, several protocols for editing plant genome have been developed. The CRISPR-Cas9 complex has been applied to develop new grape varieties, which require assessment (24).

This paragraph highlighted the fundamental role of biotechnology in developing cultivars resistant to adversities, thereby reducing the reliance on chemical products in viticulture.

1.2 Vineyard Agroecosystem

The vineyard is an artificial ecosystem, that is managed by human for grape production in high-specialization agriculture resulting in a reduction of biodiversity. In an agroecosystem, external production factors such as fertilizers, machines, irrigation, treatments, etc.) are used to modify the energy and the material flows, with the aim of improving productivity and quality. This involves eliminating natural factors that may be harmful or compete with the crops (weed plants, insects, pathogenic microorganisms) as opposed to the natural ecosystem. The vineyard agroecosystem is characterized by abiotic factors such as climatic conditions (air humidity, rainfall, windiness, variable insolation over time), as well as latitude, longitude, inclination, exposure, and the soil features (which remain immutable over the time). Biotic factors include the grapevine, the rootstock, and all the living organisms, which play a crucial role in defining the vineyard's most important features. To achieve a healthy vine and ensure quality production it is necessary to establish a dynamic equilibrium among the actors in the agroecosystem (1). The concept of balance agroecosystem is closely related the definition of "terroir" as defined to the Organization of Vine and Wine (OIV) «Vitivinicultural "terroir" is a concept that refers to an area in which collective knowledge of the interactions between the identifiable physical and biological environment and applied viticultural and oenological practices develops, providing distinctive characteristics for the products originating from this area. Terroir includes specific soil, topography, climate, landscape characteristics, and biodiversity features » (25).

To ensure the efficiency of the vineyard the main aspect is choosing

a suitable area, where the vineyard ecosystem elements combine favourably, requiring minimal human intervention and fewer external inputs (Figure 1.10). Low-input viticulture leads to a reduced environmental impact and increased sustainability, encompassing ecological, economic, and social aspects.

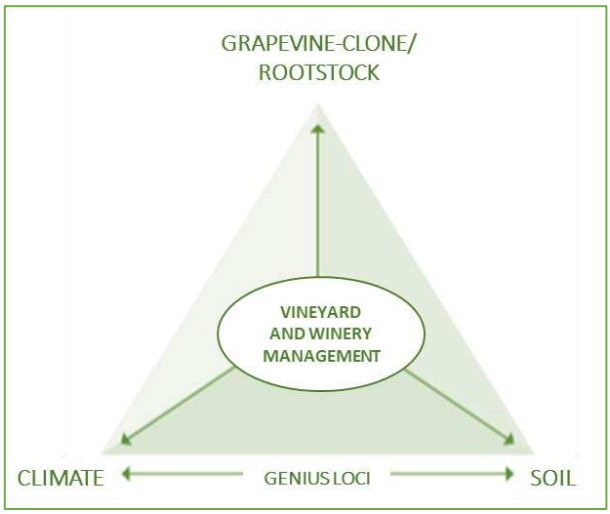

Figure 1.10. Representation of biotic, abiotic, and anthropic factors determining the terroir in grape production and wine quality. (Modified from Fregoni (2013) Viticoltura di qualità (Italian Edition) (p.306). Tecniche Nuove. Kindle Ed.).

The weather is strictly related with the climatic zone. Climate change is challenging the structure of the wine. Due to the global warming, the domesticated varieties are no longer adapted to the local conditions, and it could be necessary to carefully plan suitable areas for viticulture. Physiological needs such as water, nutrients, insolation, etc. could be better satisfied at higher latitudes, or longitudes closer to the poles (9,26-28).

The soil factor is important in determining the best condition for the vine nutrition and health. The concept of "terroir" is strongly influenced by the soil chemical and physical features (29). In fact, the soil plays a

fundamental role in plant mineral nutrition, and in containing the macro and microorganisms necessary for the efficiency of the root system (organic fraction of the soil). The role of soil is complex and heterogeneous. An exemplification is reported in figure 1.11 (29,32,33).

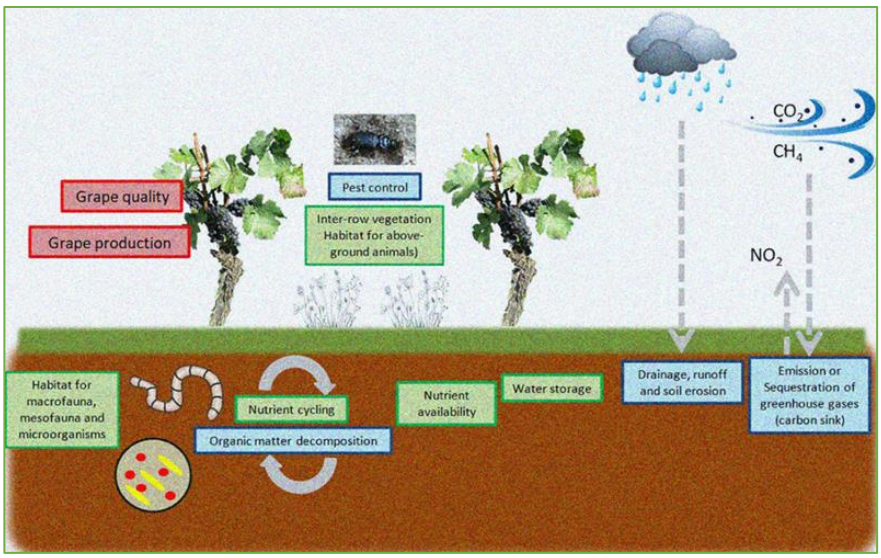

Figure 1.11. Agroecosystem vineyard: the ecosystem services provided by the soil. Biodiversity is strongly linked to habitats availability in soil and plant cover above-ground. Biodiversity plays a crucial role in several regulating services (blue boxes) such as the organic matter decomposition, rain drainage, pest control. The regulating services are related to supporting services (green boxes) that are involved in creating the macro, meso and microfauna habitat, water storage. And the supporting services may influence some provisioning services (red boxes), as grape production and quality. (Modified from Giffard *et al*., 2022 (29)).

The influence of grapevine and rootstock on vineyard ecosystem has been discussed in the paragraph 1.1.3 Grapevine genetics.

The vineyard agroecosystem cannot maintain its health due to its high specialization and density of cultivation, thus requiring intervention from the winegrower. Additionally, plants of *V. vinifera* spp. *sativa* may be susceptible to biotic adversities like phytophagous insects and pathogenic fungi, which must be managed accordingly.

Numerous microorganisms can cause diseases in grapevines. The most significant fungal adversities affecting grapevine yield include downy mildew (*Plasmopara viticola*), powdery mildew (*Oidium tuckeri*) and grey mould (*Botrytis cinerea*). Fungi as *Phaeoacremonium aleophilum*, *Phaeomoniella chlamydospore* and *Fomitiporia mediterranea* can simultaneously colonize the grapevine, impairing its physiology and leading to the Esca Disease (34). Moreover, fungal pathogens could develop from insect feeding areas. Bacterial diseases such as *Agrobacterium tumefaciens*, virosis including Grapevine leafroll associated virus- GLRaV and Grapevine Rupestris Stem Pitting Associated Virus- GRSPaV), phytoplasma disease like Grapevine flavescence dorée 16SrV are serious ampelopathies. Effective prophylaxis and phytoiatric strategies are necessary to control them (35).

The grapevine moth (*Lobesia botrana* and *Eupoecillia ambiguella*) and the grapevine yellow spider-mite (*Eotetranychus carpini* f. *vitis*) are the arthropods that most damage plant health and yield (36).

Yeasts can act as bioremediation agents in the agroecosystems, for example in the degradation of pollutant and heavy metals. They can also serve as indicators of environmental quality and as biocontrol agents such as in ensuring food and feed safety, taking action as probiotics, and protecting crops (37). Some yeast species demonstrate a remarkable metabolic versatility, able of growing on a wide variety substates, including complex and recalcitrant compounds (amines, lipid compounds, alkanes, hydrocarbons, aromatic molecules). They have the capability to transform toxic compounds into innocuous derivatives (38-42).

The yeasts' biocontrol traits can be categorized in two activities:

against the pathogens affecting the above-ground part of the plants, and against the soil-borne fungal plant pathogens. Epiphytic yeasts are the dominant fraction of the microbiota on aerial plant parts.

Many studies, primarily conduct *in vitro* conditions, have demonstrated that yeasts or their mycotoxins may inhibit the onset of plant disease. For instance, *Aureobasidium pullulans* (dimorphic filamentous Ascomycete) has been identified as an antagonist of *Monilia fructicola.* *Phytophtora infestans* was partially controlled by *Candida* sp. and *Cryptococcus* sp. (44; 45). It was observed that *Erysiphe* sp. (powdery mildews) growth was inhibited by *Pseudozyma flocculosa* (46). The reduction of some soil-borne diseases (e.g. *Rhizoctonia solani*, *Fusarium oxysporum, Chephalosporium maydis*) by antagonistic yeast (*Kazachstania unispora*, *Candida steatolytica*, *Rhodotorula spp., Trichosporon spp.*) has been detected in many crops (47- 49). The capability of the yeasts to promote plant growth has been evaluated *in vivo* (49), including grapevine (50).

The use of certain yeasts on grapes has been reported for the biological control of *Botrytis cinerea* (grey mold) (51-53). Numerous yeast species have been evaluated both *in vitro* and *in vivo* for the biological control of filamentous fungi, which are agents of grapevine disease. *In vitro* studies shown that *Wickerhamomyces anomalus*, *Aureobasidium pullulans*, *C. intermedia*, *Rhodotorula glutinis*, *Zygoascus meyerae* and *Holtermanniella takashimae* can inhibit the mycelial growth and sporulation of the filamentous fungi by 75-100%. Similarly, *Metschnikowia pulcherrima* and *Starmerella bacillaris* were effective in reducing mold growth by 50-75 %. *In vivo* trials have shown that *W. anomalus*, *A. pullulans*, *M. pulcherrima*, *C. intermedia* and *R. glutinis* can reduce disease incidence caused by fungal pathogens (54).

M. pulcherrima and *A. pullulans* have been proven effective in inhibiting *B. cinerea* in vineyards and show promise as biological control agents (BCAs) to replace agrochemical treatments (55).

Compared to the major groups of pathogenic fungi, certain yeast species may occasionally be pathogenic in crop environments. Yeasts are more pathogenic during the post-harvest time on foodstuff (51).

In addition to others cultivated plants, such as vines, the etiological agents of untreatable diseases are considered quarantine organisms and are listed in Regulation (EU) 2019/2072 (Annex II).

This paragraph discusses the strategies for containing vine diseases in vineyard management (Figure 1.12), including the use of chemical or biological treatments.

Currently, in viticulture, two primary management strategies are used: organic and integrated. In the past, vine diseases were treated with synthetic biocide such as dithiocarbamates, organophosphorus, sterol biosynthesis inhibitors (SBI), strobilurins, copper-based or Sulphur fungicides, etc at fixed intervals through the year. The extensive use of these molecules led to the selection of resistant pathogens and to the pollution of the biosphere with consequent loss of biological fertility in soils (1, 29).

Integrated vine protection techniques rely on sustainable active molecules to control pathogenic microbes and arthropods. These agrochemicals are applied in the vineyard only when necessary (56-58). Biological control against agricultural pathogenic agents is a complex alternative to conventional control, here follows a partial description.

Organic crop protection methods for controlling harmful insects involve the application of biological control tools. These tools include fostering the presence of natural predators like ladybugs, spiders, and

predatory insects, as well as parasitoids that lay eggs on or inside pests. This approach reduces pest populations to levels that are harmless to the plant and enhances the conservation of natural enemies in the ecosystem (57, 59, 60). In organic management, copper- and sulphur-based products are frequently used to combat pathogenic microbes. To achieve effective disease protection, especially against downy mildew and powdery mildew in grapevine, epidemiological forecasting models and decision support devices (DSD) are instrumental. By predicting the infection potential, the timing and the sustainability of treatments can be optimized (58, 59).

Over the past 30 years, phytoalexins have been extensively tested as elicitors in priming to protect plants against grey mold, downy mildew, powdery mildew, and Esca Diseases has been extensively tested (61). The potential use of yeast as BCAs has also been previously described.

Furthermore, beneficial bacterial inoculum can be applied on the plant as biostimulant (62) or as biopesticides against harmful organisms (63, 64) to improve crop production and protection.

Thus, instead of using traditional agrochemicals, alternative active ingredients, or natural antagonists with a stimulating action for plant self-defence can be used. A description of biostimulants is provided in the following paragraph. Furthermore, this PhD work focuses on a study of yeasts present on grape skin.

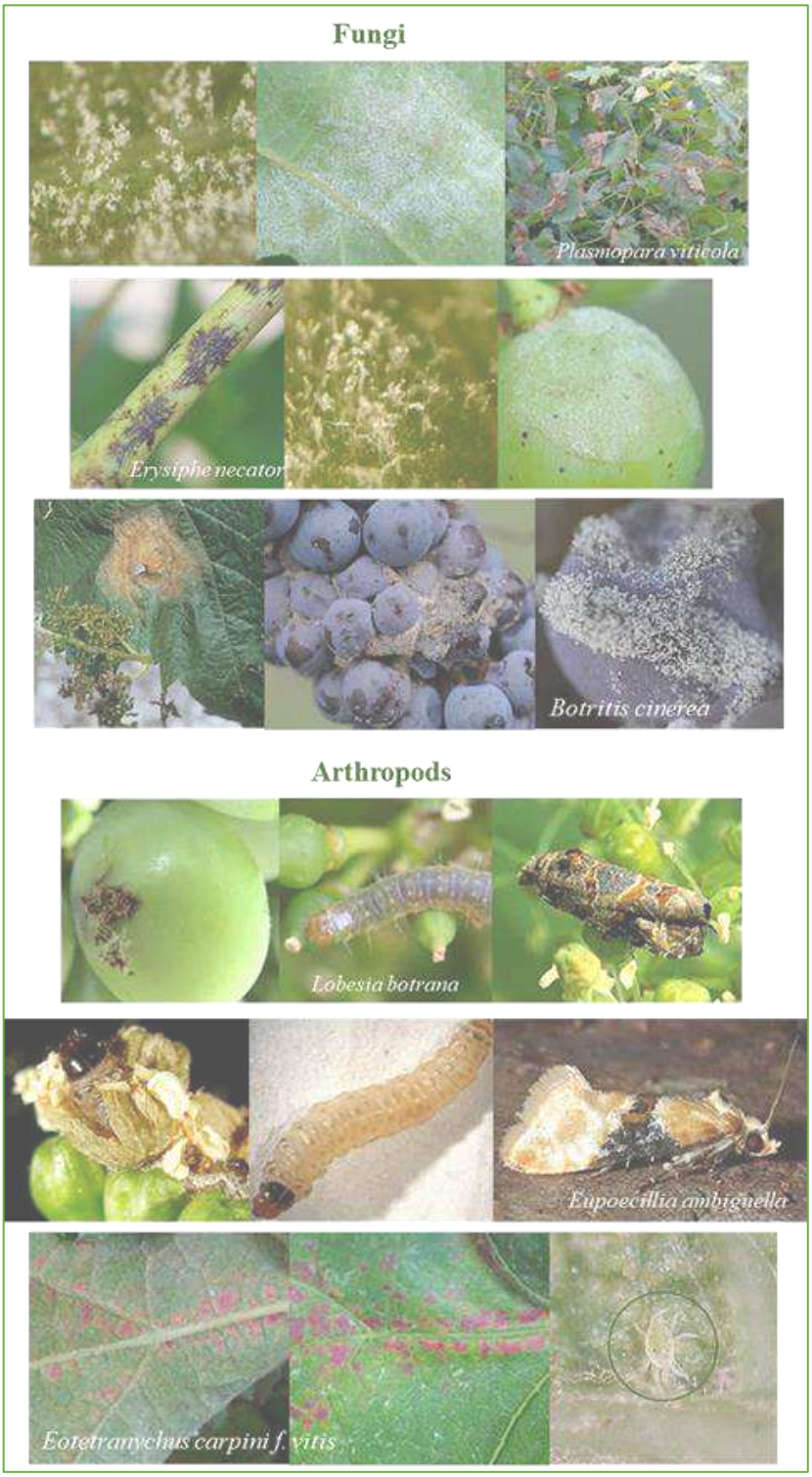

Figure 1.12. The most relevant disease in Vitis vinifera spp. *sativa.* (Modified from https://ephytia.inra.fr/it/P/97/Vite)(43).

1.2.1 Plant Biostimulant

In his review article "Plant biostimulants: Definition, concept, main categories and regulation", published on *Scientia Horticulturae* in 2015, Professor Patrick du Jardin defined a plant biostimulant as "any substance or microorganism applied to plants with the aim to enhance nutrition efficiency, abiotic stress tolerance and/or crop quality traits, regardless of its nutrients content. By extension, plant biostimulants also designate commercial products containing mixtures of such substances and/or microorganisms".

The previous paragraph mentioned the well-documented positive effect of certain microbial consortia on plants health. The biostimulant effect of arbuscular mycorrhizal fungi (AMF) and plant growth-promoting bacteria (PGPB, e.g. Rhizobacteria) on vine has extensively studied. This includes their impact on the uptake of nutritive elements, protection from copper toxicity in the soil, and resistance to abiotic stress (61, 65-69). In addition to the biostimulant behaviour of some microorganisms, especially telluric ones, in recent years much attention has been given to the mode of action of elicitors. Elicitors encompass all molecule or substance, whether biological or synthetic, that trigger a plant's response to diseases.

These elicitors can be classified as biotic if they originate from the host, endogenous for the plant (e.g., plant hormone, phytoalexins, salicylic acid) or by the etiological agent, exogenous for the plant (e.g., bacterial, viral, pathogen origin). And if elicitors originate from the environment (e.g., acetic acid, metal ions, etc.) they are called abiotic. Elicitors can also be recognised as general

or specific depending on their molecule structure and specificity towards the host wall (70, 71).

The use of elicitors in disease control in scientific studies on vine has been a topic of debate. Plant immunity is based on the development of an inducible response (IR) strategy against pathogens, which can be activated by diverse elicitors. These elicitors are defined as patterns that elicit immunity (PEIs) or that trigger immunity (PTI), and can be classified as:

- microbe-associated molecular patterns (MAMPs): microbe-derived molecules including those from helpful microbes;

- pathogen-associated molecular patterns (PAMPs): specific molecules from phytopathogenic bacteria, fungi and microbes;

- damage (or dangerous)-associated molecular patterns (DAMPs): produced by the plant after degradation or dysfunction of host molecules by microbes, or after wounding by insects or herbivores.

In dicotyledonous plants, the elicitors are identified by transmembrane pattern recognition receptors (PRRs) of the vegetal cells (72-74). This recognition results in systemic induced resistance, which restricts the growth of intruder (pathogen), enabling the plant to become more resistant to harmful microbes (72). In this case, the mechanism is defined as Systemic Acquired Resistance (SAR). The expression of pathogenesis-related proteins (PR) (e.g., chitinase, glucanase, endoprotease, peroxidase) genes has been activated. This activation implies the salicylic acid (SA) (Fig.13) pathway, that causes local necrosis of plant tissues (74). Other molecules involved in SAR, as expression of PR proteins, are reactive oxygen species (ROS), such as the phytoalexins. When

the interaction between plant and microbes is related to beneficial microorganisms (as Rhizobacteria or other symbiotic microorganisms) the phenomenon is named induced systemic resistance (ISR), that involves endogenous production of jasmonic acid (JA) (Fig. 1.13) and ethylene (ET). However, it has been observed that multiple metabolic pathways can be activated simultaneously (61, 72, 73, 75).

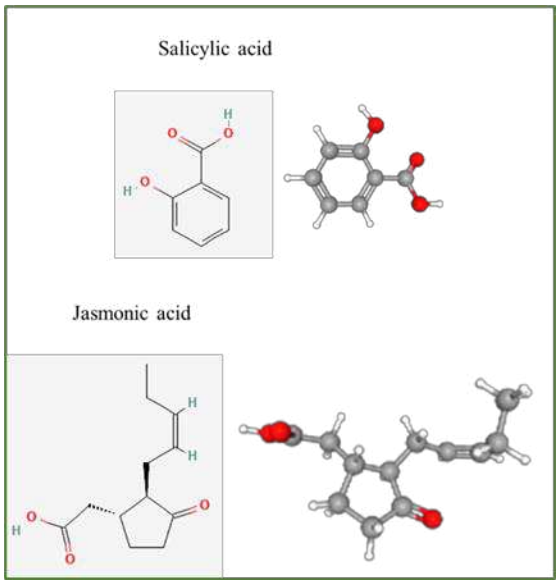

Figure 1.13. Structural formula of salicylic acid (SA) and jasmonic acid (JA). The first one involved chiefly in SAR related to the interaction between a plant host and a pathogen; the second one involved chiefly in IRS related to interaction between two symbionts, plant and microbe (from PubChem website: https://pubchem.ncbi.nlm.nih.gov/).

The discovery of the action mode of IR, has opened up at the possibility of developing new strategies for the crop protection against the pathogens (72, 73).

In the last twenty years, natural elicitor compounds extracted from plants (e.g. oligogalacturonides, fucans, laminarin), bacteria

(e.g. pseudobactin), oomycetes (e.g. eicosapentaenoic acid), and fungi (e.g. β-glucans, chitosan, ergosterol) have been hypothesized and tested for their effectiveness in controlling challenging pathogenic microorganisms in vineyards, as an alternative to pesticides (76-82).

Elicitor molecules can have biological or synthetic origin and can mimic the action mode of PTI (72, 73). Experimentation works compared the efficacy of chemical and natural resistance inducers on crops. Certain studies investigated the use of elicitors to confer tolerance to *Plasmopara viticola*, *Erysiphe necator* and *Botrytis cinerea* on vine. Vine metabolism can rapidly biodegrade natural elicitors by vine metabolism can be rapid, making them less effective in vineyards (70, 83). Substances such as benzothiadiazole (BTH), methyl jasmonate and ethephon have been used as resistance inducers in grapevines against biotrophic, hemi-trophic or necrotrophic pathogens. These molecules, alone or in combination, have been employed to modify polyphenol metabolism in grapevine (61, 84, 86). The expression of genes coding the enzymes in the phenylpropanoid/stilbene pathway resulting in an increase in stilbene biosynthesis (61, 85, 87).

One of the synthetic molecules with high effectiveness in preventing fungal and bacterial disease is the propesticide Acibenzolar-S-Methyl (ASM), belonging to the benzothiazoles chemical category (BTH derivative). Due to the similarity of structural formula and functional chemical groups it can mimic the SA behaviour (Figure 1.14) (74, 88, 89). Numerous studies have explored the efficacy of ASM in controlling fungal pathogens. In the cases study on tobacco and wheat protection, ASM (S-Methyl

benzo [1,2,3] thiadiazole-7-carbothioate), commercialized as BION® by Syngenta, was used for priming SAR through SA-dependent pathways (90, 91). This molecule was also applied to enhance resistance to *Botrytis cinerea* in *V. vinifera* spp. *sativa* cv Merlot. The experiment involved in three different treatments conducted over one week, starting from detached grape bunches to veraison.

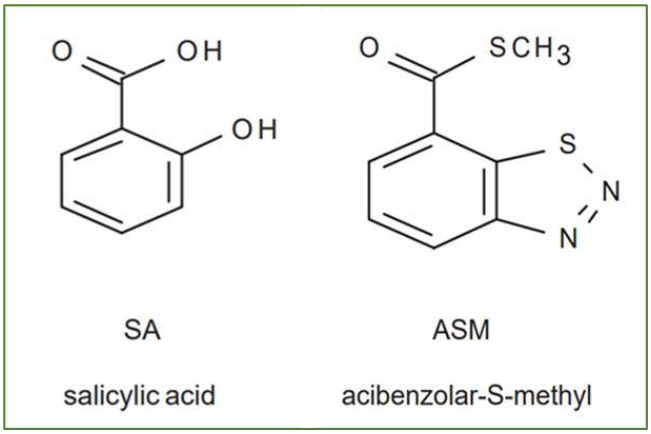

Figure 1.14. Structural formula of salicylic acid (SA) and acibenzolar-S-methyl (ASM; Benzothiadiazole derivative) compared. (Modified from Oostendorp *et al*., 2001(74)).

Research has demonstrated that ASM's protective effect involves increased anthocyanin (resveratrol) synthesis by activating the stilbene pathway in the berries (61, 86-87).

Acibenzolar-S-Methyl is an element of the experimental plan for this PhD study, which focuses on fungal communities on grapevine berry skin.

1.2.2 Sustainability: international framework

Sustainability is a current and important concept. The United Nations General Assembly (UN) approved the 2030 Agenda, which outlines seventeen Sustainable Development Goals (96).

In parallel with the UN, the European Union (EU) has implemented various initiatives and policies to reduce the environmental impact of human activities. The European Green Deal (COM (2019) 640 final and ANNEX) outlines new regulation for the European economy, covering climate change mitigation, biodiversity, pollution prevention, and circular economy principles. The agricultural sector is committed to reduce the use of agrochemical and many fungicides will be withdrawn from the market.

From several decades Food and Agriculture Organization of the United Nations (FAO) promotes strategies to minimize the environmental impact of agriculture by reducing synthetic chemicals and adhering to good practices. This approach is described in the FAO textbook "Policy Support Guidelines for the Promotion of Sustainable Production Intensification and Ecosystem Services". It involves several actions, as listed below:

- using no tillage where suitable;
- maintaining the soil cover with residues;
- implementing crop rotation or association;
- ensuring balanced nutrition (no excessive nitrogen fertilization);
- implementing Integrated Pest Management (IPM) using selective active molecules with minimal impact on the

environment and human health;

- managing damaging species (arthropods and cryptogams) when a certain infestation threshold is reached.

Both cultivation techniques and biotic threat management are directed towards minimizing environmental pollution. Pest, disease, and weed control involves the implementation of suitable practices, harnessing biodiversity, and employing selective, low-risk pesticides when deemed necessary (97-99). IPM involves assessing various factors that may promote plant diseases. This includes monitoring climate conditions, identifying initial signs of diseases, and screening phytophagous populations to determine infection thresholds. The decision on whether agrochemical treatment is necessary is guided by numerous. Subsequent actions are then taken for disease agent control. The foundation of this approach is based on the following criteria:

• Prevention: the preliminary step in pest control, aiming to hinder pests from becoming a threat. In agriculture, this can be achieved through cultural methods such as rotating between different crops, selecting pest-resistant varieties, and planting pest-free crops.

• Establishing Action Thresholds: Before implementing any pest control measures, it's crucial to set action thresholds. These thresholds indicate when pest populations or environmental conditions suggest that the pest is becoming harmful and requires control measures. Typically, the action threshold corresponds to critical levels of factors, such as population or climatic parameters, which represent an economic threat.

• Monitoring and Identification of Pests: in presence of an actual

biotic adversity, control actions may be initiated. Making appropriate control decisions, aligned with established action thresholds, prevents the risk of using incorrect pesticides or mistimed treatments.

• Control: if preventive methods are ineffective or unavailable, treatment may be initiated based on monitoring, identification, and action thresholds. Effective, less risky pest controls are given initial preferences, such as highly targeted chemicals, pheromones for disrupting pest mating, parasite trapping, mechanical control, and superficial soil tillage for weed containment. If ongoing monitoring and assessments reveal that these less risky controls are ineffective, targeted spraying of pesticides on the host becomes necessary. The application of broad-spectrum pesticides is considered a last resort (97-99).

In this scenario, the main strategy for maintaining vine physiology, productivity, and grape quality involves the using alternative products to traditional synthetic agrochemicals. These include resistance inducers or elicitors formulated for soil or foliar applications (57, 100).

Therefore, it is important to study the ecological impact of these new agrochemicals.

1.3 Economic and cultural importance of grapevine

To contextualize this study, some general economic observations on Barbera grapes cultivar in Piedmont are included.

In 2022, Spain had the largest vineyard area, globally 995,000 hectares, followed by France (812,000 ha), China (785,000 ha), and Italy (718,000 ha). Over the last five years, Italy has consistently led the world in wine production. In 2022, Italy produced 49.8 million hectolitres (mhl), followed by France (45.6 mhl), Spain (35.7 mhl), and the United States (22.4 mhl). The wine sector is one of the most relevant in the Italian economy (Tab. 1.3 and 1.4) (103).

Table 1.3 Italian data referred to Vineyard area a) *and wine production* b) *related to the World ones in last five years.* (Sources: STATE OF THE WORLD VINE AND WINE SECTOR IN 2022, April 2023 - OIV, FAO. National Statistical Offices) (102,103).

a)

Vineyard surface area							
(data refers to total surface area vine planted including young vines not yet in production, for all purposes, wine, juices, table grapes and raisins)							
	2018	2019	2020	2021	2022	22/21 Variation	2022 world percentage
	ha (x1000)					%	
Italy	705	714	719	718	718	0.0%	9.9%
World total	7342	7352	7364	7312	7280	-0.4%	100.0%

b)

Wine production							
(juices and musts excluded)							
	2018	2019	2020	2021	2022	22/21 Variation	2022 world percentage
	millions of hl					%	
Italy	54.8	47.5	49.1	50.2	49.8	-1%	19.3%
World total	294	258	262	261	258	-1%	100%

According to the Italian statistical yearbooks, the wine grapevine cultivation area in Italy has increased from 2016 to 2021. In 2021, Italy had 651,000 hectares of vineyards, producing over 7 million tons of grapes (102,103).

Furthermore, due to the recent COVID-19 pandemic, the energy crisis due to Russia-Ukraine conflict, and global supply chain disruptions, the wine market experienced significant price increases with only a slight decrease in worldwide consumption volumes. In 2022, the global wine exports reached their highest recorded value. The international wine trade was dominated by Italy, Spain, and France which collectively accounting for 53% of global wine exports by shipping 57 million hectolitres. In terms of volume, they declined with respect to 2021: Italy exported 21.9 million hl (-0.6% compared to 2021), Spain exported 21.2 million hl (-10%, the largest decrease compared to 2021), and France exported 14.0 million hl (-5% compared to 2021). In terms of value, France remains the first exporter at world level, with 12.3 bn EUR (+10.9% / 2021), followed by Italy (7.8 bn EUR, +10.1% / 2021) and Spain (3.0 bn EUR, +3.1% / 2021). These three countries account for 61% of the global export value (103). Wine production is a crucial component of Italy's agri-food exports. In 2022, Italy imported wine worth € 500 million and exported wine worth € 7,834 million, accounting for 13.7% of all agri-food exports (104,107). In table 1.4 is reported the import-export of wine in Italy.

In 2021, the Italian wine supply chain, as reported by ISMEA (Istituto di Servizi per il Mercato Agricolo Alimentare), generated a turnover of 3 billion euro, based on a wine production of 50

million hectolitres. Of these 55% had a geographical indication certification (104,107). These data underscore the strategic importance of Italy's winemaking sector and emphasize the need for research and innovation across all phases of chain production to remain competitive globally.

Table 1.4 Wine import-export in Italy (m=million). (Sources: STATE OF THE WORLD VINE AND WINE SECTOR IN 2022, April 2023 - OIV, FAO. National Statistical Offices) (103).

Wine export from Italy								
Volume (mhl)		Value (mEUR)		Type	Vertical Structure in 2022		Variation 2022/2021	
2021	2022	2021	2022		volume	value	volume	value
22.0	21.9	7,116	7,834	Bottle (< 2 l)	57%	67%	-3%	7%
				Sparkling	24%	28%	6%	19%
variation of -0.6%		variation of 10.1%		Bag in Box®	2%	1%	-3%	6%
				Bulk (> 10 l)	17%	4%	0%	13%

Wine import to Italy								
Volume (mhl)		Value (mEUR)		Type	Vertical Structure in 2022		Variation 2022/2021	
2021	2022	2021	2022		volume	value	volume	value
3.1	2.2	408	500	Bottle (< 2 l)	9%	20%	-18%	9%
				Sparkling	6%	63%	0%	36%
variation of -28.8%		variation of 22.6%		Bag in Box®	1%	0%	137%	44%
				Bulk (> 10 l)	85%	17%	-28%	1%

To narrow down the discussion to the subject of the PhD study, here's some information on “Barbera d'Asti” PDO. In Piedmont, which is a significant wine-growing region in Italy, vineyard cultivation trend (Fig. 1.15) closely follows the national trend.

In 2021, this Region had approximately 42,000 hectares of Protected Designation of Origin (PDO) vineyards, resulting in a wine and must production of 2,770,000 hectolitres (104,107). Piedmont boasts 60 types of PDO wines, including “Barbera d'Asti DOCG”, which is found in the Asti area (105). Barbera grapevine is the main red berry cv of the Monferrato zone, in the Southwest

of Piedmont, occupying 30% of the vineyard area in this Region (106).

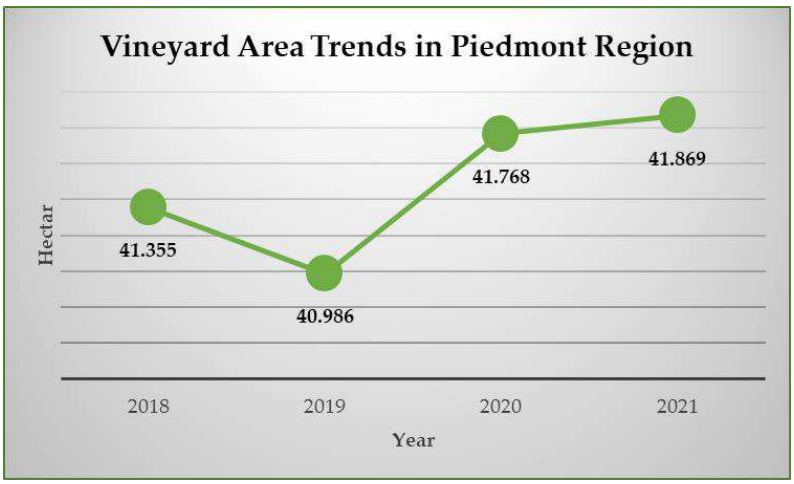

Figure 1.15. The Growing Expansion of Wine-Capable Vineyard Land Area in Piedmont from 2018 to 2021 (Source Istat database) (101).

In the Italian market, 'Barbera d'Asti DOCG' wine is positioned at the top end of the price range for red and rosé wines in 2023, with a price of €160 per hectolitre, compared to €125 the previous year, exceeding the medium price of €103/hl. (104,107).

Beyond its economic importance, grapevine cultivation holds a distinct place in the Mediterranean landscape, cultural heritage, and enogastronomy of Italy (Figure 1.16).

For instance, the presence of cultivar Barbera in the Monferrato territory dates back to the Middle Ages (1512). This historical significance is underscored by the UNESCO recognition of the "Vineyard landscape of Langhe, Roero and Monferrato" as a World Heritage Site in June 2014 (106,108).

Figure 1.16. A picture of the Monferrato, Vineyard Landscapes of Piedmont: Langhe-Roero and Monferrato UNESCO World Heritage (Modified from *https://www.destinazionemonferrato.it/il-monferrato/*)(108).

REFERENCES

(1) Fregoni M. *Viticoltura di qualità. Trattato di eccellenza da terroir*, 3rd ed.; Tecniche Nuove: Milano, Italy (2013); pp. 49–77. ISBN 978-88-481-7919-5.

(2) Viticoltura, Giuseppe Sicheri, (2008) Ulrico Hoepli Editore – Milano

(3) Eynard I. e Dalmasso G., (1990) Viticoltura moderna, IX edizione, Hoepli, Milano, 53-79.

(4) X.-Q. Liu, S.M. Ickert-Bond, Z.-L. Nie, Z. Zhou, L.-Q. Chen, J. Wen (2016) Phylogeny of the Ampelocissus–Vitis clade in Vitaceae supports the New World origin of the grape genus, *Mol. Phylog. Evol.* Vol. 95: 217–228. DOI: 10.1016/j.ympev.2015.10.013

(5) Grapevine morphology: web site https://www.shutterstock.com/it/image-vector/parts-plant-morphology-grape-vine-root-1637619400 (accessed in May 2023)

(6) Grassi F., Arroyo-Garcia R., (2020) Origins and Domestication of the Grape. *Fron. Pl. Sc.* Vol. 11. DOI: 10.3389/fpls.2020.01176

(7) Jones G. and Davis R.E. (2000). Climate Influences on Grapevine Phenology, Grape Composition, and Wine Production and Quality for Bordeaux, France. *Am. J. Enol. Vitic.,* 51

(8) Pinto C. and Gomes A.C. (2016). *Vitis vinifera* microbiome:

from basic research to technological development. *BioControl* DOI: 10.1007/s10526- 016-9725-4

(9) Van Leeuwen C. and Seguin G. (2006). The Concept of Terroir in Viticulture. *Journal of Wine Research*, 2006, Vol. 17: 1-10

(10) Grapevine flower morphology: web site www.extention.org (supported in part by New Technologies for Agriculture Extension grant no. 2020-41595-30123 from the USDA National Institute of Food and Agriculture.) (accessed in May 2023)

(11) Mullins, M. G., A. Bouquet, and L. E. Williams (1992) *Biology of the Grapevine*. Ed. Cambridge University Press. ISBN 0521305071

(12) Grapevine berry section: web site https://it.depositphotos.com/ (accessed in May 2023)

(13) Chitwood D.H., Ranjan A., Martinez C.C., Headland L.R., Thiem T., Kumar R., Covington M.F., Hatcher T., Naylor D.T., Zimmerman S., Downs N., Raymundo N., Buckler E.S., Maloof J.N., Aradhya M., Prins B., Li L., Myles S., Sinha N.R. (2014) A Modern Ampelography: A Genetic Basis for Leaf Shape and Venation Patterning in Grape. *Plant Physiology*, Vol. 164 (1): 259–272. DOI: 10.1104/pp.113.229708

(14) A. Calò, A. Scienza, A. Costacurta (2001) Vitigni d'Italia. Schede ampelografiche. Editore Calderini Edagricole, Pagine 831. ISBN: 8820643677

(15) The French–Italian Public Consortium for Grapevine Genome Characterization (2007) The grapevine genome sequence

suggests ancestral hexaploidization in major angiosperm phyla. *Nature,* Vol.449: 463–467. DOI: 10.1038/nature06148

(16) Rayapati, N., Maree H., Burger J. (2015). Grapevine Leafroll Disease and Associated Viruses: A Unique Pathosystem. Annual Review of Phytopathology. 53, 613-634. DOI: 10.1146/annurev-phyto-102313-045946

(17) González-Barreiro, C., Rial-Otero, R., Cancho-Grande, B. & Simal-Gándara, J. (2015) Wine Aroma Compounds in Grapes: A Critical Review, Critical Reviews. *Food Sc. Nutr.*, 55:2, 202-218. DOI: 10.1080/10408398.2011.650336

(18) Alleweldt, G., & Possingham, J. V. (1988). Progress in grapevine breeding. *Theoretical and Applied Genetics*, 75, 669-673. DOI: 10.1007/BF00265585

(19) Töpfer, R., Hausmann, L., Harst, M., Maul, E., Zyprian, E., & Eibach, R. (2011). New horizons for grapevine breeding. *Fruit, vegetable and cereal science and biotechnology*, 5(1), 79-100.

(20) Navarro-Payá D., Santiago A., Orduña L., Zhang C., Amato A., D'Inca E., Fattorini C., Pezzotti M., Tornielli G.B., Zenoni S., Rustenholz C., and Matus J.T. (2022). The Grape Gene Reference Catalogue as a Standard Resource for Gene Selection and Genetic Improvement. *Front. Plant Sci*. 12:803977. DOI: 10.3389/fpls.2021.803977

(21) Velasco R., Zharkikh A., Troggio M., Cartwright D.A., Cestaro A., et al. (2007) A High Quality Draft Consensus Sequence of the Genome of a Heterozygous Grapevine Variety. *PLOS ONE* 2(12): e1326. DOI: 10.1371/journal.pone.0001326

(22) Foria, S., Magris, G., Jurman, I., Schwope, R., De Candido, M., De Luca, E., Ivanišević, D., Morgante, M., Di Gaspero, G. (2022) Extent of wild–to–crop interspecific introgression in grapevine (*Vitis vinifera*) as a consequence of resistance breeding and implications for the crop species definition. *Hortic. Res.* Volume 9, uhab010. DOI: 10.1093/hr/uhab010

(23) Grando S., Velasco R. (2004). Ricerche sui caratteri genetici che determinano le produzioni viticole. L'informatore Agrario, 46: 59-62

(24) Osakabe, Y., Liang, Z., Ren, C., Nishitani, C., Osakabe, K., Wada, M., Komori, S., Malnoy, M., Velasco, R., Poli, M., Jung, M.-H.,Koo, O.-J., Viola, R., Nagamangala Kanchiswamy, C. (2018) CRISPR–Cas9-mediated genome editing in apple and grapevine. *Nature Prot.* 13(12), 2844-2863. DOI:10.1038/s41596-018-0067

(25) Organisation Internationale de la Vigne et du Vin (OIV) Web site: RESOLUTION OIV/VITI 333/2010: https://www.oiv.int/public/medias/379/viti-2010-1-en.pdf (accessed in May 2023)

(26) Caffarra, A. and Eccel, E. (2011), Projecting the impacts of climate change on the phenology of grapevine in a mountain area. *Australian Journal of Grape and Wine Research*, 17: 52-61. DOI: 10.1111/j.1755-0238.2010.00118.x

(27) Naulleau A., Gary C., Prévot L., Hossard L. (2021) Evaluating Strategies for Adaptation to Climate Change in Grapevine Production–A Systematic Review. *Frontiers in Plant Science.*

11,1664-462X. DOI: 10.3389/fpls.2020.607859

(28) Hinojos Mendoza, G.; Gutierrez Ramos, C.A.; Heredia Corral, D.M.; Soto Cruz, R.; Garbolino, E. (2020) Assessing Suitable Areas of Common Grapevine (*Vitis vinifera* L.) for Current and Future Climate Situations: The CDS Toolbox SDM. *Atmosphere.* 11, 1201. DOI:10.3390/atmos11111201

(29) Giffard B., Winter S., Guidoni S., Nicolai A., Castaldini M., Cluzeau D., Coll P., Cortet J., Le Cadre E., d'Errico G., Forneck A., Gagnarli E., Griesser M., Guernion M., Lagomarsino A., Landi S., Bissonnais Y.L., Mania E., Mocali S., Preda C., Priori S., Reineke A., Rusch A., Schroers H.-J., Simoni S., Steiner M., Temneanu E., Bacher S., Costantini E.A.C., Zaller J. and Leyer I. (2022) Vineyard Management and Its Impacts on Soil Biodiversity, Functions, and Ecosystem Services. *Front. Ecol. Evol*. 10:850272. DOI: 10.3389/fevo.2022.850272

(30) Gambino, G., Dal Molin, A., Boccacci, P., Minio, A., Chitarra, W., Avanzato, C. G., Tononi, P., Perrone, I., Raimondi, S., Schneider, A., Pezzotti, M., Mannini, F., Gribaudo, I., Delledonne, M. (2017) Whole-genome sequencing and SNV genotyping of 'Nebbiolo' (*Vitis vinifera* L.) clones. *Scientific Reports* 7(1), 2045-2322. DOI: 10.1038/s41598-017-17405-y

(31) Martínez-Zapater, J.M., Carmona, M.J., Díaz-Riquelme, J., Fernández, L., Lijavetzky, D. (2010) Grapevine genetics after the genome sequence: Challenges and limitations. *Australian Journal of Grape and Wine Research* 16(s1), 1322-7130. DOI: 10.1111/j.1755-0238.2009.00073.x

(32) Blouin, M., Hodson, M. E., Delgado, E. A., Baker, G., Brussaard, L., Butt, K. R., et al. (2013). A review of earthworm impact on soil function and ecosystem services. *Eur. J. Soil Sci*. 64, 161–182. DOI: 10.1111/ejss.12025

(33) Orgiazzi, A., Bardgett, R. D., Barrios, E., Behan-Pelletier, V., Briones, M. J. I., Chotte, J.-L., et al. (2016). Global Soil Biodiversity Atlas. Luxembourg, LUX: *Publication Office of the European Union*. https://esdac.jrc.ec.europa.eu/content/global-soil-biodiversity-atlas

(34) Surico, G., Mugnai, L., Marchi, G. (2008) The Esca Disease Complex. In Integrated Management of Diseases Caused by Fungi, Phytoplasma and Bacteria. Integrated Management of Plant Pests and Diseases; Ciancio, A., Mukerji, K. Eds; *Springer*: Dordrecht, Netherlands, Volume 3, pp. 119-136. DOI: 10.1007/978-1-4020-8571-0_6

(35) Musetti, R. (2008) Management and Ecology of Phytoplasma Diseases of Grapevine and Fruit Crops. In Integrated Management of Diseases Caused by Fungi, Phytoplasma and Bacteria. Integrated Management of Plant Pests and Diseases; Ciancio, A., Mukerji, K. Eds; *Springer:* Dor-drecht, Netherlands, Volume 3, pp. 43-60. DOI: 10.1007/978-1-4020-8571-0_3

(36) Altimira, F., Vitta, N., Tapia, E. Integrated Pest Management of *Lobesia botrana* with Microorganism in Vineyards: An Alternative for Clean Grapes Production [Internet]. In Grapes

and Wine. IntechOpen; 2022. Available online: https://www.intechopen.com/books/10901. DOI: 10.5772/intechopen.99153 (accessed on 04 April 2023)

(37) Kurtzman, C. P.; Fell, J. W. and Boekhout T. The Yeast a Taxonomic study (set) 5t ed.; Elsevier: 32 Jamestown Road, London NW1 7BY, UK, 2011; Vol.1, p. 22.

(38) Kurtzman, C. P.; Fell, J. W. and Boekhout T. The Yeast a Taxonomic study (set) 5th ed.; Elsevier: 32 Jamestown Road, London NW1 7BY, UK, 2011; Vol.1, pp. 41-42.

(39) Margesin, R., Neuner, G. & Storey, K.B. (2007) Cold-loving microbes, plants, and animals—fundamental and applied aspects. Naturwissenschaften 94, 77–99. DOI: 10.1007/s00114-006-0162-6

(40) Lee, H. M., Hong R. K., Eunbeen J., Hee C. Y., Sukkyoo L., Jiaojie L., and Dae-Hwan K. (2020) "Evaluation of the Biodegradation Efficiency of Four Various Types of Plastics by Pseudomonas aeruginosa Isolated from the Gut Extract of Superworms" Microorganisms 8, no. 9: 1341. DOI: 10.3390/microorganisms8091341

(41) Lettieri T. (2006) Recent Applications of DNA Microarray Technology to Toxicology and Ecotoxicology. Environmental Health Perspectives 114:1 DOI: 10.1289/ehp.8194

(42) Sun, G.L., Reynolds, E.E. & Belcher, A.M. (2020) Using yeast to sustainably remediate and extract heavy metals from waste waters. *Nat Sustain* 3, 303–311. DOI: 10.1038/s41893-020-0478-9

(43) Images of various pathogens and pests responsible for grapevine diseases: on web site e-phytia, INRAE (Institut National de Recherche pour l'Agriculture, l'alimentation et l'Environnement) portal hosts various phytosanitary applications; https://ephytia.inra.fr/it/P/97/Vite (accessed in September 2023)

(44) Kurtzman, C. P.; Fell, J. W. and Boekhout T. The Yeast a Taxonomic study (set) 5th ed.; Elsevier: 32 Jamestown Road, London NW1 7BY, UK, 2011; Vol.1, p. 45.

(45) Di Francesco, A.; Ugolini, L.; D'Aquino, S.; Pagnotta, E.; Mari, M. (2017) Biocontrol of Monilinia laxa by Aureobasidium pullulans strains: Insights on competition for nutrients and space Int. Jour. Food Microb. 248: 32-38. DOI: 10.1016/j.ijfoodmicro.2017.02.007.

(46) Jarvis, W. R., Traquair, J. A. and Bélanger, R. R. (2007) 'Sporodex®, fungal biocontrol for powdery mildew in greenhouse crops.', CABI Books. CABI. doi: 10.1079/9781845932657.0224.

(47) El-Mehalawy, A. A. (2004) Rhizosphere y east fungi as biocontrol agents. Int. J. Agri. Biol., Vol. 6, No. 2, 310-316.

(48) El-Mehalawy, A. A., Hassanein, N. M., Khater, H. M., El-Din, E. K., & Youssef, Y. A. (2004). Influence of maize root colonization by the rhizosphere actinomycetes and yeast fungi on plant growth and on the biological control of late wilt disease. Int J Agric Biol, 6(4), 599-605.

(49) El-Tarabily, Khaled A.; Sivasithamparam, K. (2006) Potential

of yeasts as biocontrol agents of soil-borne fungal plant pathogens and as plant growth promoters. Mycoscience 47(1), pp. 25-35. DOI: 10.1007/S10267-005-0268-2

(50) Fernandez-San Millan, A.; Farran, I.; Larraya, L.; Ancin, M.; Arregui, L.M.; Veramendi, J. (2020) Plant growth-promoting traits of yeasts isolated from Spanish vineyards: benefits for seedling development. Microbiological Resear. 237: 126480. DOI: 10.1016/j.micres.2020.126480

(51) Kurtzman, C. P.; Fell, J. W. and Boekhout T. The Yeast a Taxonomic study (set) 5th ed.; Elsevier: 32 Jamestown Road, London NW1 7BY, UK, 2011; Vol.1, p. 47.

(52) Altieri, V.; Rossi, V.; Fedele, G. (2023) Biocontrol of Botrytis cinerea as Influenced by Grapevine Growth Stages and Environmental Conditions. Plants, 12, 3430. DOI: 10.3390/plants12193430

(53) Sepúlveda, X.; Vargas, M.; Vero, S.; Zapata, N. (2023) Indigenous Yeasts for the Biocontrol of Botrytis cinerea on Table Grapes in Chile. *J. Fungi*, 9, 557. DOI: 10.3390/jof9050557

(54) Ayogu, P., Teixeira, A., Gerós, H., & Martins, V. (2023). Identification of grape berry indigenous epiphytic yeasts with in vitro and in vivo antagonistic activity towards pathogenic fungi. *OENO One*. 57(1): 253–264. DOI: /10.20870/oeno-one.2023.57.1.7273

(55) Agarbati, A., Canonico, L., Pecci, T., Romanazzi, G., Ciani, M., & Comitini, F. (2022). Biocontrol of Non-*Saccharomyces*

yeasts in vineyard against the gray mold disease agent Botrytis cinerea. Microorganisms, 10(2), 200. DOI: 10.3390/microorganisms10020200

(56) Reiff, J.M., Pennington, T., Kolb, S. *et al*. (2023) Consistent benefits of fungicide reduction on arthropod predators and predation rates in viticulture: a five-year experiment. *BioControl*. DOI: 10.1007/s10526-023-10213-6

(57) Kaczmarek, M., Entling, M.H. & Hoffmann, C. (2023) Differentiating the effects of organic management, pesticide reduction, and landscape diversification for arthropod conservation in viticulture. *Biodivers Conserv* 32, 2637–2653. DOI: 10.1007/s10531-023-02621-y

(58) Jez, E.; Pellegrini, E.; Contin, M. (2023) Copper Bioavailability and Leaching in Conventional and Organic Viticulture under Environmental Stress. *Appl. Sci*., 13, 2595. DOI: 10.3390/app13042595

(59) Maddalena, G.; Marone; Fassolo, E.; Bianco, P.A.; Toffolatti, S.L. (2023) Disease Forecasting for the Rational Management of Grapevine Mildews in the Chianti Bio-District (Tuscany). *Plants*. 12, 285. DOI: 10.3390/plants12020285

(60) Cortez-Madrigal, H., Gutiérrez-Cárdenas, O.G. (2023) Enhancing biological control: conservation of alternative hosts of natural enemies. Egypt J Biol Pest Control 33, 25. DOI: 10.1186/s41938-023-00675-2

(61) Jeandet, P.; Trotel-Aziz, P.; Jacquard, C.; Clément, C.; Mohan, C.; Morkunas, I.; Khan, H.; Aziz, A. (2023) Use of Elicitors and

Beneficial Bacteria to Induce and Prime the Stilbene Phytoalexin Response: Applications to Grapevine Disease Resistance. *Agronomy*, 13, 2225. DOI: 10.3390/agronomy13092225

(62) Vuolo, F.; Novello, G.; Bona, E.; Gorrasi, S.; Gamalero, E. (2022) Impact of Plant-Beneficial Bacterial Inocula on the Resident Bacteriome: Current Knowledge and Future Perspectives. Microorganisms, 10, 2462. DOI: 10.3390/microorganisms10122462

(63) Hassan, T., Rashid, G. (2023). Biofertilisers and Biopesticides: Approaches Towards Sustainable Development. In: Dar, G.H., Bhat, R.A., Mehmood, M.A. (eds) Microbiomes for the Management of Agricultural Sustainability. Springer, Cham. https://doi.org/10.1007/978-3-031-32967-8_5

(64) Bona, E.; Lingua, G.; Manassero, P.; Cantamessa, S.; Marsano, F.; Todeschini, V.; Copetta, A.; D'Agostino, G.; Massa, N.; Avidano, L.; Gamalero, E.; Berta, G. (2015) "AM fungi and PGP pseudomonads increase flowering, fruit production, and vitamin content in strawberry grown at low nitrogen and phosphorus levels." Mycorrhiza, 25:181–193. DOI: 10.1007/s00572-014-0599-y

(65) Ambrosini, V. G.; Voges, J. G.; Canton, L., *et al*. (2015) Effect of arbuscular mycorrhizal fungi on young vines in copper-contaminated soil. *Brazilian J. Micr*. 46 (4): pp 1045-1052. DOI: 10.1590/S1517-838246420140622

(66) Moukarzel, R., Ridgway, H.J., Waller, L. *et al*. (2023) Soil

Arbuscular Mycorrhizal Fungal Communities Differentially Affect Growth and Nutrient Uptake by Grapevine Rootstocks. *Microb Ecol* 86, 1035–1049. DOI: 10.1007/s00248-022-02160-z

(67) Brunetto, G.; Marques, A. C. R.; Trentin, E.; *et al*. (2023) Arbuscular mycorrhizal fungi inoculation as strategy to mitigate copper toxicity in young field-grown vines. *Ciência Téc. Vitiv*., 38 (1): pp. 60-66. DOI: 10.1051/ctv/ctv20233801060

(68) Orozco-Mosqueda, M.d.C.; Kumar, A.; Fadiji, A.E.; Babalola, O.O.; Puopolo, G.; Santoyo, G. (2023) Agroecological Management of the Grey Mould Fungus *Botrytis cinerea* by Plant Growth-Promoting Bacteria. *Plants*, 12, 637. DOI:10.3390/plants12030637

(69) Ye, Q.; Wang, H.; Li, H. (2023) Arbuscular Mycorrhizal Fungi Enhance Drought Stress Tolerance by Regulating Osmotic Balance, the Antioxidant System, and the Expression of Drought-Responsive Genes in *Vitis vinifera* L. Aust. J. Grape Wine Res. 2023: 7208341. DOI: 10.1155/2023/7208341

(70) Héloir, M-C; Adrian, M; Brulé, D; *et al*. (2019) Recognition of Elicitors in Grapevine: From MAMP and DAMP Perception to Induced Resistance. *Front. Plant Sci.* 10:1117. DOI: 10.3389/fpls.2019.01117

(71) Salifu, R.; Chen, C.; Sam, F.E.; Jiang, Y. (2022) Application of Elicitors in Grapevine Defense: Impact on Volatile Compounds. *Horticulturae*, 8, 451. DOI: 10.3390/horticulturae8050451

(72) Wiesel, L.; Newton, A. C.; Elliott, I.; Booty, D.; Gilroy, E. M.;

Birch, P. R.; Hein, I. (2014) Molecular effects of resistance elicitors from biological origin and their potential for crop protection. *Fr. Plant Sc*. 5: 655. DOI: 10.3389/fpls.2014.00655

(73) Walters, D., & Fountaine, J. (2009). Practical application of induced resistance to plant diseases: An appraisal of effectiveness under field conditions. *The J. of Agricultural Science*, 147(5), 523-535. DOI:10.1017/S0021859609008806

(74) Oostendorp, M.; Kunz, W.; Dietrich, B.; Staub, T. (2001) Induced Disease Resistance in Plants by Chemicals. *Eur. J. Plant Pathol*. 107, 19–28.

(75) Newman, M. A., Sundelin, T., Nielsen, J. T., and Erbs, G. (2013). MAMP (microbe-associated molecular pattern) triggered immunity in plants. Front. *Plant Sci*. 4:139. DOI: 10.3389/fpls.2013.00139

(76) Galletti, R., Ferrari, S., and De Lorenzo, G. (2011). *Arabidopsis* MPK3 and MPK6 play different roles in basal and oligogalacturonide- or flagellin-induced resistance against *Botrytis cinerea*. *Plant Physiol*. 157, 804–814. DOI: 10.1104/pp.111.174003

(77) Craigie, J. S. (2011). Seaweed extract stimuli in plant science and agriculture. *J. Appl. Phycol*. 23, 371–393. DOI: 10.1007/s10811-010-9560-4

(78) Vera, J., Castro, J., Gonzalez, A., and Moenne, A. (2011). Seaweed polysaccharides and derived oligosaccharides stimulate defense responses and protection against pathogens in plants. *Mar. Drugs*. 9, 2514–2525. DOI: 10.3390/md9122514

(79) De Vleesschauwer, D., and Höfte, M. (2009). Rhizobacteria-induced systemic resistance. *Adv. Bot. Res*. 51, 223–281. DOI: 10.1016/S0065-2296(09)51006-3

(80) Henriquez, M. A., Wolski, E. A., Molina, O. I., Adam, L. R., Andreu, A. B., and Daayf, F. (2012). Effects of glucans and eicosapentaenoic acid on differential regulation of phenylpropanoid and mevalonic pathways during potato response to *Phytophthora infestans*. *Plant Physiol. Biochem*. 60, 119–128. DOI: 10.1016/j.plaphy.2012.07.027

(81) Laquitaine, L., Gomès, E., François, J., Marchive, C., Pascal, S., Hamdi, S., *et al*. (2006). Molecular basis of ergosterol-induced protection of grape against *Botrytis cinerea*: induction of type I LTP promoter activity, WRKY, and stilbene synthase gene expression. Mol. Plant Microbe Interact. 19, 1103–1112. DOI: 10.1094/MPMI-19-1103

(82) Vatsa, P., Chiltz, A., Luini, E., Vandelle, E., Pugin, A., and Roblin, G. (2011). Cytosolic calcium rises and related events in ergosterol-treated Nicotiana cells. *Plant Physiol. Biochem*. 49, 764–773. DOI: 10.1016/j.plaphy.2011.04.002

(83) Harm, A.; Kassemeyer, H.-H.; Seibicke, T.; Regner, F. (2011) Evaluation of Chemical and Natural Resistance Inducers against Downy Mildew (*Plasmopara viticola*) in Grapevine. *Amer. J. Eno. Vit*. 62 (2): pp 184-192 DOI: 10.5344/ajev.2011.09054

(84) Fernandez-Marin, M.I.; Guerrero, R.F.; Puertas, B.; Garcia-Parrilla, M.C.; Collado, I.G.; Cantos-Villar, E. (2013) Impact of

preharvest and postharvest treatment combinations on increase of stilbene content in grape. *J. Int. Sci. Vigne Vin*., 47, 203–212. DOI: 10.20870/oeno-one.2013.47.3.1548

(85) Miliordos, D.-E.; Alatzas, A.; Kontoudakis, N.; Unlubayir, M.; Hatzopoulos, P.; Lanoue, A.; Kotseridis, Y. (2023) Benzothiadiazole Affects Grape Polyphenol Metabolism and Wine Quality in Two Greek Cultivars: Effects during Ripening Period over Two Years. *Plants*. 12, 1179. DOI: 10.3390/plants12051179

(86) Iriti, M.; Rossoni, M.; Borgo, M.; Faoro, F. (2004) Benzothiadiazole enhances resveratrol and anthocyanin biosynthesis in grapevine, meanwhile improving resistance to *Botrytis cinerea*. *J. Agric. Food Chem*. 52, 4406–4413. DOI: 10.1021/jf049487b

(87) Dufour, M.C.; Lambert, C.; Bouscaut, J.; Mérillon, J.M.; Coriot-Costet, M.F. (2013) Benzothiadiazole-primed defence responses and enhanced differential expression of defence genes in *Vitis vinifera* infected with biotrophic pathogens *Erysiphe necator* and *Plasmopara viticola*. *Plant Pathol*. 62, 370–382. DOI: 10.1111/j.1365-3059.2012.02628.x

(88) Durrant, W.E.; Dong, X. (2004) Systemic acquired resistance. *Ann. Rev. Phytopathol*. 42, 185–209. DOI: 10.1146/annurev.phyto.42.040803.140421

(89) Rahman, F.U.; Khan, I.A.; Aslam, A.; Liu, R.; Sun, L.; Wu, Y.; Aslam, M.M.; Khan, A.U.; Li, P.; Jiang, J.; *et al*. (2022) Transcriptome analysis reveals pathogenesis-related gene 1

pathway against salicylic acid treatment in grapevine (*Vitis vinifera* L.). *Front. Genet*. 13, 1033288. DOI: 10.3389/fgene.2022.1033288

(90) Friedrich, L.; Lawton, K.; Ruess, W.; Masner, P.; Specker, N.; Gut Rella, M.; Meier, B.; Dincher, S.; Staub, T.; Uknes, S.; *et al*. (1996) A benzothiadiazole derivative induces systemic acquired resistance in tobacco. *Plant J.* 10, 61–70. DOI: 10.1046/j.1365-313X.1996.10010061.x

(91) Görlach, J.; Volrath, S.; Knauf-Beiter, G.; Hengy, G.; Beckhove, U.; Kogel, K.H.; Oostendorp, M.; Staub, T.; Ward, E.; Kessmann, H.; *et al*. (1996) Benzothiadiazole, a novel class of inducers of systemic acquired resistance, activates gene expression and disease resistance in wheat. *Plant Cell.* 8, 629–643

(92) Liu, S.-l.; Wu, J.; Zhang, P.; Hasi, G.; Huang, Y.; Lu, J.; Zhang, Y.-l. (2016) Response of phytohormones and correlation of SAR signal pathway genes to the different resistance levels of grapevine against *Plasmopara viticola* infection. *Plant Physiol. Biochem*. 107, 56–66. DOI: 10.1016/j.plaphy.2016.05.020

(93) Gutiérrez-Gamboa, G.; Romanazzi, G.; Garde-Cerdán, T.; Pérez-Álvarez, E.P. (2019) A Review of the Use of Biostimulants in the Vineyard for Improved Grape and Wine Quality: Effects on Prevention of Grapevine Diseases: Use of Biostimulants in the Vineyard for Improved Grape and Wine Quality. *J. Sci. Food Agric.* 99, 1001–1009. DOI:10.1002/jsfa.9353.

(94) Du Jardin, P. (2015) Plant Biostimulants: Definition, Concept, Main Categories and Regulation. *Sci. Hortic*. 196, 3–14. DOI: 10.1016/j.scienta.2015.09.021.

(95) Bano, A.; Waqar, A.; Khan, A.; Tariq, H. (2022) Phytostimulants in Sustainable Agriculture. *Front. Sustain. Food Syst*. 6, 801788. DOI:10.3389/fsufs.2022.801788. (accessed in October 2022)

(96) United Nation web site of the Department of Economic and Social Affairs - Sustainable Development: https://sdgs.un.org/goals (accessed in October 2022)

(97) Food and Agriculture Organization of the United Nation (FAO) web site: https://www.fao.org/family-farming/detail/en/c/327688/ (accessed in October 2022)

(98) Food and Agriculture Organization of the United Nation FAO. Integrated Crop Management, Policy Support Guidelines for the Promotion of Sustainable Production Intensification and Ecosystem Services (2013) Vol. 19 available at: http://www.fao.org/3/a-i3506e.pdf (accessed in October 2022)

(99) Food and Agriculture Organization of the United Nation FAO. Integrated Pest Management. Available online: https://www.fao.org/pest-and-pesticide-management/ipm/integrated-pest-management/en/ (accessed in October 2022).

(100) Beaumelle L., Gifard B., Tolle P., Winter S., Entling M.H., Benítez E., Zaller J.G., Auriol A., Bonnard O., Charbonnier Y., Fabreguettes O., Joubard B., Kolb S., Ostandie N., Reif J.M.,

Richart-Cervera S., Rusch A. (2023) Biodiversity conservation, ecosystem services and organic viticulture: a glass half-full. *Agric Ecosyst Environ*. 351:108474. DOI: 10.1016/j.agee.2023.108474

(101) Vineyard Land Area in Piedmont: Istat - StatBase: "l'accesso ai principali dati" (provided from Istat on 30/05/2022, 09h44 UTC (GMT) https://www.istat.it/it/dati-analisi-e-prodotti/banche-dati/statbase)

(102) Organisation Internationale de la Vigne et du Vin (OIV) Web site: STATE OF THE WORLD VINE AND WINE SECTOR IN 2022, https://www.oiv.int/sites/default/files/documents/2023_SWVWS_report_EN.pdf (accessed in April 2023)

(103) 2022 and 2021 Italian statistical yearbook, on the Istituto Nazionale di Statistica - ISTAT web site: https://www.istat.it/it/archivio/annuario+statistico+italiano (accessed in April 2023)

(104) Import-export wine data from Istituto di Servizi per il Mercato Agricolo Alimentare (ISMEA) web site: www.ismeamercati.it: SchedaVino_2022_04.pdf (accessed in April 2022)

(105) "Asti" Protected Designation of Origin from "Regione Piemonte" web site: Disciplinare di produzione della denominazione di origine controllata e garantita dei vini "ASTI" https://www.regione.piemonte.it/web/temi/agricoltura/viticoltura-enologia/vini-denominazione-origine-docg-doc (accessed in

April 2023)

(106) PDO Barbera d'Asti Consortium web site: https://www.viniastimonferrato.it/vitigni/barbera/ (accessed in April 2022)

(107) Prices data ISMEA mercati web site: https://www.ismeamercati.it/flex/cm/pages/ServeBLOB.php/L/IT/IDPagina/5390 (accessed in May 2023)

(108) UNESCO world heritage convention web site: https://whc.unesco.org/en/list/1390 (accessed in April 2022)

Chapter II

Outline of the thesis

2. Outline

This doctoral research was carried out in the context of the project entitled "*Microbiota of Vitis vinifera cv. Barbera grapes: a focus at the mycobiota and a look on culturable indigenous Saccharomyces spp. strains under three different experimental conditions in vineyard*". Although there was no scholarship, there was financial support from Consiglio per la ricerca e l'analisi dell'economia agraria – Centro di ricerca Viticoltura ed Enologia (CREA-VE) for the infrastructure, laboratory, equipment, and experimental vineyard.

Furthermore, the PhD was conducted jointly with University of Piemonte Orientale (DISIT), which funded expenses related to attending conferences and publishing scientific articles. IGA Technology srl provided service of Next Generation Sequencing (NGS) focused on metagenomic analysis and engaging in productive discussions on optimal sequencing conditions.

This doctoral project was inspired from the research project "Elicitori di resistenza a supporto della difesa dalla Flavescenza dorata della vite" ("Resistance elicitors to support vine defense against the Flavescence dorée"), coordinated by Istituto per la protezione Sostenibile delle Piante of the Consiglio Nazionale delle Ricerche (CNR-IPSP) and funded by the Regione Piemonte. This last research evaluated the efficacy of BION®50WG in the recovery of grapevines from Flavescence doré and ESCA diseases.

The CREA-VE experimental vineyard was conducted in accordance with the Integrated Crop Management (ICM) principles. During the 2018 and 2019 growing seasons some tests were ran with the biostimulant BION®50WG produced by Syngenta (Basel, Switzerland). This synthetic biostimulant contains 50% Acibenzolar

S-methyl (ASM) and is formulated in hydrodispersible granules. The trials were carried out according to the CRN-IPSP experimental design, as described in Chapter 3, which includes details on the vineyard parcel characteristics and on the experimental protocol.

The focus was on the yeast fraction of grape microorganisms, which play a crucial role in the vinification processes. Therefore, to gain a comprehensive understanding of yeast communities, three distinct approaches have been employed to characterise them.

In order to investigate the mycobiota community on the grape skin and the effect of the biostimulant on its composition the massive sequencing through metabarcoding technique was performed. The use of this culture-independent method allows for a thorough exploration of the complexity of microbial communities in a given environment, without the limitations of traditional culture-dependent methods. These last may result in the loss of a significant portion of microorganisms during in vitro cultivation. The sequencing results enable the estimation of the most used biodiversity indexes, namely alpha and beta diversity. The term "alpha" is used to describe the diversity within a community in a particular habitat, without considering the diversity in surrounding areas. It is usually studied in ecology to describe the diversity of species within a single community or habitat. The terms “beta” refers to the diversity of species between two or more ecosystems, habitats, or communities. It measures how species composition changes when you move from one location to another or from one community to another.

Following the NGS opportunity and the data analysis through the Microbiome Analysis Platform, the fungal communities living on the grape bunches can be observed and described at various taxonomic level. The fungal groups abundance at species level was reported

focusing on the biodiversity within each treatment and on the differences among the treatments. Additionally alpha diversity estimator, such as Shannon and Simpon indexes were evaluated to describe the eventual shift in biodiversity at species level within the theses and among the three different experimental conditions (considered as three micro-habitats). The Shannon Index was chosen in this study because it considers both species richness (number of different species) and species evenness (relative abundance of each species). Higher values of the Shannon index indicate greater species diversity and evenness within the community, and a value of “0" indicates that the community consists of a single species. This index is widely used because of its applicability to various ecological studies, including those related to ecosystems, microbial communities, and biodiversity assessments. The Simpson Index also consider species richness and evenness and is widely used as alpha diversity estimator. It calculates the probability that two randomly selected individuals from the community will belong to the same species. A higher value indicates lower diversity, while a lower value suggests higher diversity. A value of “1” indicates perfect dominance by a single species.

When Shannon and Simpson Indexes are used in conjunction, they provide a more comprehensive view of alpha diversity within a community. Often, as in this study, both indexes are considered together to gain insight into the different aspects of community diversity.

Beta diversity is used to describe the diversity and to measure of compositional dissimilarity in species between the three experimental conditions. This measure based on Bray-Curties metrics ranges from 0 to 1, with 0 indicating identical species composition and 1 indicating

no shared species between the “sites” or between the communities. This analysis was reported as PCoA graphics.

The Microbiome Analyst Platform was used also for the presentation of species richness in a pie chart format, displaying the relative abundance of communities from three parcels. A heatmap representation was shown to compare the community composition in each sample and identify any trends, even with a large number of OTUs per sample. The “pattern search” tool shows the positive and negative corelation between the treatment and the species more affected by the considered experimental conditions. In order to identify if some OTUs could be relevant combining standard statistical significance tests with biologically meaningful, a Linear discriminant analysis Effect Size (LEfSe) was elaborated.

The culture dependent method in microbiology, involves the study of the yeast species present on the berry skin. Restriction Fragment Length Polymorphism (RFLP) analysis was performed to identify at species level the yeasts. This is a classic molecular analysis always useful in the identification of microorganism species. It involves studying the DNA Internal Transcribe Spacer (ITS), which delimits the ribosomal 5.8S subunit coding region. As the ribosomal DNA is highly conserved during the phylogeny, it is suitable for species assignment. Although through this method it is impossible to find less abundant species, it could be of interest discovering if any culturable species could be favourite in one of the theses. The identification at species level was performed grouping the population of the isolates by RFLP analysis and comparing their pattern using Bionumerics™ Data Base and type strains genetic profile present in the CREA-VE microorganisms Collection in Asti. When this strategy is not effective to the identification, the isolate were grouped per homogeneous

profile based on the RFLP results. One type per group, underwent to Sanger sequencing method of 26S DNA region to determine the actual species.

A final trial was planned to investigate any potential shift in yeast communities on the grape that may not have been detected by the metabarcoding approach or by culture-dependent methods. This test focused on the presence of the wine yeast indirectly through spontaneous alcoholic fermentation. Wine fermenting strains, particularly *S. cerevisiae* species, are in low abundance on the grape. Thus 5 spontaneous fermentation per treatment, one from each sampled grape, was performed. Commonly, the spontaneous fermentation was driven by *S. cerevisiae*, using grape must from ICM vineyard. Therefore, the study of the wine yeasts at the end of spontaneous fermentations referred to each treatment revealed if one experimental condition can promote one fermenting yeast species. An effectual molecular approach to identify both *S. cerevisiae* species and its strains was used. This technique involves amplifying three specific hypervariable microsatellite *loci* of *S. cerevisiae* using multiplex PCR analysis. By this approach, genotypes of *S. cerevisiae* and the presence of non-*Saccharomyces* yeast can be assessed. The non-*Saccharomyces* species are identified using the RFLP protocol mentioned earlier. Also, the spontaneous fermentations aim at the evaluation of eventual inhibition of the fermenting yeasts in general.

The project aimed at three goals, primarily addressing the potential side effects of BION®50WG on mycobiota:

- to access biodiversity indexes using metabarcoding technique and explore the potential differences in the composition of the yeast communities on the grape surface across three parcels involved in the trial;

- to describe the composition of cultivable yeasts on the berry skin and comparing the three theses;

- to induce spontaneous fermentations from each sample and observe if any anomalies occur on the process trend. Also, verify if there is any shift in the yeast species at the end of alcoholic fermentation depending on the treatment.

This study is the first to evaluate the mycobiota on the grapevine berry skin after three different treatments, focusing on the biostimulant BION®50WG. In addition, it represents an attempt to provide further information on the new phytostimulant effect on yeast communities associated to Barbera grapevine bunches, and their possible implications in oenology, such as in the alcoholic fermentation process.

The comparison of the mycobiota from each treatment was examined in depth. The composition of the yeast communities through culture-dependent method was assessed. The identification of the wine yeasts at the end of the spontaneous fermentation allowed the estimation of eventual effect on the process and on the indigenous fermenting yeasts. After the study from these three points of view resulted that the treatments did not affect the fungal populations examined.

In conclusion the phytostimulant BION®50WG did not significantly affect the fungal biodiversity in the vineyard at ripening time. Therefore, this chemical biostimulant can be applied in the vineyard pest management (IPM) because it has no relevant impact on the fungal biodiversity of the mature berries surface. Concerning the winemaking, Acibenzolar S-Methyl substantially did not modify the wine yeast species and apparently it will not cause any problem for the vinification processes.

Metabarcoding analysis can be used to assess biodiversity indexes and monitor environmental biodiversity by public entities, particularly during the authorization phases of new crop protection products. Additionally, collecting metabarcoding data annually and in different locations, could be a valuable resource for estimating microbial bioindicators during climate change or at polluted sites.

Several aspects of the project should be studied in depth as described below.

Due to past observations of fermentation stoppages or slow fermentations, caused by certain fungicides, further studies on the alcoholic fermentation process in presence of ASM could be very relevant. It could affect the yeast growth and the AF performance.

To evaluate eventual variation in metabolisms, the indigenous *S. cerevisiae* isolated from the three parcels should be examined for their technological properties. Additionally in order to estimate the *Saccharomyces* yeast contribution to the wine terroir, chemical parameters of oenological interest and aromatic compounds should be analysed. On the other hand, it is necessary verify the possible onset of aromatic defects derived from the metabolization of ASM by yeast cell.

Therefore, it would be advisable to evaluate the effect of the BION®50WG on plant metabolism, particularly on the chemical composition of the berries.

Chapter III

Materials and Methods to analyse the yeast communities on grape skin and at the end of alcoholic fermentation

3. Materials and Methods

3.1 Pedo-climatic conditions

Piedmont is characterized by a continental climate. In 2019, this Region experienced a minimum temperature of 1.92 ◦C and a maximum temperature of 25.54 ◦C and recorded an annual rainfall of 803.4 mm (1).

According to the ISPRA (Istituto Superiore per la Protezione e la Ricerca Ambientale - Italian Institute for Environmental Protection and Research) annual report, the year 2019 marked the twenty-third consecutive year with a positive anomaly in both temperature and precipitation. Globally, 2019 was the second warmest year since 2016 for both land and ocean temperatures, and the third warmest year since 1961. Except for January and May, all months of the year were significantly warmer than normal, peaking in June, when the positive anomaly reached +4.25°C in the North (2).

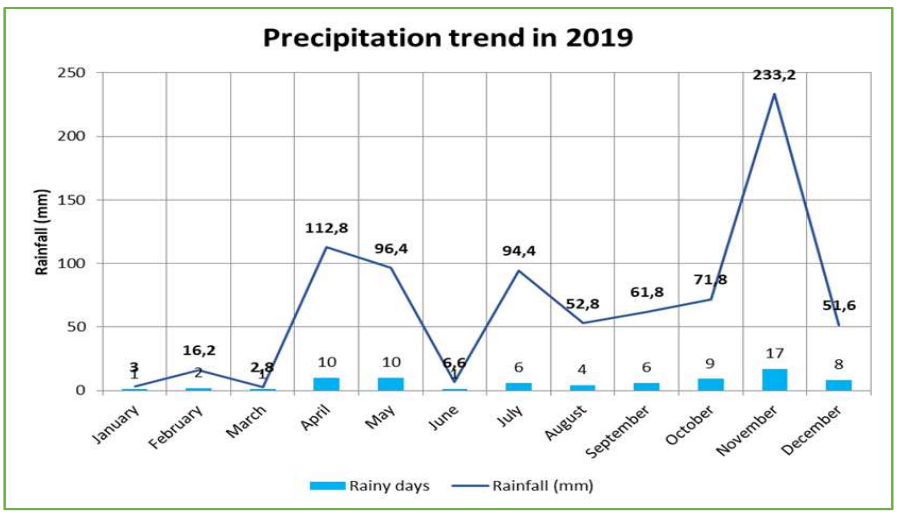

Figure 2.1. The graph illustrates the monthly rainfall in Asti province for the year 2019, and that spring and autumn were the rainiest months in terms of both intensity and duration (data source: ARPA

Piemonte)(1).

The climatic situation in Piedmont during the growing season was typical, except for a short period of drought in March. Minimum temperatures in May were lower than normal. At the end of June, maximum temperatures of + 10 °C occurred. On 14 July, the maximum daily rainfall for the month of July was recorded throughout the region (2). The following figures provide an overview of the climatic conditions in 2019. These are derived from the monthly data recorded by the weather station of Agenzia Regionale per la Protezione Ambientale Piemonte (1), situated closest to the experimental vineyard.

The precipitation graph clearly indicates that in the initial days of October, during the vineyard sampling, there was no rainfall that could have led to the washing away of microorganisms from the berries (Fig. 2.1) (1).

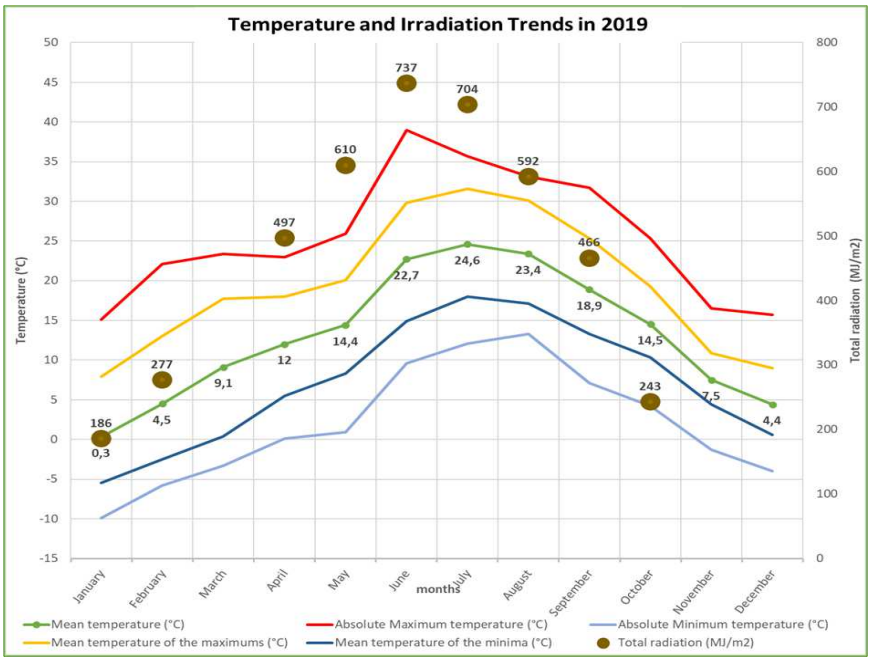

Figure 2.2. The graph illustrates the monthly temperatures and global solar radiation in 2019 in Asti. Summer months resulted the

warmest, also due to the high sun radiation. Spring and Autumn were characterised by mild temperatures. Y axis on the left: temperature (°C); Y axis on the right: sun radiation (MJ/m^2) (data source: ARPA Piemonte) (1).

From the graph in figure 2.2 the temperatures trend was in line with the total radiation, as expected. Therefore, the table below depicted that the monthly mean temperatures in August, September, and October were temperate, aligning with the seasonal norms and meeting the thermal requirements of wine yeasts. The monthly mean temperatures in August, September, and October were temperate, aligning with the seasonal norms and meeting the thermal requirements of wine yeasts (tab 2.1) (1).

Table 2.1. The table displays the average monthly temperature (°C) and the global sun radiation in monthly average (MJ/m^2) in Asti for the year 2019. The highest temperature corresponds to the maximum radiation value (source: ARPA Piemonte) (1).

Parameter	Jan.	Feb.	Mar.	Apr.	May	Jun.	Jul.	Aug.	Sep.	Oct.	Nov.	Dec.
Mean temperature (°C)	0.3	4.5	9.1	12.0	14.4	22.7	24.6	23.4	18.9	14.5	7.5	4.4
Monthly average of global solar radiation (MJ/m^2)	186	277		497	610	737	704	592	466	243		

Due to the slow speed of the breeze recorded in September and October (average 1.5 and 1.2 m/s, respectively) the microflora on the grape during harvest was minimally affected by windiness (Fig 2.3).

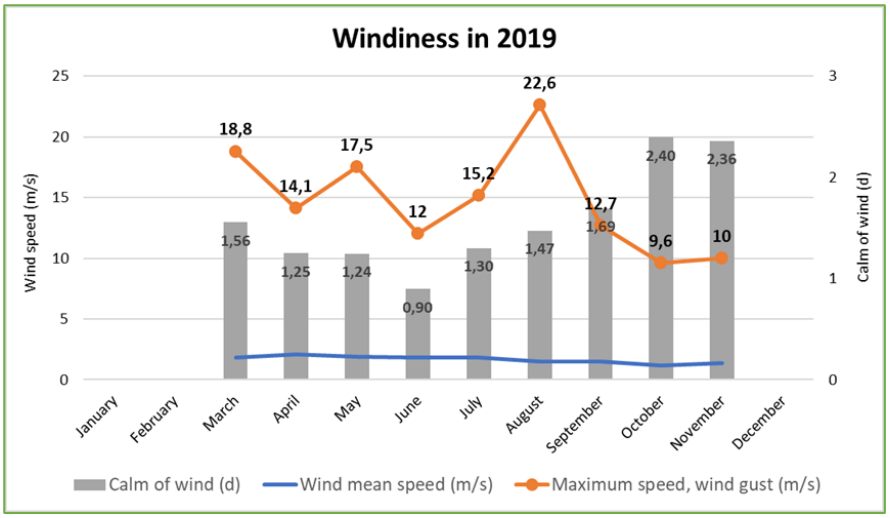

Figure 2.3. The graph illustrates monthly windiness in 2019 in Asti. Through this year the breeziness was low, the mean speed was around 1,8 m/s, with maximum of 2,1 m/s in April and minimum of 1,4 m/s in November. Generally, the no wind days range had 0,9 to 2,36. Y axis on the left: wind speed (m/s); Y axis on the right: calm of wind (day); (data source: ARPA Piemonte) (1).

In October, the harvest period for Barbera cv, the average monthly rainfall registered close to Asti, was similar to the climatological values for Piedmont. The following graph illustrates daily temperature and rainfall during the last three months of the ripening stage (Fig. 2.4).

These climatic data are from European Centre for Medium-Range Weather Forecasts (3,4), an independent intergovernmental organisation supported by 35 states, including Italy. ECMWF produces numerical weather forecasts, monitors the Earth system, conducts scientific and technical research to improve forecast skill, and maintain an archive of meteorological data within the EU's Copernicus Earth observation programme. Among the services provided by ECMWF is ERA5-LAND, which compiles climatic datasets since 1950 from the 5 major continents of the world (China, EU/EFTA, USA, India, United Kingdom of Great Britain, and

Northern Ireland) (3,4).

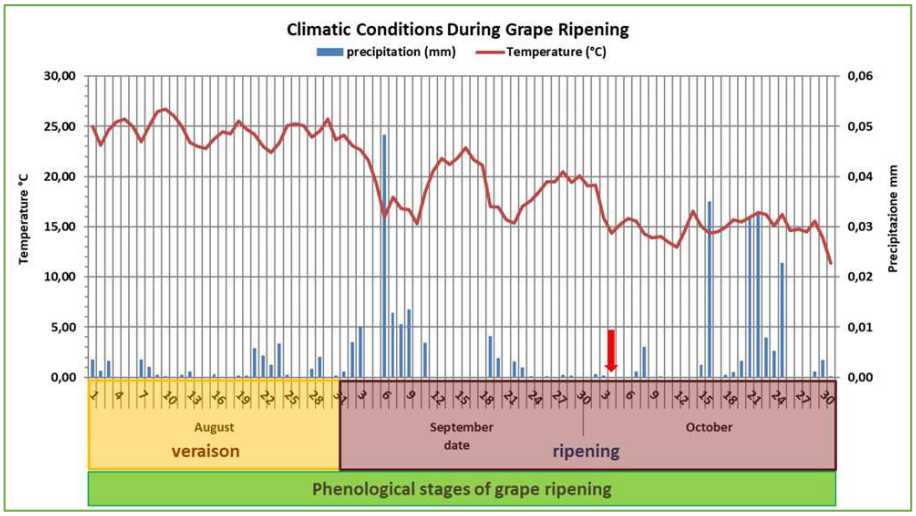

Figure 2.4. Focus on the climatic conditions during the grape ripening in 2019. Graph generated from ERA5-Land platform, utilizing monthly averaged data from 1950 to present (https://www.ecmwf.int/en/era5-land). Precipitation data represents the daily sum of rain, and temperature data reflects the daily average temperature measured 2 meters above the ground at the geo-localized survey point located at longitude 8.2°N and latitude 44.9°E, with a resolution of 10 km per grid point. This point corresponds to the weather cabin closest to Asti in the ERA5-Land Database. The red arrow indicates the sampling time.

It is noteworthy that during the harvest time, the climatic conditions were optimal, and the rainfall was so minimal (0.004 mm of rain, and 19.67 °C of temperature as three months average) that it did not induce significant variation in the microbial composition following the last biostimulant treatment on 7th August. On the sampling day, the air temperature was 14.37°C, and no rainfall was recorded.

The evaluation of soil chemical composition was conducted to assess the grapevine cultivation conditions. Soil sampling was performed according a "W" scheme on 1 ha of vineyard, simultaneously at grape sampling. Samples were collected at a depth

of 30 cm after removing the surface layer. Five samples were gathered and mixed to form a single bulk soil pattern. Physical and chemical analyses were then performed on the bulk soil following the guidelines of D.M. 13/09/99 (5) (Tab. 2.2).

Table 2.2. Soil physical and chemical composition of the vineyard.

Parameter	Unit of measure	Results
Granulometry		
Total sand	%	31.25
Total silt	%	38.75
Clay	%	30.00
Analyzed compound		
pH (in Water)	-	7.43
Total limestone ($CaCO_3$)	%	0.41
Organic Matter	%	1.50
Organic Carbon	%	0.87
Total Nitrogen	%	0.0706
C/N ratio	-	12.32
Absorbable Phosphorus	ppm	10
Exchangable Potassium	ppm	59
Exchangeble Calcium	ppm	2362
Exchangable Magnesium	ppm	245
CEC	meq/100g	27.91

Based on the granulometry data, the soil texture was identified as clayey loam, typical of Monferrato soil (Fig. 2.5).

The soil chemical composition was in line with the chemical characteristics of medium-textured clay soils, with neutral pH. The Cation exchange capacity (CEC) measuring the soil ability to hold nutrients, is of 27.91 meq/100g, that indicated a relatively high soil fertility. The exchangeable potassium and assimilable phosphorus soli reserve was very low, leading to physiological problems in the vine and uneven ripening of the grape bunches (7-9). The Grapevines phytosanitary state was considered during the bunches sampling as specified in paragraph 3.2.2.

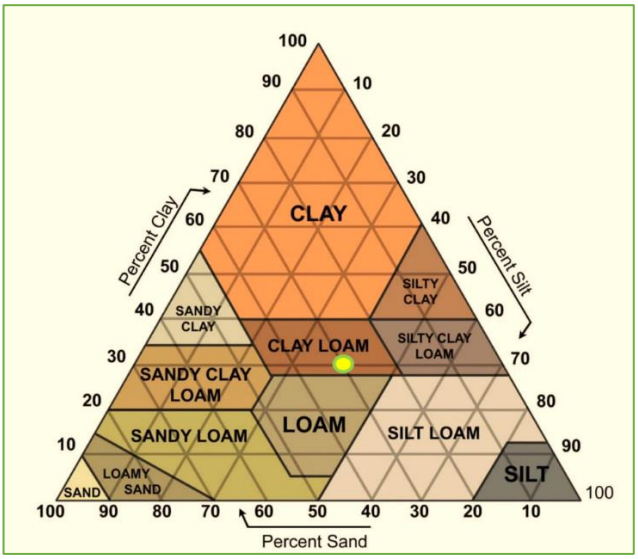

Figure 2.5. Representation of soil texture triangle according to United States Department of Agriculture (USDA); yellow spot indicates the soil texture of CREA-VE experimental vineyard soil, considering the granulometry data: total sand= 31.25%; total silt= 38.75% and clay= 30.00%. (Modified from: https://soilsensor.com/articles/soil-textures/)(6).

3.2 Experimental conditions

CREA-VE experimental vineyard (Fig. 2.6) was located in Asti countryside, Piedmont (44° 55' 28" N; 8° 11' 12" E).

Figure 2.6. GPS vision of the vineyard from Google Earth.

The field was close to the city of Asti, extended on 2 hectare (ha) at an altitude from 166 to 198 m a.s.l.. It has a slope of about 17% and an orientation at south. The vineyard was planted in 2006. It was composed of 63 rows, arranged in an East–West direction, and cultivated with 6 *V. vinifera* varieties. All the cultivars were grafted on 1103 Paulsen rootstock (high vigour; adapts well to clayey, compact, and saline soils; absorbs a lot of magnesium and postpones the ripening). The plant of about 1 m height is cultivated in the Guyot training system, which consists in the cultivation with poles, metal treads and cord as support for the climbing shrubs. The pruning guaranteed the foliage structure of Guyot style by the pruning

technique based on leaving a spur and a new shoot for future fruiting (Fig. 2.7). After the pruning, 6-12 buds occur on the shoot and 2 ones on the spur. This is the most common vine management in Piedmont (10).

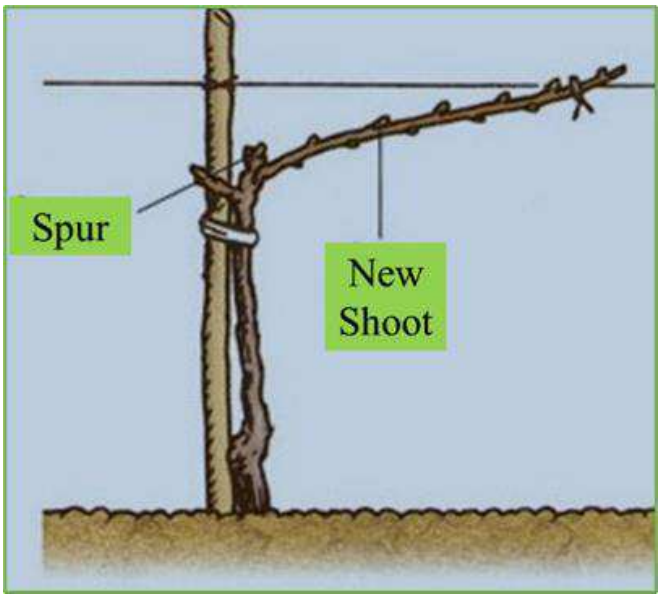

Figure 2.7. A schematic representation of a Guyot system.

The vineyard adhered to Integrated Crop Management (ICM) strategies as described in the introduction of the thesis. Notably, pest control, especially on arthropods, disease management, and weed control were implemented using selective and low-risk pesticides when necessary. Practices aligned with the principles of Integrated Pest Management (IPM) were employed (11,12).

3.2.1 Experimental plan

The trial adhered to the experimental protocol designed within the project "Elicitori di resistenza a supporto della difesa dalla Flavescenza dorata della vite" coordinated by CNR-IPSP, as detailed

in Outline.

The entire vineyard was segmented into areas, each corresponding to grapevine varieties in the CREA-VE experimental field. Each variety's surface area was further divided into three parcels, each subjected to a distinct treatment.

This thesis focused on examining the cv Barbera area, covering 0.5 ha, illustrated in Figure 2.8.

The treatments were intended as:

- **Control (C)**: Integrated pest management (IPM) of the vineyard. Consisting of the use of insecticides and fungicides against the main parasites and pathogenic fungi when the infestation threshold occurs during vegetative stage and especially during ripening phase.

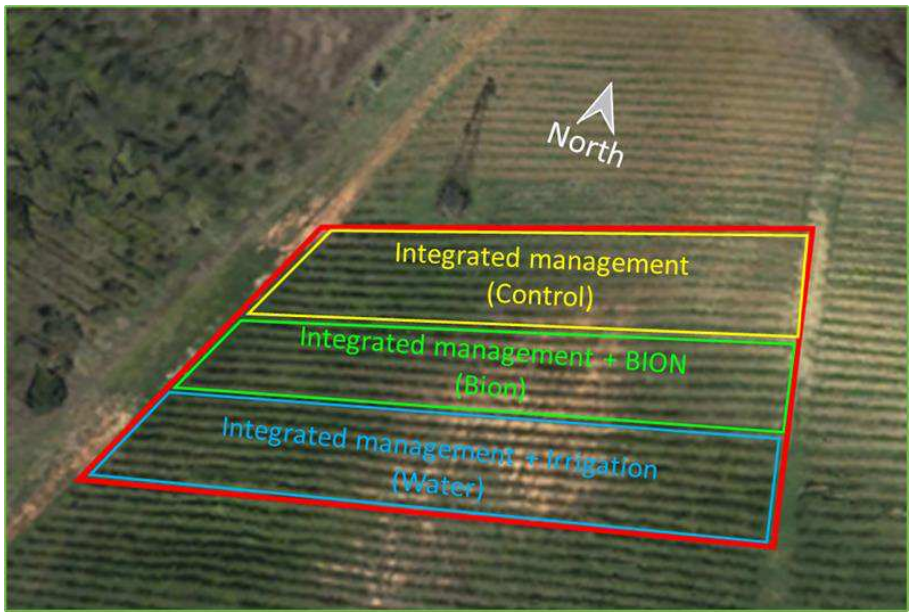

Figure 2.8. Sampling area dedicated to Barbera cultivar, partitioned into three parcels corresponding to distinct treatments.

- **Bion (B)**: IPM was augmented with the phytostimulant BION®50WG from Syngenta. BION®50WG was applied

every two weeks (see Table 2.3) throughout the growing season via foliar irrigation with a 500 L water suspension. The treatment dosage was derived from the posology recommended for *Actinidia* sp. plants, as indicated on the label. This was chosen due to the analogous vegetative habitus shared between *Vitis* and *Actinidia*.

- **Water (W)**: IPM combined with the nebulization of 500 L of water on leaves to simulate the possible effect of the humidity increase without the active molecule. It could be analogous to a light rain with a washout effect on previous treatments.

The treatments were taken during the 2018 and 2019 growing seasons as reported in table 2.3.

Table 2.3. Timing of BION®50WG treatment. Application of 5 hl of water suspension with the dose of 20g/hl in parcel Bion.

Year	timing of BION® 50WG treatments				
2018	26 June	10 July	24 July	7 August	21 August
2019	26 June	10 July	24 July	7 August	-

3.2.2 Grape sampling

To collect indigenous fermentative yeasts and to evaluate the berry microbiological conditions, the ripening phase is considered the best time (13). The sampling was conducted on October 3rd, 2019, the day before grape harvest. A random scheme was employed to select five grapevines within each parcel (fig. 2.9). Considering the occurrence of Flavescence doré and Esca diseases, unhealthy plants were avoided. Moreover, vineyard zones showing typical signs of soil aridity and erosion were excluded from sampling (14,15).

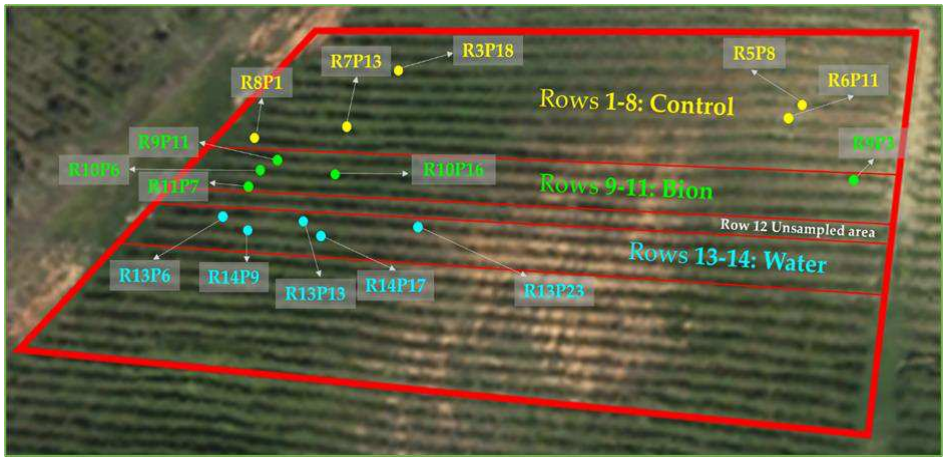

Figure 2.9. Cultivar Barbera vineyard area divided into plots according to the three treatments and respective sampling points.

Two to three ripe grapes per plant, amounting at 700g, were detached, and collected in sterile bags. Five biological replicas for each treatment were sampled, resulting in a total selection of 15 grapevine plants (tab. 2.4, fig. 2.9) (16).

In order to preserve the bunches conditions and the berries integrity, the harvested grapes were stored in a thermal bag at 10°C with frozen tablets.

Table 2.4. Sampling overview.

Treatment	Description	sample	Row	Plant
Control	Integrated Pest Management	1	**R3**	**P18**
		2	**R5**	**P8**
		3	**R6**	**P11**
		4	**R7**	**P13**
		5	**R8**	**P1**
Bion	IPM + BION®50WG 20g/hl (spraying 5 hl of water suspension)	6	**R9**	**P11**
		7	**R9**	**P3**
		8	**R10**	**P6**
		9	**R10**	**P10**
		10	**R11**	**P7**

Water	IPM + Water (spraying 5 hl of water)	11	**R13**	**P6**
		12	**R13**	**P13**
		13	**R13**	**P23**
		14	**R14**	**P9**
		15	**R14**	**P17**

3.3 Yeast collection and storage

In order to collect the yeasts from the grape skin, 50 berries (average weight of the berries 2,60 g with ± 0,24 g of standard deviation) were randomly sampled from each bunch, using a sterilized scissors and avoiding juice release. Berries were put into a sterile flask containing 200 ml of sterile saline solution (0,9% NaCl) and incubated overnight at 25 °C. The suspension was then incubated for 2 hours in a rotary shaker at 75 rpm (16) and centrifuged at 5000 rpm for 15 minutes at 4°C in order to obtain a pellet.

The pellets were resuspended in 5 ml of fresh saline solution and split in five aliquots. An aliquot of 1 ml was added with 50% V/V of glycerol and stored in duplicate at -80°C. Two aliquots of 1 ml, intended for the characterization of yeast community by metabarcoding analysis, were collected in sterile microtubes (2 ml volume) and pelleted again by centrifugation at 4°Cand 14.000 rpm for 5 minutes. One millilitre of the cellular suspension from each grape sampled was used for the culturable yeast identification (17,18).

3.4 Yeast characterization through Culture-dependent Method

Traditional culture dependent methods were applied to identify yeast isolated from the berry surface, as well as the yeast occurring at the final phase of spontaneous fermentation.

3.4.1 Selection, isolation, and storage conditions of yeast on the berry surface

One hundred µl of five 1:10 serial dilutions of the cellular suspension for each sample, obtained as previously described, were distributed in triplicate onto Wallerstein Laboratory nutrient agar (WL Nutrient Agar for microbiology, MERCK KGaA, Darmstadt, Germany) added of Ampicillin sodium salt (100 mg/l, Sigma-Aldrich) and Biphenyl (400mg/l, Sigma-Aldrich) in order to prevent bacterial and mould growth, respectively. WL agar is a selective and differential medium commonly used for the isolation of fungi and bacteria from food allowing a presumptive strain identification based on colony morphology (16,19) (Fig. 2.10).

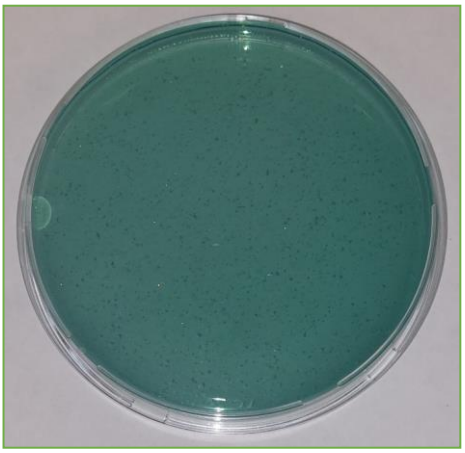

Figure 2.10. Plate of WL medium with inhibitors

Then, the Petri plates were incubated at 25° C for eight days to allow

yeast growth. Plates containing 20-200 colonies were considered as significant dilutions to statistically evaluate the microbial load of yeasts in different samples. From the significant plates, one repetition per bunch, colony isolation and yeast selection were performed according to the different morphologies. The colonies morphology was described with the help of a stereomicroscope referring to the margin, the form, the surface, the elevation, and the colour (Fig. 2.11 and 2.12).

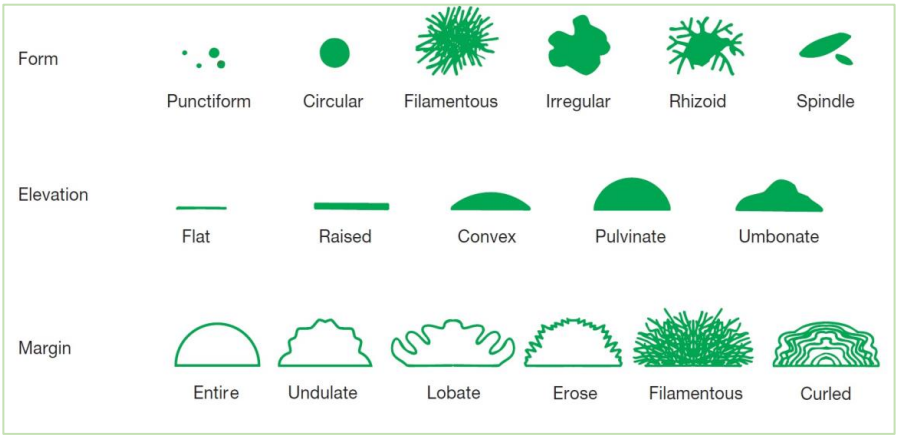

Figure 2.11. Some figures of the reference morphologies useful for the description of the yeast colonies.

An amount of 20-25 colonies per grape bunch (one repetition plate of the significant dilution), showing different morphology on WL medium were further isolated onto YEPG Agar (yeast extract: 10g/l; peptone: 10g/l; glucose: 20g/l) to prevent the contamination and in order to obtain a library. Overall, about 300 colonies were collected to be identify at species level with RFLP method.

After incubation at 25° C for three days, each strain was cultivated into YEPG broth, at 25° C for 24 hours stirring it, and used for the long-term conservation in 50% v/v glycerol at -80°C (16). Unique and rare morphologies occurring on plates were also isolated.

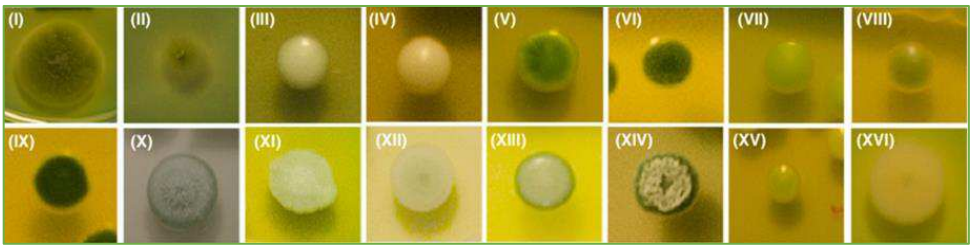

Figure 2.12. Sixteen colony morphotypes of non-Saccharomyces isolates on WL Nutrient Agar. I: Aureobasidium pullulans var. melanigenum; II: Aureobasidium pullulans var. pullulans; III: Candida albicans; IV: Candida apicola; V: Candida glabrata; VI: Candida stellimalicola; VII: Clavispora lusitaniae; VIII: Cryptococcus albidus; IX: Hanseniaspora spp.; X: Hyphopichia (Pichia) burtonii; XI: Issatchenkia orientalis; XII: Issatchenkia terricola; XIII: Kluyveromyces marxianus; XIV: Kodamaea (ex Pichia) ohmeri; XV: Meyerozyma (ex Pichia) caribbica; XVI: Pichia norvegensis (From: Polizzotto et al., 2016)(19).

3.4.2 Identification of the culturable yeast from berry surface

Identification of yeast strain at the species level was performed by a combined approach consisting of Restriction Fragment Length Polymorphism (RFLP) and sequencing analysis.

After the DNA purification from the pure culture in broth each isolate was subjected to the RFLP analysis, according to Esteve-Zarzoso et al. (1999) (20). The DNA extraction and purification was performed according to a modified protocol proposed by Cocolin et al. (2000) (21). A culture pellet was mixed with 200 µl of extraction buffer, 200 µl of Phenol: chloroform: iso-amyl alcohol (25:24:1) ≥ 99% (VWR Chemicals) and 0.3 g of glass beads. The suspension was incubated at 65 ° C for 15 minutes at 1400 rpm in the Thermomixer® (Eppendorf). In order to extract the DNA, the mixture was centrifugated to separate the hydrophilic supernatant phase from the

non-polar one. Then, the hydrophilic supernatant was subjected to precipitation of nucleic acid with glacial ethanol and washed with ethanol 70%. Finally, a centrifugation phase at 16.000 rcf for 10 minutes at 4°C leads to the extraction. The resulting pellet was resuspended in 50 µl ultrapure water (Milli-Q® CLX 7000 and Super-Q®). The RFLP analysis consists in the study of the coding zone for the RNA ribosomal 5.8S and of two non-coding regions at ITS ends (Fig. 2.13). Basically, it consists of a PCR amplification of the ITS region (22), followed by enzymatic digestion using three different endonucleases, HinfI, CfoI and HaeIII to access the different species. The PCR reaction and the subsequent enzymatic digestion were performed as described in table 2.5 and 2.6.

Table 2.5. Recipe for 20 µl PCR mix.

Reagent	Brand	Final concentration	Mix volume
Buffer (5 X), containing 5 mM dNTPs, 15 mM $MgCl_2$	Wonder Taq EUROCLONE SpA, Milano, Italy	1 X	4 µl
Recombinant thermostable DNA polymerase (5U/µl)	Wonder Taq EUROCLONE SpA, Milano, Italy	1U	0,2 µl
ITS 1 (10mM) Forward Primer	Eurofins Genomics, Ebersberg, Germany	0,25 mM	0,5 µl
ITS 4 (10mM) Reverse Primer	Eurofins Genomics, Ebersberg, Germany	0,25 mM	0,5 µl
Sterile and ultrapure water	-	-	13,8 µl
template DNA	-	10-100 ng/ µl	µl

The polymerase chain reaction was performed with a positive (known species DNA) and negative (No DNA) control using T100 thermal cycler (Bio-Rad Laboratories Inc., Hercules – CA, USA).

The PCR amplification program was set up as:

- initial denaturation at 94 ° C for 4 minutes;

- 35 cycles for the amplification: denaturation of DNA double strands at 95 ° C for 45 seconds, annealing phase at 55 ° C for 45 seconds to pair the primers and DNA synthesis at 72 ° C for 1 minute;
- final elongation of neosynthesised DNA at 72 ° C for 10 minutes.

Table 2.6. Mix with endonucleases Hha I (Cfo I), Hae III and Hinf I for 10 µl of total reaction volume eachone. Enzymatic digestion at 37°C for at least four hours.

Reagent	Brand	Final concentration	Mix volume
Buffer (10 X)	New England Biolab Ltd., United Kingdom	1 X	1 µl
Restriction enzyme (20 U/ µl)	New England Biolab Ltd., United Kingdom	1U	0,05 µl
Sterile and ultrapure water	-	-	3,95 µl
ITS amplified DNA	-	1 µg	5 µl

After the PCR and each enzymatic digestion, a 2.5% W/V agarose (Bio-Rad) gel in 1X TBE buffer was prepared. It was run in 1X TBE buffer electrophoresis at 150 V for 1hour to separate both, PCR and the digestion products using PowerPack Basic (Bio-Rad Laboratories Inc., Hercules - CA, USA). Band sizes were estimated by comparison against a 100 base pair (bp) DNA ladder (NIPPON Genetics Co, Japan) and a blue coloured dye was added to the amplicons before loading. The image acquisition, to identify the bands pattern for each isolate, was accomplished by "GelDoc Go", Gel Imaging System (Bio Rad Laboratories Inc., Hercules - CA, USA) after ethidium bromide staining and visualized under UV light. The images analysis of the electrophoresis gel was performed through BioNumerics™ version 6.6 software (Applied Maths NV,

Sint-Martens-Latem, Belgium).

BioNumerics™ allows the grouping of the isolates according to the DNA profiles and few genotypes per group were analysed through Sanger sequencing method using the ABI prism 310 genetic analyser (Applied Biosystems ®, Waltham – Massachussets). One representative per genotype was molecularly characterised by 26S region sequencing (23, 24, 25).

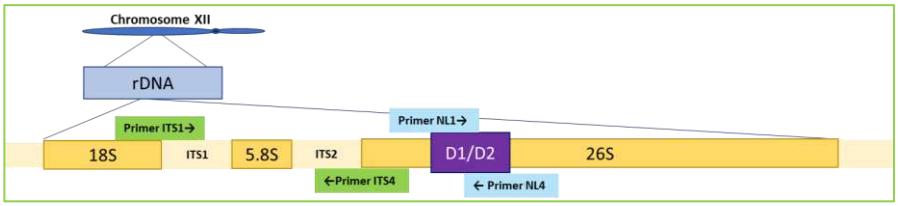

Figure 2.13. The yeast genome region encoding for ribosomal subunits, which show the highest genetic variability used for the species identification. In the image are drawn the primers driving the amplification of ITS region and D1/D2 dominion, respectively: ITS1(5'-TCCGTAGGTGAACCTGCGG-3') and ITS4 (5'-TCCTCCGCTTATTGATA TGC-3'); NL-1 (5'-GCATATCAATAAGCGGAGGAAAAG-3) and NL-4 (5'-GGTCCGTGTTTCAAGACGG-3').

To define the D1/D2 region (26S), characterized of a DNA fragment of approximately 600 bp (27), a PCR reaction was performed using the primers NL1 and NL4 (Fig. 2.13, tab. 2.7). The thermal cycler protocol condition was:

- initial denaturation at 95°C for 5 min;
- 35 cycles: of denaturing at 94°C for 1 min, annealing at 47°C for 1 min. and elongation at 72°C for 2 min;
- final elongation at 72°C for 6 min.

The 600 bp amplicons for each genotype detected, was purified with a handmade protocol (ethanol precipitation), then applied as template for a second PCR called cycle sequencing, using the Big Dye Terminator (BDT) cycle sequencing kit (Applied Biosystems,

Inc.).

The DNA concentration required for the cycle sequencing PCR is of about 10 ng/µl. The estimation of DNA weight was performed by the comparison with a DNA ladder (FastGene 100 bp DNA Marker, NIPPON Genetics Co, Japan), showing 500 bp band dimension, corresponding to a DNA mass of 90 ng/5µl of ladder solution loaded. The cycle sequencing PCR is aimed to substitute normal nucleotides (Adenine, Thymine, Cytosine and Guanine) with di-deoxynucleotide (ddNTPs), that are modified nucleotides differing from the natural ones for the lacking C2 and C3 hydroxylic group. Thus, they prevent the formation of phosphodiester bonds with additional nucleotides and block the DNA strand polymerization. Moreover, during the DNA sequencing reaction, fluorescent markers were attached to the single DNA strains.

Table 2.7. Master mix for Big Dye Terminator PCR for 10 µl of total reaction volume.

Reagent	Brand	Final concentration	Mix volume
Buffer (5 X)	Applied Biosystems™ v3.1 Cycle Sequencing Kit (Massachusetts-USA)	1 X	3,25 µl
Big Dye Terminator	Applied Biosystems™ v3.1 Cycle Sequencing Kit (Massachusetts-USA)	5 X	2 µl
NL 1 (10mM) Forward Primer	Eurofins Genomics, Ebersberg Germany	0,32 µM	0,32 µl
Sterile and ultrapure water	-	-	13,8 µl
template DNA (10ng/ml)	-	10 ng/ µl	1 µl

At the end of the reaction, fragments with different length and with different light signal, depending on the base of incorporated ddNTP after the laser ray excitation, were synthesized. A second handmade

purification step was performed before the capillary electrophoresis. A final denaturation phase consisting in incubation at 95°C for 2 minutes of 5 µl of samples mixed with 10 µl of formamide is necessary for the sequencing through ABI prism 310 genetic analyser (Applied Biosystems®, Waltham – Massachusetts). The sequences, obtained from the signal detected by the instrument and translated into nitrogen bases by the ABI software, were submitted to a Blast analysis on the NCBI platform (https://blast.ncbi.nlm.nih.gov/Blast.cgi). The Blast tool facilitated alignment based on sequence similarity. Results were compared to all libraries available on the NCBI database, and a single species displaying the highest identity percentage with the sequence under study was identified. A similarity of 98% is considered sufficient for species-level identification (28).

3.4.3 Identification of yeast at the end of spontaneous alcoholic fermentation

The identification of the yeast at the end of the spontaneous fermentation concerned the description of the indigenous microflora which can carried on the alcoholic fermentation. Because of *S. cerevisiae* very small presence on the grapes surface, its detection by isolation from the washing suspension was unworkable. Furthermore, *S. cerevisiae* identification by NGS technique was not possible due to the inability of this analysis to identify the microbes in very low concentration. The spontaneous fermentation of the grape must was a suitable strategy to compare the wine yeast from the fifteen sampled bunches (29).

Two bunches were crushed, and 250 ml of must was added into sterile flasks and closed with a silicone Pasteur stopper (Fig 2.14).

The spontaneous fermentation was driven at 24°C and monitored by daily weight loss until the flask weight remained constant, because the alcoholic fermentation (AF) was concluded (30-32).

Figure 2.14. a detail of the "Pasteur cap"; b: an example of weighing to monitor the AF.

The measurement of alcohol production for each fermentation was assessed based on the weight loss (Fig 2.14) using the following formula:

$$\text{Ethanol\% V/V} = \Delta W/V*1.28*100$$

where ΔW is the weight loss (g), V is the volume of fermenting must (ml) and 1.28 is the conversion factor of CO_2 into ethanol, per 100 ml.

At the end of the spontaneous alcoholic fermentation, an aliquot of wine was diluted in sterile saline solution (0,9% NaCl) until 10^{-5} and distributed in triplicate on WL nutrient agar, without antibiotics

nor fungicides. After the colony development (at 25°C for 72h), significant dilutions (20-200 colonies) were considered for the isolation of yeast colonies, as described in paragraph 3.4.2. Twentyfour colonies from a significant dilution were randomly collected and isolated on YEPGA. Their molecular intraspecific identification, within *S. cerevisiae* species, was performed according to Vaudano and Garcia-Moruno method (2008) (33, 34).

Moreover, for each fermentation, an aliquot of wine was collected and stored at -80°C after the addition of glycerol 50% v/v for further analysis.

Table 2.8. Recipe for 20 µl of multiplex PCR mix

Reagent	Brand	Final concentration	Mix volume
DNA polymerase kit (2X)	KAPA2G Fast Multiplex Mix (Roche)	1 X	10 µl
SC8132X Forward Primer	Eurofins Genomics, Ebersberg, Germany	0,25 mM	1 µl
SC8132X Reverse Primer	Eurofins Genomics, Ebersberg, Germany	0,25 mM	1 µl
YOR267C Forward Primer	Eurofins Genomics, Ebersberg, Germany	0,25 mM	1 µl
YOR267C Reverse Primer	Eurofins Genomics, Ebersberg, Germany	0,25 mM	1 µl
SCPTSY7 Forward Primer	Eurofins Genomics, Ebersberg, Germany	0,25 mM	1 µl
SCPTSY7Reverse Primer	Eurofins Genomics, Ebersberg, Germany	0,25 mM	1 µl
Sterile and ultrapure water	-	-	13,8 µl
template DNA	-	100-150 ng/µl	1 µl

Each isolate was processed with microsatellite multiplex PCR (Tab 2.8) using three primers pairs targeting three highly polymorphic microsatellite loci (SC8132×, YOR267C and SCPTSY7) in *S. cerevisiae* species.

This protocol allowed the discrimination of *S. cerevisiae* through

the detection of 100-500 bp length fragments after amplification. On the contrary, no amplifications or amplicons bigger than 500 bp indicate that the DNA was from other species. The occurrence of different strains (genotype) within the species can be assessed. Moreover, non-*S. cerevisiae* strains, occurring at the end of spontaneous fermentation can be identified as described in the previous paragraph according Esteve-Zarzoso et al.1999 protocol (20).

3.5 Yeast characterization through Culture-independent Method

The NGS technique was applied in the (35) metabarcoding analysis of the mycobiota associated to the surface of the berries was performed on microbe cells pelleted as described previously (par.3.3).

DNA extraction and purification was completed by a handmade CTAB (Cetyltrimethylammonium Bromide) treatment starting from a pellet of about 1 mg (36). The pellet was mixed with 0,3 g of glass beads, 800 µl of CTAB (ITW Reagents) extraction buffer, 5 µl 2-Mercaptoethanol (Sigma-Aldrich), 7U/reaction of Lyticase (enzyme from *Bacillus subtilis*, Sigma Aldrich) and incubated at 65°C for 30 minutes to promote the cell wall rupture. Then, to facilitate the release of the nucleic acids Phenol: chloroform: iso-amyl alcohol (25:24:1) ≥ 99% (VWR Chemicals) was added to the mixture proceeding as described above.

The amount of extracted DNA was assessed by spectrophotometer measurement at 260 nm (Beckman Coulter DU700) and its purity evaluated as 260/280 ratio (37).

The primers selection was scrupulous, because yeast ITS region can overlap with ITS region of higher plants. Thanks to the accurate preparation of the washing suspension avoiding the damage of berries, no plant DNA was released in the suspension, and did not affect the NGS analysis. Thus, the analysis was exclusively focused on the whole genome of Fungi communities. Moreover, Primers ITS1 and ITS4 were chosen for their high specificity and coverage of ITS region (38,39).

As recommended by the Illumina protocol, a PCR reaction with a hot start high fidelity DNA polymerase (Roche, Monza, Italy) and the ITS1F and ITS4 R primers (Eurofins Genomics, Ebersberg Germany) was performed to verify the quality of the purified DNA (22,38,39).

The metabarcoding analysis was conducted by IGA Technology service S.r.l., and Illumina procedure was performed. The preparation of the ITS DNA libraries (hypervariable regions ITS1-5.8S-ITS2) was obtained in two amplification steps. An initial PCR amplification using *locus*-specific PCR primers and a subsequent amplification that integrates relevant flow-cell binding domains and unique indices (NexteraXT Index it, FC-131-1001/FC-131-1002, Illumina Inc.). The libraries were sequenced using 300-bp paired-end mode and the processing of the amplicon pool was performed on MiSeq instrument (Illumina Inc., San Diego, CA) (Fig. 2.15).

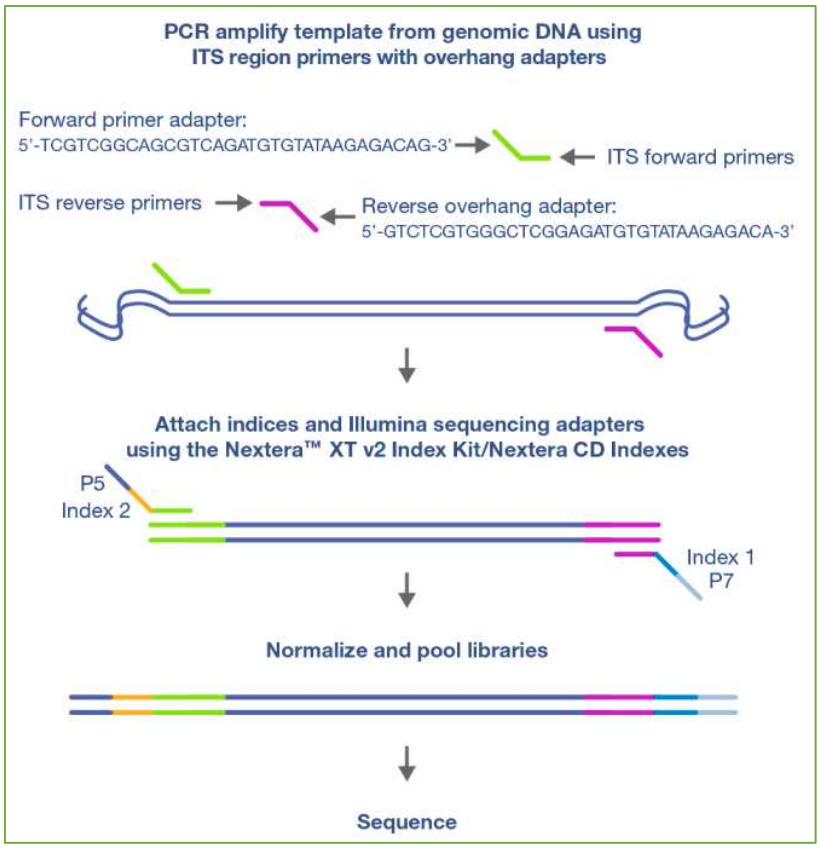

Figure 2.15. Preparation of ITS DNA libraries (modified from: Illumina Fungal sequencing and classification with the ITS Metagenomics Protocol).

3.6 Data analysis and statistics

3.6.1 Culturable Yeast

Yeast count

A viable cell count method was employed to assess cell number, providing abundance at the species level in absolute terms. Colonies with the same morphology were counted from the representative Petri dish, as described above. The overall colony-forming units,

calculated based on the total microorganisms found in each sample, represent the frequency of the species.

Data pertaining to culturable yeast, in terms of CFU per gram on the berry surface or millilitre at the end of AF, underwent statistical analysis using XL-STAT software. Analysis of variance was conducted through an ANOVA test, and any significant differences were assessed using either Fisher's or Tukey's test (32).

Chemical analysis at the end of the spontaneous AF

At the conclusion of spontaneous fermentation to assess the effective alcohol production, each wine was analysed to determine the ethanol percentage (%vol) using the official OIV method for direct distillation (41). The wine was distilled using a Gibertini "Distillatore Elettronico Enochimico" (Gibertini - Novate Milanese (MI), Italy) to extract the alcohol (see Fig. 2.16 a). In the distillation flask, 100 ml of wine was mixed with 5 ml of CaCO3 (calcium carbonate solubilized in water), 3-4 drops of silicone defoamer diluted 1:20, and a splash of distilled water. The distillate was collected into a 100 ml flask, and purified water was added to achieve a volume of 100 ml. Both the wine and the distillate density were measured using the DMA 5000 Anton Paar Density Meter (Anton Paar GmbH – Graz, Austria) (see Fig. 2.16 b). This instrument is a Fourier-transform infrared (FT-IR) spectrometer, which allowed the evaluation of liquid density at 20°C (D20/20), determining the alcohol percentage (%V/V). Using the wine and the distillate density was achieved the total dry matter (g/l) through conversion tables as described in OIV-MA-AS2-03B: R2012 (42). Statistical differences were assessed through a statistical analysis using XL-STAT software.

Figure 2.16. Measure of alcohol content: the distiller Gibertini; b: the DMA 5000 Anton Paar Density Meter; both used for the determination of ethanol percentage in wine.

Image analysis in molecular biology

BioNumerics™ is a database that offers integrated analysis of some applications in Bioinformatics, such as electrophoresis gels, all kinds of chromatographic and spectrometric profiles, phenotype characters, microarrays, and sequences. It is useful to combine information from various genomic and phenotypic sources into one global database and conduct conclusive analyses through the software Applied Maths (site http://www.applied-maths.com/bionumerics) if the case.

A fingerprint type experiment was created in the data base as reference for each parameter according to the RFLP analysis including the ladder DNA.

Yeast identification was achieved by electrophoresis gels picture in "Tiff" extension. All obtained data as band patterns resulting from PCR-RFLP or microsatellite PCR (in some cases DNA sequences)

were added into the database, which contains information regarding all the identified yeasts by the CREA-VE in Asti. Each accession corresponded to a single entry of the database and the data were processed with cluster analysis software.

To grouping the accessions and create a dendrogram according to the similarity of electrophoresis patterns the software performs a Comparison analysis. In the case of the identification at species level the analysis included ITS amplicons and restriction fragment patterns. To compare the accession considering both the amplicons and the three restriction patterns was recommended the choice “Total Fingerprinting” and use the option “average of experiments”. The resulting dendrogram was constructed using the unweighted pair group method with arithmetic mean (UPGMA) algorithm, with a cut-off of 90% similarity for determining species identity. For the differentiation at the strain level of S. cerevisiae, microsatellite profiles were analysed to group genotypes, and the 'Dice coefficient' was selected as the similarity coefficient in the software. The dendrogram resulted from UPGMA algorithm and considering 80% similarity as the cut-off for the strain identification (16). In the software, the cophenetic correlation coefficient was employed to distinguish reliable and unreliable clusters, presented as a biostatistical index in the form of a percentage of identity. The cophenetic correlation coefficient estimates how faithfully a dendrogram preserves the pairwise distances between the original unmodeled data points (43).

ABI software and NCBI platform

The ABI Software for Data Collection stores the raw data from

the DNA sequencing and converts them to DNA sequence data. Sequencing Analysis software considers raw sequencing data and calls bases (*de novo* sequencing). For each detected base, the software assigns four different colours and estimates the robustness of the detection through a graphical representation of histograms. The reliability of the data increases with the height of the histogram, and a base is considered certain if coloured in blue. Then, the software returns the electropherogram obtained by the normalization of the row data highlighting clear peaks.

To assess the efficiency of the sequencing, it is recommended to use M13mp18 as a single-stranded DNA control and pGEM-3Zf(+) as a double-stranded control.

The sequence obtained through the sequencing of the D1/D2 domain (ribosomal DNA, 26S region) is approximately 400-600 bp long and has been used for alignment with sequence libraries based on similarity (23).

On the NCBI platform, the Basic Local Alignment Search Tool (nucleotide BLAST) allows for a basic local alignment based on sequence similarity with GenBank database (25). The query page was filled out with information regarding the nature and origin of the sample, and the desired output options were selected. For species identification, 'Highly similar sequences (megablast)' was applied. To ensure a correct run, certain parameters were provided in the algorithm section, such as the target sequence length (100-500 bp) and the expect threshold (0.05).

Results were compared to all available databases on the platform, and the statistical significance of matches was calculated according to the BLAST algorithm. The species showing the highest identity percentage in terms of base sequence with the submitted one was

selected. The highest percentage of alignment must be chosen, as a 99% overlap in sequences allows for a confident identification at the species level.

3.6.2 Metabarcoding data analysis

Typically, after NGS, data bioinformatic analysis comprises four main steps:

- Processing raw sequencing data to eliminate low-quality reads and sequencing artifacts.
- Using bioinformatics tools to cluster sequences into Operational Taxonomic Units (OTUs) or Amplicon Sequence Variants (ASVs), representing different species or taxa.
- Assigning taxonomic identities to the grouped sequences by comparing them to reference databases.
- Performing statistical analyses to assess the diversity and abundance of taxa within the samples, conducting statistical tests, and generating charts to understand community structure and dynamics.

A full description follows.

After bulk sequencing row reads ('.fastq' format) were demultiplexed based on Illumina indexing system. In cases where the amplicon length was permissive with the respective sequencing length, the 3'-ends of pairs were overlapped to generate consensus pseudo-reads, while the remaining pairs were kept as separate entities. Subsequently, a standard clipping was applied to remove low-quality bases at the 3'-tails. Additionally, any primer sequence at the 5'-ends was deleted and not considered during the process. The reads maintained after this control must have 200bp minimum length. Paired reads allowing overlap at the 3' ends were merged into

a single fragment. The assembled fragment is used to improve the assignment accuracy.

Further filtering of the reads takes place using the QIIME software (44). QIIME pipelines referred at USEARCH algorithm (version 8.1.1756.32-bit, a heuristic algorithm designed to optimize speed) allowed chimera filtering, duplicate sequences clustering, sequences sorting by decreasing abundance, and operational taxonomic unit (OTU) identification (45,46). The OTU picking step aims to cluster query sequences with 97% similarity level (pick-open-reference-otus script from USEARCH algorithm) constituting centroids (or OTUs). The query sequences not sharing similarity with a centroid were discarded. Then representing sequence counts for each centroid were normalized using cumulative sum scaling (CSS, a QIIME tool) to standardize the number of sequences among samples (47). This last step allows the comparison between samples. The clustered sequences (tags) were aligned to the reference database UNITE2016, specific for molecular identification of fungi (48-50). This database provides the access to 1,000,000 public fungal ITS sequences for establishing taxonomic references, annotate taxonomic information based on Blast algorithm (49). Only matches with a minimum identity of 94% were retained and a minimum confidence threshold of 0.50 was used to assign the taxonomy. The sequences from the database were retained as representative sequences of OTUs (53).

The total count of OTUs ('.txt' and '.biom' formats) was retained for the estimation of alpha and beta diversity and of taxonomic abundances and used accordingly for ad-hoc statistical tests.

Further statistics was performed on Microbiome-Analyst software (http://www.microbiomeanalyst.ca/), that in first seps repeats filtering and normalization of the reads. This software operates with

R version 4.0.2 (2020-06-22) (51). Data in BIOM format were loaded on Microbiome-Analyst, where “Marker Data Profiling – MDP” tool consolidated Taxon Set libraries, accessing Phylum, Class, Order, Family, Genus and Species of the yeast found in the samples (52).

Before the analysis, a data integrity check was conducted to ensure that all necessary information was collected. Subsequently, a data filtering process was implemented to enhance the results, by identifying and removing features that are unlikely to be useful in modelling the data. During the filtration step, features (types) with low counts and low variance were removed. Additionally, features with very few counts were filtered based on their abundance levels, with a minimum count threshold of 10 across samples (prevalence). To standardize samples for comparison, a three-step normalization procedure, consisting of data rarefaction, data scaling, and data transformation, was performed. Rarefaction and scaling methods permit to deal with the uneven sequencing depths, ensuring that samples were brought to the same scale for comparison (53,54).

Subsequently the biodiversity estimators can be assessed. Alpha diversity provides insights into the richness and evenness of species in an actual sample. Beta diversity is a measure of biodiversity that assesses the differences in species composition among more distinct samples.

Both alpha and beta diversity estimators and graphs was extrapolated from Microbiome-Analyst using the phyloseq package (53,55,56). Species Richness, representing the total number of observed species, that measures the similarity in terms of abundance of yeast species among the samples, were assessed. The Shannon and Simpson indexes estimate alpha diversity in terms of evenness of fungal community, was considered. The statistical significance

among alpha diversity indexes for groups based on experimental conditions was assessed using the Kruskal-Wallis non-parametric test. The results were plotted across samples and presented as box plots for each considered group (treatment) (53,55,56).

Beta diversity analysis was conducted by measuring the dissimilarity (distance) between samples. Each sample was compared to every other sample, generating a distance matrix. Utilizing Bray-Curtis distance and Principal Coordinate Analysis (PCoA), it was possible to visualize these matrices in a 2-D plot, where each point represents the entire mycobiome of a single sample.

Each axis on the PCoA plot reflects the percentage of variation between the samples, with the X-axis representing the highest dimension of variation and the Y-axis representing the second-highest dimension. Each point (sample) displayed on the PCoA plots is color-coded based on its adhering treatment. Additionally, the statistical significance of the clustering pattern in ordination plots can be evaluated using Permutational ANOVA (PERMANOVA) (55).

Hierarchical cluster analysis was conducted at the species level. In this analysis, each sample initially starts as a separate cluster, and the algorithm proceeds to combine them until all samples belong to one cluster. Two key parameters were considered:

i) Distance Metric: this metric quantifies the dissimilarity or the distance between data points (samples).

ii) Clustering Algorithm: Ward's Method was employed, minimizing the variance within each cluster (the sum of squares of any two clusters). This method determines how distances between clusters are calculated.

The hierarchical clustering was performed using the 'hclust' function in the 'stat' package of Microbiome-Analyst. The results are

presented as a heatmap, with the distance measure using Euclidean matrix and clustering algorithm using 'ward.D' at the OTU level.

Heat tree method was used to compare abundance at species level. Heat tree uses hierarchical structure of taxonomic classifications to depict quantitatively and statistically the taxon differences among fungi communities. The quantitative data refers to the median abundance and the non-parameter statistical test Wilcoxon Rank Sum was applied, comparing one pair of theses at a time. The resulting differential heat tree indicates which species are more abundant in the different considered treatments. Heat tree analysis was performed using metacoder R package, according to Foster (55).

The analysis of the core microbiome was conducted to identify species on the berry skin that remained consistent in their composition across the entire fungal community in different treatment (57,58). The analysis utilized the 'core' function in the microbiome R package. The results of this analysis are presented in the form of a heatmap of core taxa. The Y-axis represents the prevalence level of core features, while the X-axis represents the detection threshold range (Relative abundance). In addition, Principal Component Analysis (PCA) was conducted, considering all the parameters and based on the factor 'sampling site.' The analysis was performed using R (version 3.5.1) with the FactoMineR and Facto extra packages (58,59). PCA is a statistical method used to emphasize variation and bring out strong patterns in a dataset. In this context, it helps discern patterns and relationships among various parameters in relation to the 'sampling site' factor.

For biomarker discovery and elucidation, we applied the Linear Discriminant Analysis Effect Size (LDA-LEfSe) method at the species level. This method combines statistical significance and

biological consistency in high-dimensional metagenomic data. It employs a non-parametric Kruskal-Wallis test for identifying species with significantly differential abundance concerning the factor of interest (treatment). Subsequently, Linear Discriminant Analysis (LDA) is employed to estimate the effect size of each differentially abundant feature. The outcomes include species with the highest mean and logarithmic LDA score (Effect Size), with significance determined by adjusted p-values (default cut-off: 0.05) (8,60).

REFERENCES

(1) Meteorological data provided by personal communication from Dr. Cristiana Monferrato of Agenzia Regionale per la Protezione Ambientale (ARPA), Piemonte

(2) ISPRA web site: https://www.isprambiente.gov.it/it/pubblicazioni/stato-dellambiente/gli-indicatori-del-clima-in-italia-nel-2019-2013-anno-xv : Fioravanti, G.; Fraschetti, P.; Lena, F.; Perconti, W.; Piervitali, E.; Pavan, V. (2020) ISPRA Stato dell'Ambiente 94/2020 - Gli indicatori del Clima in Italia nel 2019-anno XV; Istituto Superiore per la Protezione e la Ricerca Ambientale. ISBN978-88-448-0998-0 (accessed in September 2020)

(3) Historical notions on European Centre for Medium-Range Weather Forecasts (ECMWF) available on line at: https://www.ecmwf.int/ (accessed in Sptember 2022)

(4) Meteorological data downloaded from ERA5-Land platform: https://www.ecmwf.int/en/era5-land, provided by personal communication from Dr. Alessandro Dell'Aquila of Agenzia nazionale per le nuove tecnologie, l'energia e lo sviluppo economico sostenibile (ENEA).

(5) Gazzetta Ufficiale della repubblica web site: Ministero delle Politiche Agricole e Forestali, Decreto Ministeriale 13/09/1999 Metodi ufficiali di analisi chimica del suolo: https://www.gazzettaufficiale.it/eli/gu/1999/10/21/248/so/185/sg/pdf (accessed in September 2021)

(6) Soil texture triangle according to United States Department of

Agriculture (USDA): https://soilsensor.com/articles/soil-textures/ (accessed in June 2022)

(7) Sparks, D. L. (Ed.). (1998). Soil physical chemistry. CRC press.

(8) Yunan, D.; Xianliang, Q.; Xiaochen, W. Study on Cation Exchange Capacity of Agricultural Soils. IOP *Conf. Ser. Mater. Sci. Eng*. 2018, 717 392, 042039, DOI:10.1088/1757-899X/392/4/042039

(9) Freeman, B. M.; Kliewer, A W. M. (1983) Effect of Irrigation, Crop Level and Potassium Fertilization on Carignane Vines. II. Grape and Wine *Quality. Am. J. Enol. Vitic.* V 34, N 3: pp 197-207. DOI: 10.5344/ajev.1983.34.3.197

(10) Fregoni M. *Viticoltura di qualità. Trattato di eccellenza da terroir*, 3rd ed.; Tecniche Nuove: Milano, Italy, 2013; pp. 519–521. ISBN 978-88-481-7919-5

(11) Food and Agriculture Organization of the United Nation (FAO) web site: https://www.fao.org/family-farming/detail/en/c/327688/ (accessed in October 2022)

(12) Integrated Crop Management, Policy Support Guidelines for the Promotion of Sustainable Production Intensification and Ecosystem Services (2013) Vol. 19 available at: http://www.fao.org/3/a-i3506e.pdf (accessed in October 2022)

(13) Ramírez, M.; López-Piñeiro, A.; Velázquez, R.; Muñoz, A.; Regodón, J.A. (2020) Analysing the vineyard soil as a natural reservoir for wine yeasts. *Food Res. Inter*. 129, 108845. DOI: 10.1016/j.foodres.2019.108845

(14) Miliordos, D.E.; Galetto, L.; Ferrari, E.; Pegoraro, M.; Marzachì, C.; Bosco, D. (2017) Acibenzolar-S-methyl may prevent vector-mediated flavescence dorée phytoplasma transmission, but is ineffective in inducing recovery of infected grapevines. *Pest. Manag. Sci*. 73, 534–540. DOI: 10.1002/ps.4303

(15) Ripamonti, M.; Pegoraro, M.; Rossi, M.; Bodino, N.; Beal, D.; Panero, L.; Marzachì, C.; Bosco, D. (2020) Prevalence of Flavescence Dorée Phytoplasma-Infected *Scaphoideus Titanus* in Different Vineyard Agroecosystems of Northwestern Italy. *Insects.* 11, 301. DOI: 10.3390/insects11050301

(16) Vaudano, E.; Quinterno, G.; Costantini, A.; Pulcini, L.; Pessione, E.; Garcia-Moruno, E. (2019) Yeast Distribution in Grignolino Grapes Growing 684 in a New Vineyard in Piedmont and the Technological Characterization of Indigenous Saccharomyces Spp. Strains. *Int. J. Food Microbiol*. 289, 154–161. DOI: 10.1016/j.ijfoodmicro.2018.09.016.

(17) Zhang, J.; Wang, E.T.; Singh, R.P.; Guo, C.; Shang, Y.; Chen, J.; Liu, C. (2019) Grape Berry Surface Bacterial Microbiome: Impact from the Varieties and Clones in the Same Vineyard from Central China. *J. Appl. Microbiol*. 126, 204–214. DOI:10.1111/jam.14124.

(18) Barata, A.; Malfeito-Ferreira, M.; Loureiro, V. (2012) The Microbial Ecology of Wine Grape Berries. *Int. J. Food Microbiol*. 153, 243–259. DOI: 10.1016/j.ijfoodmicro.2011.11.025.

(19) Polizzotto, G.; Barone, E.; Ponticello, G.; Fasciana, T.; Barbera, D.; Corona, O.; Amore, G.; Giammanco, A.; Oliva, D. (2016) Isolation, identification and oenological characterization of non-*Saccharomyces* yeasts in a Mediterranean island. *Lett. Appl. Microbiol*. 63(2), pp 131-138. DOI: 10.1111/lam.12599

(20) Esteve-Zarzoso, B., C. Belloch, F. Uruburu, A. Querol, (1999) "Identification of yeasts by RFLP analysis of the 5.8S rRNA gene and the two ribosomal internal transcribed spacers", *International Journal od Systematic Bacteriology*, 49, 329-337. DOI:10.1099/00207713-49-1-329

(21) Cocolin, L., N. Innocente, M. Biasutti, G. Comi (2004) "The late blowing in cheese: a new molecular approach based on PCR and DGGE to study the microbial ecology of the alteration process" *International Journal of Food Microbiology*, 90 (1): 83-9. DOI: 10.1016/S0168-1605(03)00296-4

(22) White, T. J., Bruns, T., Lee, S., & Taylor, J. (1990) A guide to methods and applications: Amplification and direct sequencing of fungal ribosomal RNA genes for phylogenetics. In PCR protocols; Innis, M.A., Gelfand, D.H., Sninsky, J.J. & White, T.J. Eds. Academic Press, Inc.: San Diego, California; pp. 315–322.

(23) Kurtzman, C.P. and Robnett, C.J. (1998) Identification and Phylogeny of Ascomycetous Yeasts from Analysis of Nuclear Large Subunit (26S) Ribosomal DNA Partial Sequences. *Antonie van Leeuwenhoek*, 73, 331-371. DOI: 10.1023/A:1001761008817

(24) KAWAHATA, M.; FUJII, T.; IEFUJI, H. (2007) Intraspecies Diversity of the Industrial Yeast Strains Saccharomyces cerevisiae and Saccharomyces pastorianus Based on Analysis of the Sequences of the Internal Transcribed Spacer (ITS) Regions and the D1/D2 Region of 26S rDNA, *Bioscience, Biotechnology, and Biochemistry*, 71:7, 1616-1620, DOI: 10.1271/bbb.60673

(25) Hesham, A.E.-L.; Wambui, V.; Ogola J.O., H.; Maina, J.M. (2014) Phylogenetic analysis of isolated biofuel yeasts based on 5.8S-ITS rDNA and D1/D2 26S rDNA sequences. J. Gen. Eng. Biotec. V. 12, I. 1: pp 37-43. DOI: 10.1016/j.jgeb.2014.01.001

(26) Walker, G.M. Yeasts (2009) Editor(s): Moselio Schaechter, Encyclopedia of Microbiology (Third Edition), Academic Press, Pages 478-491. ISBN 9780123739445. DOI: 10.1016/B978-012373944-5.00335-7

(27) Romanelli, A. M.; Fu, J.; Herrera, M. L.; Wickes, B. L. (2014). A universal DNA extraction and PCR amplification method for fungal rDNA sequence-based identification. *Mycoses*, *57*(10), 612-622. DOI: 10.1111/myc.12208

(28) Costantini A.; Vaudano, E.; Pulcini, L.; Boatti, L.; Gamalero, E.; Garcia-Moruno, E. (2022) Yeast Biodiversity in Vineyard during Grape Ripening: Comparison between Culture Dependent and NGS Analysis. *Processes.* 10(5), 901. DOI: 10.3390/pr10050901

(29) Costantini, Antonella, Maria Carla Cravero, Loretta Panero, Federica Bonello, Enrico Vaudano, Laura Pulcini, and Emilia

Garcia-Moruno. (2021) Wine Fermentation Performance of Indigenous *Saccharomyces cerevisiae* and *Saccharomyces paradoxus* Strains Isolated in a Piedmont Vineyard *Beverages* 7, no. 2: 30. DOI: 10.3390/beverages7020030

(30) Capece, A.; Romaniello, R.; Siesto, G.; Pietrafesa, R.; Massari, C.; Poeta, C.; Romano, P. (2010) Selection of indigenous Saccharomyces cerevisiae strains for Nero d'Avola wine and evaluation of selected starter implantation in pilot fermentation. *International Journal of Food Microbiology*. 144(1):187-92. DOI: 10.1016/j.ijfoodmicro.2010.09.009

(31) Capece, A.; Romaniello, R.; Siesto, G.; Romano, P. (2012) Diversity of Saccharomyces cerevisiae yeasts associated to spontaneously fermenting grapes from an Italian "heroic vine-growing area". Food Microbiology, 31:159-166. DOI:10.1016/j.fm.2012.03.010

(32) Capece; A.; Pietrafesa, R.; Siesto, G.; Romaniello, R.; Condelli, N.; Romano, P. (2019) Selected Indigenous Saccharomyces cerevisiae Strains as Profitable Strategy to Preserve Typical Traits of Primitivo Wine. *Fermentation*. 5, no. 4: 87. DOI: 10.3390/fermentation5040087

(33) Vaudano, E.; Garcia-Moruno, E. (2008) Discrimination of Saccharomyces cerevisiae wine strains using microsatellite multiplex PCR and band pattern analysis. *Food Microbiology.* 25: 56–64. DOI:10.1016/j.fm.2007.08.001

(34) Legras, J.-L.; Ruh, O.; Merdinoglu, D.; Karst, F. (2005) Selection of hypervariable microsatellite loci for the

characterization of *Saccharomyces cerevisiae* strains. *International Journal of Food Microbiology*, 102(1): 73-83. DOI: 10.1016/j.ijfoodmicro.2004.12.007

(35) Shendure, J., Ji, H. (2008) Next-generation DNA sequencing. *Nat Biotechnol* 26, 1135–1145. DOI: 10.1038/nbt1486

(36) Cerutti, F.; Cravero, D.; Costantini, A. Pulcini, L.; Modesto, P.; Acutis, P.; Vaudano, E.; Peletto, S. (2019) Impact of DNA purification method and primer selection on 16S rRNA gene metabarcoding on wine. *OENO One*; 53. DOI: 10.20870/oeno-one.2019.53.3.2368

(37) Işçi, B.; Yildirim, K.; H. and Altindisli, A. (2014) Evaluation of methods for DNA extraction from must and wine. *J. Inst. Brew*. 120: 238–243. DOI: 10.1002/jib.129

(38) Scibetta, S.; Schena, L.; Abdelfattah, A.; Pangallo, S.; Cacciola, S.O. (2018) Selection and Experimental Evaluation of Universal Primers to Study the Fungal Microbiome of Higher Plants. *Phytobiomes Journal*; 2(4): 225-236. DOI: 10.1094/PBIOMES-02-18-0009-R

(39) Usyk, M., C.P Zolnik, H. Patel, M.H. Levi, R.D. Burk (2017) Novel ITS1 fungal primers for characterization of the mycobiome. *mSphere2*: e00488-17. DOI:10.1128/mSphere.00488-17.

(40) Illumina Fungal sequencing and classification with the ITS Metagenomics Protocol available on line at Illumina website: https://www.illumina.com; https://www.illumina.com/content/dam/illumina-

marketing/documents/products/appnotes/its-metagenomics-app-note-1270-2018-001-web.pdf (accessed in May 2023)

(41) Official International Organisation of Vine and Wine (OIV) method for Alcoholic strength by volume at 20 °C, OIV-MA-AS312-01A: R2016 available on line at: https://www.oiv.int/standards/revision-of-the-method-oiv-ma-as312-01a%3A-alcoholic-strength-by-volume-at-20%C2%A0%C2%B0c (accessed in January 2023)

(42) Official International Organisation of Vine and Wine (OIV) method for Dry matter OIV-MA-AS2-03B: R2012 https://www.oiv.int/public/medias/2471/oiv-ma-as2-03b.pdf (accessed in January 2023)

(43) Rossetti, L. & G.,Giraffa (2005) Rapid identification of dairy lactic acid bacteria by M13-generated, RAPD-PCR fingerprint databases. J. Microbiol. Methods 63, 135–144.

(44) Miura, T.; Sánchez, R.; Castañeda, L.E.; Godoy, K. and Barbosa, O. (2017), Is microbial terroir related to geographic distance between vineyards? *Environmental Microbiology Reports*, 9: 742-749. DOI: 10.1111/1758-2229.12589

(45) Edgar RC. (2017) Accuracy of microbial community diversity estimated by closed- and open-reference OTUs. *PeerJ* 5: e3889. DOI: 10.7717/peerj.3889

(46) Edgar, R. (2010). Search and clustering orders of magnitude faster than BLAST. Bioinformatics 26, 2460–2461. doi: 10.1093/bioinformatics/ btq461 USearch, version 6.0.307

(47) Paulson, J.N., Stine, O.C., Bravo, H.C., and Pop, M. (2013) Differential abundance analysis for microbial marker-gene surveys. Nat Methods 10: 1200–1202.

(48) Nilsson, R.H.; Larsson, K.-H.; Taylor, A. F. S.; Bengtsson-Palme, J.; Jeppesen, T.S; Schigel, D.; Kennedy, P.; Picard, K.; Glöckner, F.O.; 697 Tedersoo, L.; Saar, I.; Kõljalg, U.; Abarenkov, K. (2019) The UNITE database for molecular identification of fungi: handling dark taxa and parallel 698 taxonomic classifications, Nucleic Acids Res. 47 (D1), D259–D264. DOI:10.1093/nar/gky1022

(49) Jayawardena, R.S.; Purahong, W.; Zhang, W. et al. (2018) Biodiversity of fungi on *Vitis vinifera* L. revealed by traditional and high-resolution culture-independent approaches. *Fungal Diversity.* 90, 1–84. DOI: 10.1007/s13225-018-0398-4

(50) Abarenkov, K.; Henrik Nilsson, R.; Larsson, K.-H.; Alexander, I.J.; Eberhardt, U.; Erland, S.; et al. (2010) The UNITE database for molecular identification of fungi– recent updates and future perspectives. *New Phytol* 186: 281–285.

(51) Dhariwal, A. et al. MicrobiomeAnalyst - a web-based tool for comprehensive statistical, visual and meta-analysis of microbiome data. *Nucl. Acids Res*. 45, W180–188, DOI: 10.1093/nar/gkx295 (2017).

(52) Weiss, S.; Xu, Z.Z.; Peddada, S.; Amir, A.; Bittinger, K.; Gonzalez, A.; Lozupone, C.; Zaneveld, J.R.; Vázquez-Baeza, Y.; Birmingham, A.; et al. (2017) Normalization and Microbial Differential Abundance Strategies Depend upon Data

Characteristics. *Microbiome.* 5, 27. doi:10.1186/s40168-017-0237-y

(53) Chong, J.; Liu, P.; Zhou, G.; Xia, J. (2020) Using MicrobiomeAnalyst for comprehensive statistical, functional, and meta-analysis of microbiome data. *Nat. Protoc*. 15, 799–821. doi:10.1038/s41596-019-0264-1

(54) Paul, D. (2013) Osmotic Stress Adaptations in Rhizobacteria: Osmotic Stress Adaptations in Rhizobacteria. *J. Basic Microbiol*. 53, 101– 705. DOI:10.1002/jobm.201100288.

(55) Foster, Z.S.L.; Sharpton, T.J.; Grünwald, N.J. (2017) Metacoder: An R Package for Visualization and Manipulation of Community Taxonomic Diversity Data. *PLoS Comput. Biol*., 13, e1005404. DOI: 10.1371/journal.pcbi.1005404

(56) Neu, A.T.; Allen, E.E.; Roy, K. (2021) Defining and Quantifying the Core Microbiome: Challenges and Prospects. *Proc. Natl. Acad. Sci*. 118, e2104429118. DOI: 10.1073/pnas.2104429118

(57) The R Development Core Team. R: A Language and Environment for Statistical Computing; R Foundation for Statistical Computing: Vienna, Austria, 2018.

(58) Lê, S.; Josse, J.; Husson, F. (2008) FactoMineR: An R Package for Multivariate Analysis. *J. Stat. Softw*., 25, DOI:10.18637/jss.v025.i01.

(59) Kassambara, A.; Mundt, F. Package “Facto Extra” 2016.

(60) Segata, N.; Boernigen, D.; Tickle, T.L.; Morgan, X.C.; Garrett,

W.S.; Huttenhower, C. Computational Meta'omics for Microbial Community Studies. Mol. Syst. Biol. 2013, 9, 666, doi:10.1038/msb.2013.22

Chapter IV

Exploring the mycobiota of *Vitis vinifera* cv. Barbera grape berry

4. Exploring the mycobiota of *Vitis vinifera* cv. Barbera grape berry

This section details the fungal microbiota occurring on grape bunches, following the experimental design outlined in Chapter 3. The data encompass the examination of cultivable yeasts discovered on the berry skin and the investigation of fungal biodiversity on the berry surface through a metagenomic approach.

4.1 Culturable yeast on the berry skin

To assess the impact of the three experimental conditions on yeast abundance on grape surfaces, triplicate counts of culturable yeast were performed (tab. 4.1). Variance statistical analysis was carried out using XL-STAT software to estimate the influence of treatments on the yeast population in the three parcels: Control (C), Bion (B) and Water (W) (1; 2; 3) (Fig.4.1).

Data and figures relatives to the total count of the yeast on WLD medium, and tables and graphs on descriptive statistics are reported here below.

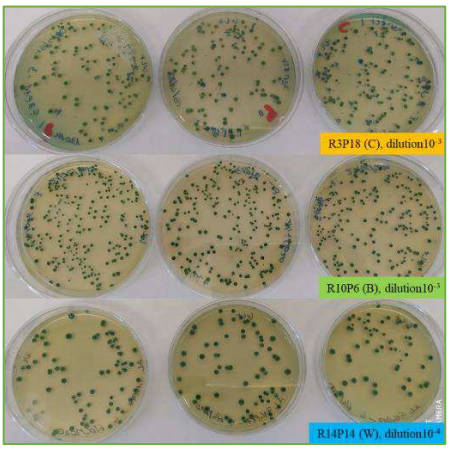

Figure 4.1. Pictures of the significant plates, containing 20-200 yeast colonies.

The descriptive statistics parameters of the 45 observations are reported in Table 4.1.

Table 4.1. Data recorded on the yeast count. Total count per millilitre derived from the count onto WLD plates. Data referred as CFU per gram have been calculated on grape weight.

treatment	samples	replicates	Total Count per millilitre (CFU/ml)	Total count per gram (CFU/g)
C	R3P18	1	2,60E+05	7,80E+05
C	R3P18	2	2,56E+05	7,68E+05
C	R3P18	3	3,56E+05	1,07E+06
C	R5P8	1	9,00E+04	2,70E+05
C	R5P8	2	4,60E+04	1,38E+05
C	R5P8	3	4,20E+04	1,26E+05
C	R6P11	1	6,00E+04	1,80E+05
C	R6P11	2	6,60E+04	1,98E+05
C	R6P11	3	5,00E+04	1,50E+05
C	R7P13	1	5,60E+04	1,68E+05
C	R7P13	2	4,40E+04	1,32E+05
C	R7P13	3	4,80E+04	1,44E+05
C	R8P1	1	1,62E+06	4,86E+06
C	R8P1	2	1,20E+06	3,60E+06
C	R8P1	3	1,58E+06	4,74E+06
B	R9P3	1	5,08E+06	1,52E+07
B	R9P3	2	1,14E+07	3,41E+07
B	R9P3	3	5,42E+06	1,63E+07
B	R9P11	1	3,60E+05	1,08E+06
B	R9P11	2	4,00E+05	1,20E+06
B	R9P11	3	4,40E+05	1,32E+06
B	R10P6	1	5,40E+05	1,62E+06
B	R10P6	2	1,12E+06	3,36E+06
B	R10P6	3	8,60E+05	2,58E+06
B	R10P16	1	1,80E+05	5,40E+05
B	R10P16	2	2,40E+05	7,20E+05
B	R10P16	3	3,40E+05	1,02E+06
B	R11P7	1	1,40E+05	4,20E+05
B	R11P7	2	1,80E+05	5,40E+05
B	R11P7	3	1,80E+05	5,40E+05
W	R13P6	1	1,68E+06	5,04E+06
W	R13P6	2	1,68E+06	5,04E+06
W	R13P6	3	1,36E+06	4,08E+06
W	R13P13	1	1,00E+05	3,00E+05

W	R13P13	2	1,00E+05	3,00E+05
W	R13P13	3	1,40E+05	4,20E+05
W	R13P23	1	2,40E+06	7,20E+06
W	R13P23	2	2,02E+06	6,06E+06
W	R13P23	3	1,92E+06	5,76E+06
W	R14P9	1	1,60E+05	4,80E+05
W	R14P9	2	4,00E+05	1,20E+06
W	R14P9	3	4,40E+05	1,32E+06
W	R14P17	1	1,02E+06	3,06E+06
W	R14P17	2	5,40E+05	1,62E+06
W	R14P17	3	4,80E+05	1,44E+06

As depicted in the histogram in Figure 4.1, the sample R9P3, a biological replicate of the Bion treatment, stands out as an outlier, indicating a higher microbial load compared to the other four samples in the same group.

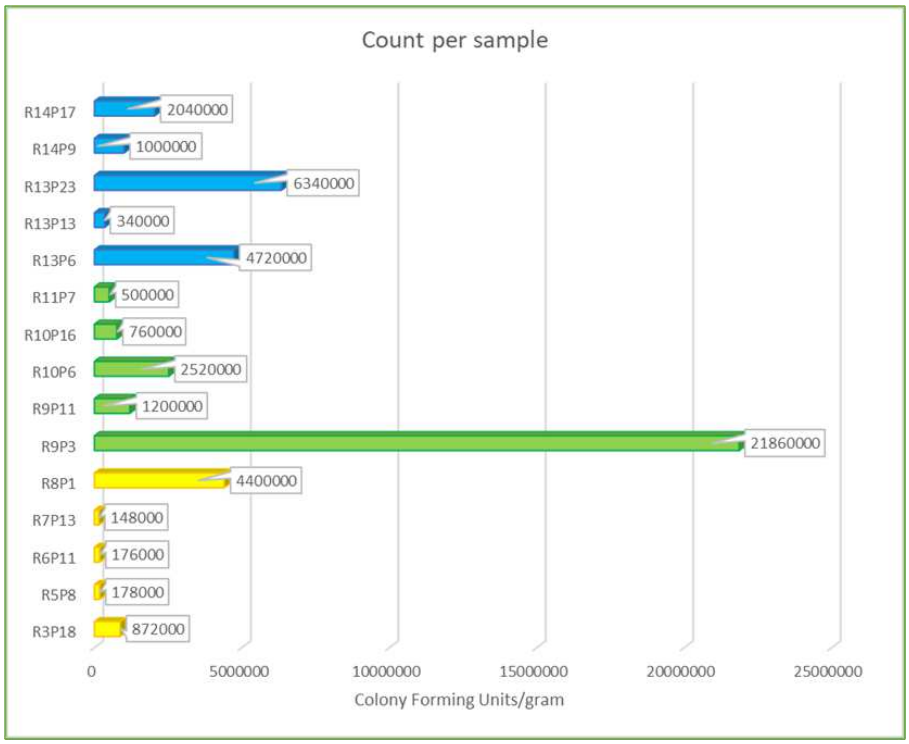

Figure 4.1. The graph illustrates the microbial density of all the samples, as mean among three counts. (blue: treatment Water; green: treatment Bion; yellow: treatment Control)

Upon the examination of the five biological replicates per treatment (or group), it was evident that there was no numerical consistency among samples within each group (Tab 4.2). Furthermore, no discernible trend characterizes the treatments.

Table 4.2. Data are referred to a gram of grape.

minimum (CFU/g)	maximum (CFU/g)	mean (CFU/g)	stad. Dev. (CFU/g)
1,26E+05	3,41E+07	3,14E+06	5,86E+06

Excluding the observation on the outlier sample, the ANOVA statistical results indicate no significant differences in yeast abundance among the means of the three groups (F>α) (Tab 4.3).

Table 4.3. ANOVA statistics results. No significant differences in yeast abundance among the samples are observed. (level of confidence: 95%; tolerance: 0,0001; df: degrees of freedom; α: 0.05)

Source	df	Sum of squares	Mean of squares	F
Model	14	1280485460800000.000	91463247199999.900	11.879
Error	30	230995512000002.000	7699850400000.060	
adjusted total Sum of squares	44	1511480972800000.000		

For each sampled grape, yeast morphology was described according to Polizzotto et al. (2016) (2) to characterize the culturable fraction, as outlined in Vaudano et al. (2019) (1). Among the three biological replicates, the one with the highest richness in morphologies was considered. The colonies displayed a high degree of similarity, appearing mostly circular and of a dark green hue. Despite utilizing WL medium, identification errors based on colony morphology can occur, prompting the need for molecular analyses. Consequently, for molecular analyses, a randomized sampling approach was employed, covering at least 10% of the colonies counted on the significant plate.

This strategy aimed to characterize the yeast population on the grape peel through a representative sample. The yeast species identification was primarily assessed through the CREA-VE database stored in BioNumerics™. In cases where the database did not allow identification, 26S sequencing was performed for accurate species-level identification. Additionally, the results of isolate RFLP analysis, including cluster analysis conducted with BioNumerics™, are presented.

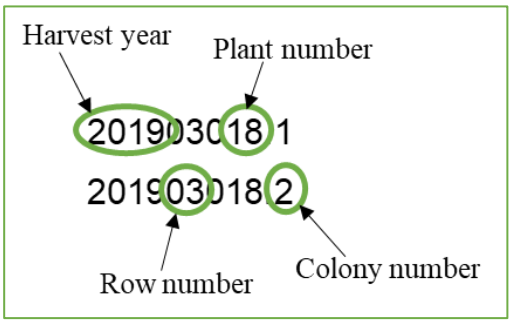

Figure 4.2. The denomination of the isolate in BioNumerics™ *database.*

The isolate under study, "entry" in database, was named as illustrated in Figure 4.2. At the conclusion of the culturable yeast description, the 26S sequences are provided, facilitating the identification of isolates at the species level.

R3P18 (Control)

Table 4.4. Data recorded on the morphological features of R3P18C (dilution 10^{-4}). Total count per millilitre derived from the count onto WLD plates. The morphology frequency is expressed as a percentage of the total count.

Morphological features (form, elevation, margin, colour, etc.)	Number per morphology	Total count (CFU/ml)	**Frequency %** (n. morph./total count)

Circular, dark green, irregular margin, opaque, raised, clear halo	13	25	52%
Irregular, raised, green, opaque	2		8%
Circular, dark green, entire margin, opaque, raised	10		40%

After the morphological description, a random sampling from the WLD plate was performed, and RFLP analysis was conducted on 29 isolates.

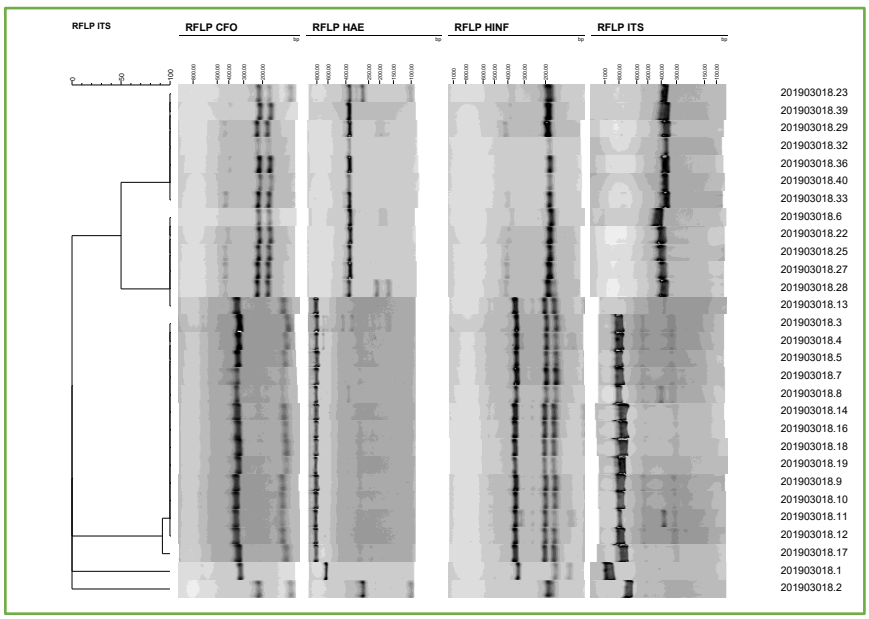

Figure 4.3. R3P18C. RFLP patterns, including ITS amplification bands and digestion profiles using Hha I (Cfo I), Hae III, and Hinf I enzymes, analysed and clustered using BioNumerics™ version 6.6 software. This sample exhibits two prevalent genotypes.

Following the grouping based on RFLP molecular profiles, the unidentified isolate was sequenced on the D1/D2 region of the 26S DNA fragment.

- 15/29 isolates analysed belong to *Hanseniaspora uvarum* species.

- 12/29 isolates analysed belong to *Candida diversa.*
- 1/29 isolates analysed belong to *Wickerhamomyces anomalus.*
- 1/29 isolates analysed belong to *Torulaspora* sp.

R5P8 (Control)

Table 4.5 Data recorded on the morphological features of R5P8C (dilution 10^{-3}). Total count per millilitre derived from the count onto WLD plates. The morphology frequency is expressed as a percentage of the total count.

Morphological features (form, elevation, margin, colour, etc.)	Number per morphology	Total count (CFU/ml)	**Frequency %** (n. morph./total count)
Circular, light green, crater profile, wrinkled surface, undulate margin, opaque	1	45	2.2%
Circular, light green, wrinkled surface, opaque, green-red underneath	2		4.4%
Circular, dark green, shiny, entire margin, convex, creamy	19		42.2%
Circular, dark green, undulate margin, clear halo, opaque	20		44.4%
Circular, light green, shiny, pulvinate	3		6.6%

After the morphological description, a random sampling from the WLD plate was performed, and RFLP analysis was conducted on 20 isolates.

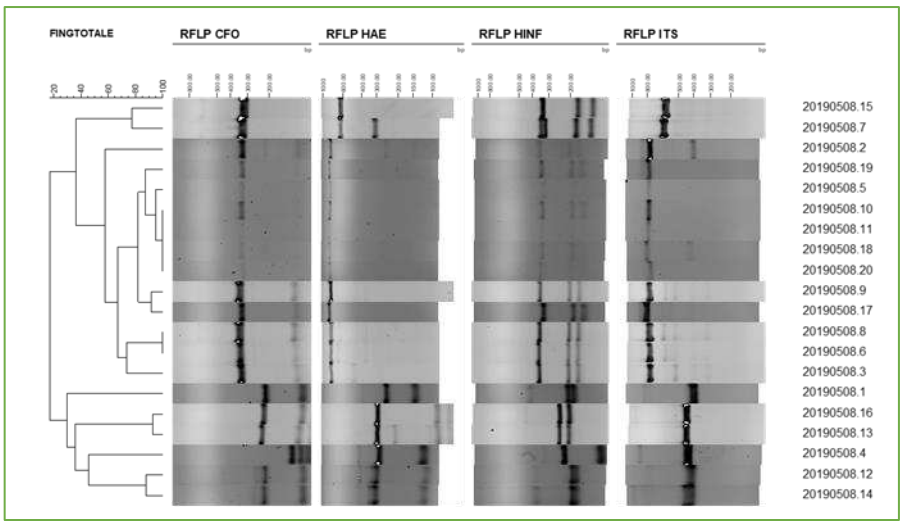

Figure 4.4. R5P8C. RFLP patterns, including ITS amplification bands and digestion profiles using Hha I (Cfo I), Hae III, and Hinf I enzymes, analysed and clustered using BioNumerics™ version 6.6 software. This sample exhibits two prevalent genotypes.

Following the grouping based on RFLP molecular profiles, the unidentified isolate was sequenced on the D1/D2 region of the 26S DNA fragment.

- 12/20 isolates analysed belong to *Hanseniaspora uvarum* species.
- 2/20 isolates analysed belong to *Pichia membranifaciens.*
- 3/20 isolates analysed belong to *Candida magnoliae.*
- 1/20 isolates analysed belong to *Torulaspora* sp.
- 1/20 isolates analysed belong to *Saccharomycodes ludvigii*.
- 1/20 isolates analysed belong to *Aureobasidium pullulans*.

R6P11 (Control)

Table 4.6. Data recorded on the morphological features of R6P11C (dilution 10^{-2}). Total count per millilitre derived from the count onto WLD plates. The morphology frequency is expressed as a percentage of the total count.

Morphological features (form, elevation, margin, colour, etc.)	Number per morphology	Total count (CFU/ml)	**Frequency %** (n. morph./total count)
Circular, concentric, light green, convex, undulate margin, opaque, creamy	2	38	5.3%
Circular, white, umbonate, opaque, undulate margin, streaked green-red underneath	1		2.6%
Circular, green, opaque, convex, entire margin, buttery texture	1		2.6%
Circular, convex, light green, entire margin, opaque	1		2.6%
Circular punctiform, pulvinate, dark green, shiny, entire margin	7		18.4%
Irregular, undulate margin, umbonate, dark green, opaque, creamy, white halo	13		34.2%
Circular, entire margin, pulvinate, bullous profile, light green, creamy	2		5.3%
Dark green, circular, umbonate, white halo, opaque, creamy	11		30%

After the morphological description, a random sampling from the WLD plate was performed, and RFLP analysis was conducted on 27 isolates.

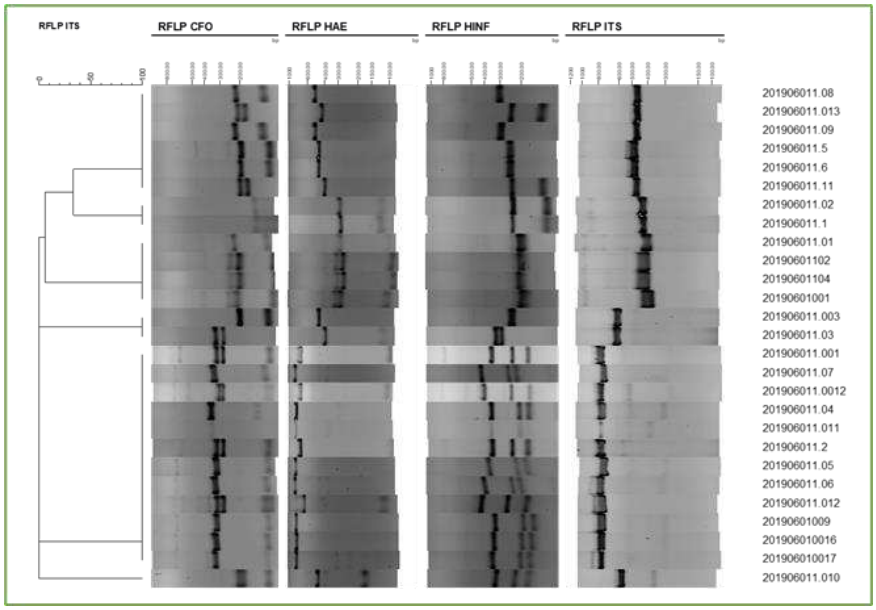

Figure 4.5. R6P11C. RFLP patterns, including ITS amplification bands and digestion profiles using Hha I (Cfo I), Hae III, and Hinf I enzymes, analysed and clustered using BioNumerics™ version 6.6 software. This sample exhibits two prevalent genotypes.

Following the grouping based on RFLP molecular profiles, the unidentified isolate was sequenced on the D1/D2 region of the 26S DNA fragment.

- 4/27 isolates analysed belong to *Metschnikowia pulcherrima* species.
- 2/27 isolates analysed belong to *Pichia terricola* (*Issatchenkia terricola*).
- 8/27 isolates analysed belong to *Hanseniaspora uvarum*.
- 4/27 isolates analysed belong to *Zygosaccharomyces bailii*.
- 1/27 isolates analysed belong to *Aureobasidium pullulans.*
- 2/27 isolates analysed belong to *Pichia* sp.
- 3/27 isolates analysed belong to *Candida bombicola*.
- 3/27 isolates analysed belong to *Pichia delftensis.*

R7P13 (Control)

Table 4.7. Data recorded on the morphological features of R7P13C (dilution 10^{-3}). Total count per millilitre derived from the count onto WLD plates. The morphology frequency is expressed as a percentage of the total count.

Morphological features (form, elevation, margin, colour, etc.)	Number per morphology	Total count (CFU/ml)	**Frequency %** (n. morph./total count)
Circular, white, convex, entire margin, opaque, creamy, streaked red underneath	2	46	5.3%
Circular, dark green, convex, undulate margin, creamy shiny, white halo	18		2.6%
Circular, dark green, convex, lobate margin, creamy shiny, white halo	2		2.6%
Circular, convex, dark green, entire margin, opaque, white halo, buttery texture	24		2.6%

After the morphological description, a random sampling from the WLD plate was performed, and RFLP analysis was conducted on 30 isolates.

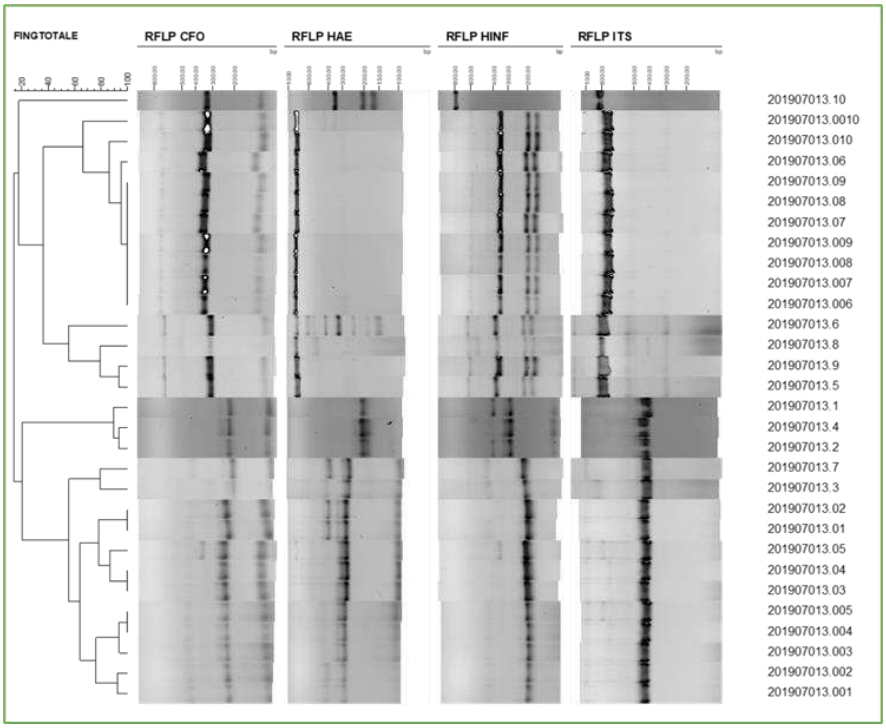

Figure 4.6. R7P13C. RFLP patterns, including ITS amplification bands and digestion profiles using Hha I (Cfo I), Hae III, and Hinf I enzymes, analysed and clustered using BioNumerics™ version 6.6 software. This sample exhibits two prevalent genotypes.

Following the grouping based on RFLP molecular profiles, the unidentified isolate was sequenced on the D1/D2 region of the 26S DNA fragment.

- 15/30 isolates analysed belong to *Hanseniaspora uvarum*.
- 12/30 isolates analysed belong to *Metschnikowia pulcherrima.*
- 3/30 isolates analysed belong to *Candida* sp.

R8P1 (Control)

Table 4.8. Data recorded on the morphological features of R8P1C (dilution 10^{-4}). Total count per millilitre derived from the count onto WLD plates. The morphology frequency is expressed as a percentage of the total count.

Morphological features (form, elevation, margin, colour, etc.)	Number per morphology	Total count (CFU/ml)	**Frequency %** (n. morph./total count)
Circular, light green, convex, entire margin, opaque, creamy, dark green underneath	1	160	0.6%
Circular, dark green, convex, entire margin, creamy, shiny	28		17.5%
Circular, light green, pulvinate, entire margin, creamy, opaque	1		0.6%
Circular, convex, dark green, entire margin, shiny, creamy	130		81%

After the morphological description, a random sampling from the WLD plate was performed, and RFLP analysis was conducted on 30 isolates.

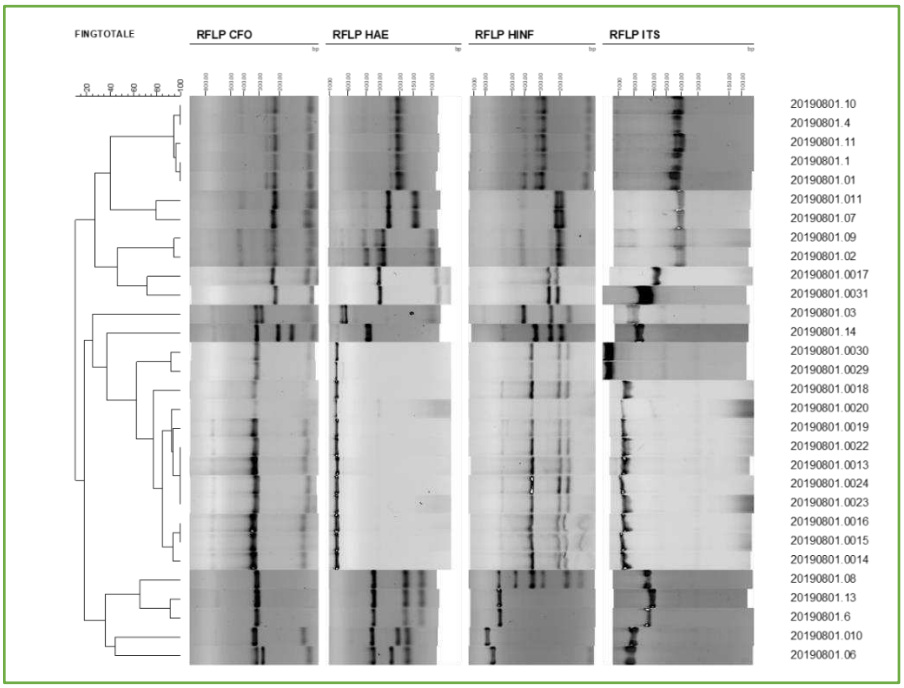

Figure 4.7. R8P1C. RFLP patterns, including ITS amplification bands and digestion profiles using Hha I (Cfo I), Hae III, and Hinf I

enzymes, analysed and clustered using BioNumerics™ version 6.6 software. This sample exhibits two prevalent genotypes.

Following the grouping based on RFLP molecular profiles, the unidentified isolate was sequenced on the D1/D2 region of the 26S DNA fragment.

- 12/30 isolates analysed belong to *Hanseniaspora uvarum* species.
- 4/30 isolates analysed belong to *Pichia* sp.
- 5/30 isolates analysed belong to *Candida californica*.
- 2/30 isolates analysed belong to *Pichia kluyveri.*
- 3/30 isolates analysed belong to *Zygosaccharomyces bailii*.
- 1/30 isolates analysed belong to *Kluyveromyces* sp.
- 3/30 isolates analysed belong to *Saccharomyces* sp.

R9P3 (Bion)

Table 4.9. Data recorded on the morphological features of R9P3B (dilution 10^{-5}). Total count per millilitre derived from the count onto WLD plates. The morphology frequency is expressed as a percentage of the total count.

Morphological features (form, elevation, margin, colour, etc.)	Number per morphology	Total count (CFU/ml)	**Frequency %** (n. morph./total count)
Circular, dark green, convex, entire margin, shiny, clean halo, creamy	3	28	10.7%
Circular, dark green, convex, entire margin, creamy, shiny	25		89.3%

After the morphological description, a random sampling from the WLD plate was performed, and RFLP analysis was conducted on 20 isolates.

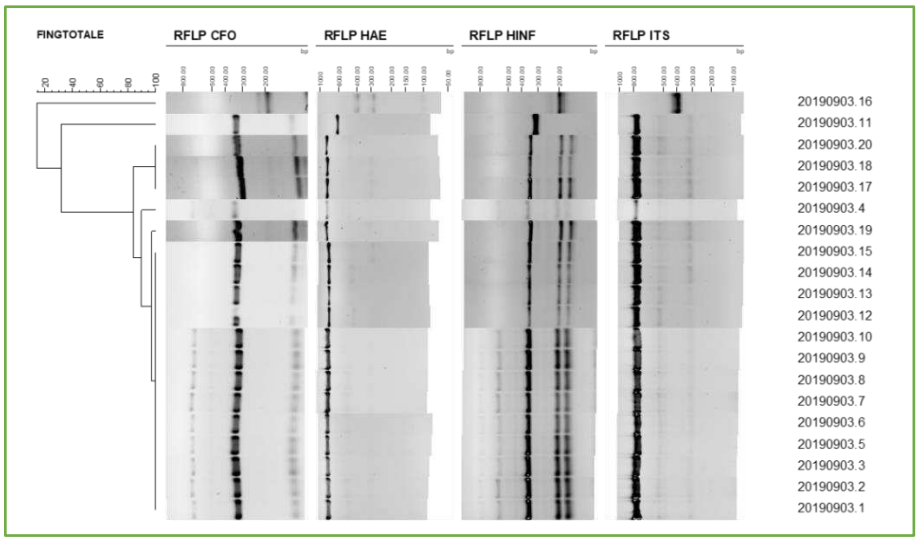

Figure 4.8. R9P3B. RFLP patterns, including ITS amplification bands and digestion profiles using Hha I (Cfo I), Hae III, and Hinf I enzymes, analysed and clustered using BioNumerics™ version 6.6 software. This sample exhibits two prevalent genotypes.

Following the grouping based on RFLP molecular profiles, the unidentified isolate was sequenced on the D1/D2 region of the 26S DNA fragment.

- 18/20 isolates analysed belong to *Hanseniaspora uvarum* species.
- 1/20 isolates analysed belong to *Candida zemplinina*.
- 1/20 isolates analysed belong to *Pichia* sp.

R9P11(Bion)

Table 4.10. Data recorded on the morphological features of R9P11B (dilution 10^{-2}). Total count per millilitre derived from the count onto WLD plates. The morphology frequency is expressed as a percentage of the total count.

Morphological features (form, elevation, margin, colour, etc.)	Number per morphology	Total count (CFU/ml)	**Frequency %** (n. morph./total

			count)
Circular, white, convex and bullous, entire margin, opaque, clean halo, creamy, dark green underneath	1	58	1.7%
Circular, dark green, convex, entire margin, buttery texture, opaque	25		43,1%
Circular, dark green, convex, entire margin, shiny	32		55,2%

After the morphological description, a random sampling from the WLD plate was performed, and RFLP analysis was conducted on 24 isolates.

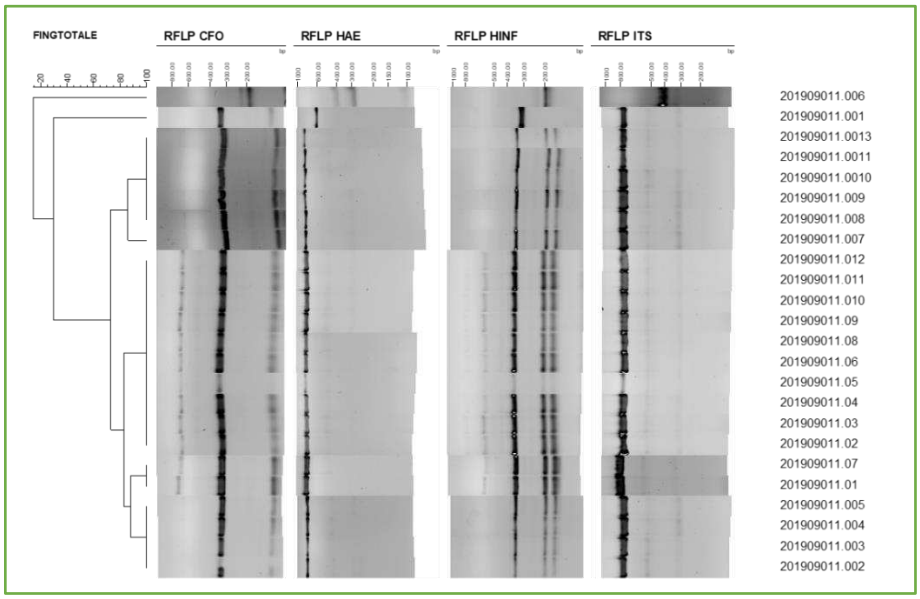

Figure 4.9. R9P11B. RFLP patterns, including ITS amplification bands and digestion profiles using Hha I (Cfo I), Hae III, and Hinf I enzymes, analysed and clustered using BioNumerics™ version 6.6 software. This sample exhibits two prevalent genotypes.

Following the grouping based on RFLP molecular profiles, the

unidentified isolate was sequenced on the D1/D2 region of the 26S DNA fragment.

- 22/24 isolates analysed belong to *Hanseniaspora uvarum* species.
- 1/24 isolates analysed belong to *Pichia* sp.
- 1/24 isolates analysed belong to *Candida* sp.

R10P6 (Bion)

Table 4.11. Data recorded on the morphological features of R10P6B (dilution 10^{-4}). Total count per millilitre derived from the count onto WLD plates. The morphology frequency is expressed as a percentage of the total count.

Morphological features (form, elevation, margin, colour, etc.)	Number per morphology	Total count (CFU/ml)	**Frequency %** (n. morph./total count)
Circular, white, convex and bullous, entire margin, opaque, creamy, dark green underneath	2	54	3.7%
Circular, dark green, convex, entire margin, shiny, creamy	10		18.5%
Circular, dark green, raised, undulated margin, shiny	40		74.1%
Circular, convex, dark green, entire margin, clean halo, dark green underneath	2		3.7%

After the morphological description, a random sampling from the WLD plate was performed, and RFLP analysis was conducted on 28 isolates.

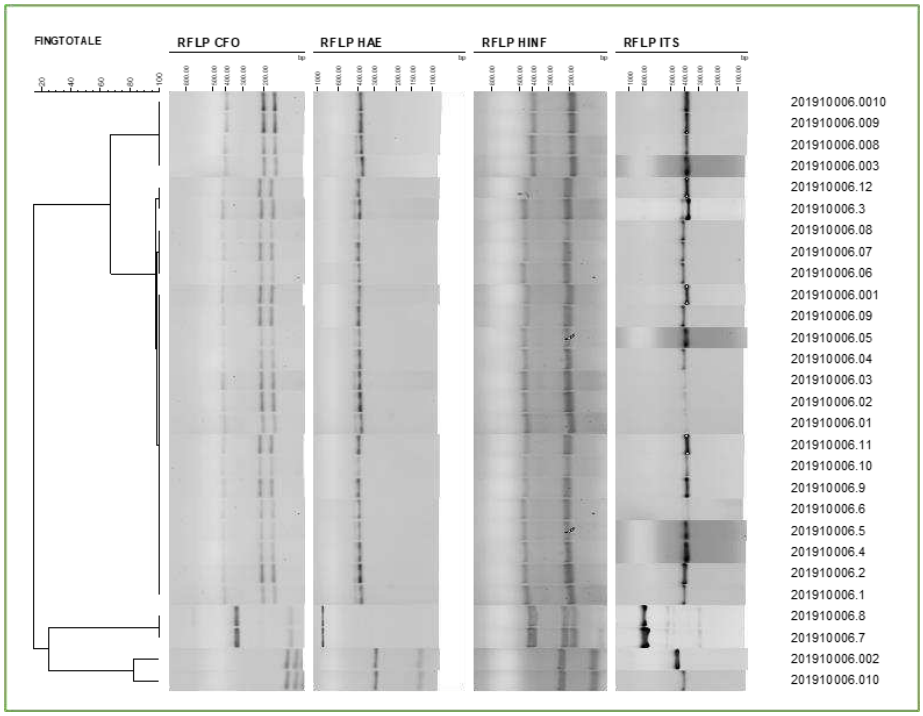

Figure 4.10. R10P6B. RFLP patterns, including ITS amplification bands and digestion profiles using Hha I (Cfo I), Hae III, and Hinf I enzymes, analysed and clustered using BioNumerics™ version 6.6 software. This sample exhibits two prevalent genotypes.

Following the grouping based on RFLP molecular profiles, the unidentified isolate was sequenced on the D1/D2 region of the 26S DNA fragment.

- 2/28 isolates analysed belong to *Pichia* sp.
- 2/28 isolates analysed belong to *Torulaspora* sp.
- 24/28 isolates analysed belong to *Candida diversa*.

R10P16 (Bion)

Table 4.12. Data recorded on the morphological features of R10P16B (dilution 10^{-4}). Total count per millilitre derived from the count onto WLD plates. The morphology frequency is expressed as a percentage of the total count.

Morphological features (form, elevation, margin, colour, etc.)	Number per morphology	Total count (CFU/ml)	**Frequency %** (n. morph./total count)
Circular, dark green, convex, and bullous, undulate margin, opaque, creamy, white halo	6	34	17.7%
Irregular form, white with red stripes, convex, green, and lobate margin, opaque, creamy, dark green underneath	2		5.8%
Circular, light green, pulvinate, bullous, shiny	2		5.8%
Circular, convex, light green, filamentous margin, white halo, opaque, buttery texture	4		11.8%
Circular, lobate margin, convex, dark green, creamy	20		58.8%

After the morphological description, a random sampling from the WLD plate was performed, and RFLP analysis was conducted on 24 isolates.

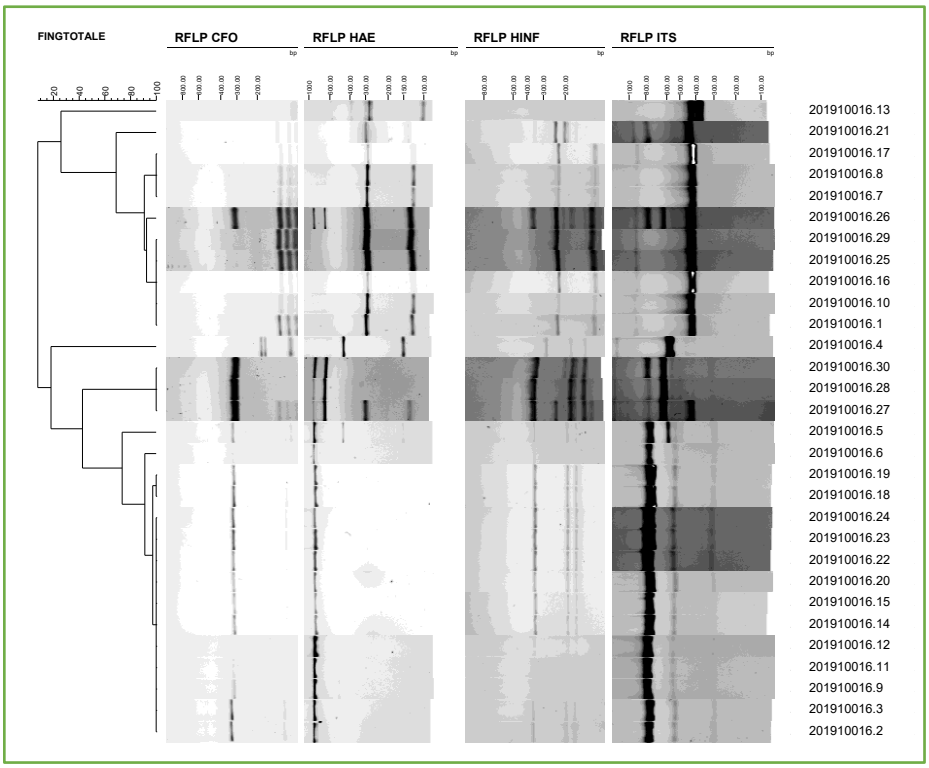

Figure 4.11. R10P16B. RFLP patterns, including ITS amplification bands and digestion profiles using Hha I (Cfo I), Hae III, and Hinf I enzymes, analysed and clustered using BioNumerics™ version 6.6 software. This sample exhibits two prevalent genotypes.

Following the grouping based on RFLP molecular profiles, the unidentified isolate was sequenced on the D1/D2 region of the 26S DNA fragment.

- 9/30 isolates analysed belong to *Pichia kluyveri*.
- 1/30 isolates analysed belong to *Pichia membranifaciens*.
- 1/30 isolates analysed belong to *M. pulcherrima.*
- 1/30 isolates analysed belong to *Candida* sp.
- 3/30 isolates analysed belong to *Pichia* sp.
- 15/30 isolates analysed belong to *Hanseniaspora uvarum.*

R11P7 (Bion)

Table 4.13. Data recorded on the morphological features of R11P7B (dilution 10^{-3}). Total count per millilitre derived from the count onto WLD plates. The morphology frequency is expressed as a percentage of the total count.

Morphological features (form, elevation, margin, colour, etc.)	Number per morphology	Total count (CFU/ml)	**Frequency %** (n. morph./total count)
Circular, dark green, raised, curled surface, undulate margin, opaque, creamy, halo	64	180	35.5%
Irregular form, convex, dark green, lobate margin, shiny, creamy, green halo	55		30.5%
Circular, dark green, convex, opaque, undulate margin	43		24%
Circular, flat, light green and darker green inside, shiny, irregular margin, white halo	18		10%

After the morphological description, a random sampling from the WLD plate was performed, and RFLP analysis was conducted on 31 isolates.

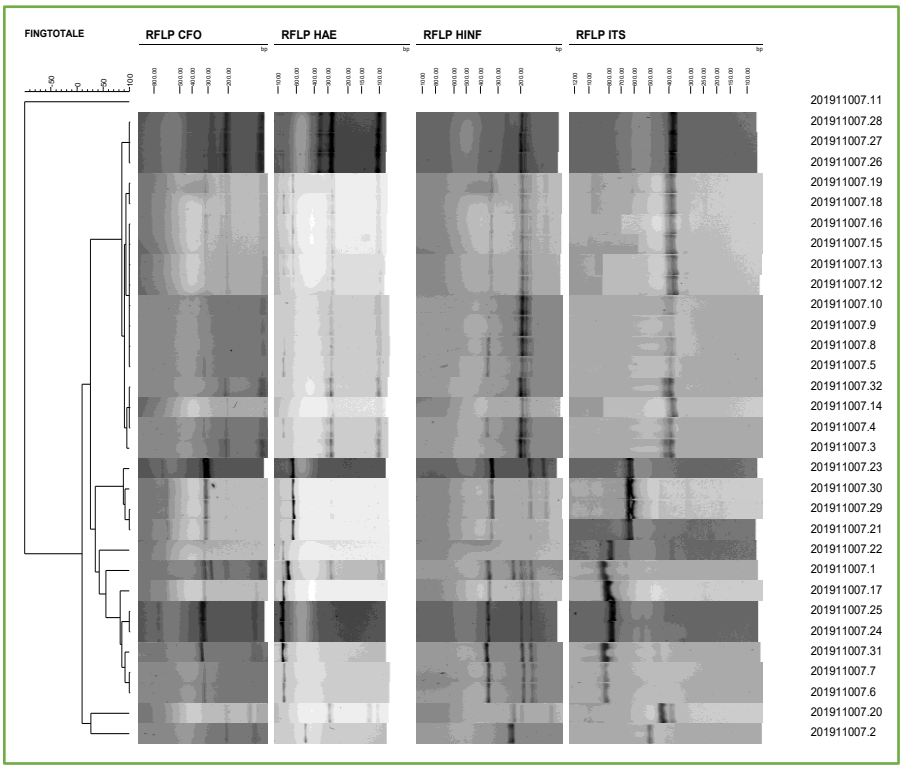

Figure 4.12. R11P7B. RFLP patterns, including ITS amplification bands and digestion profiles using Hha I (Cfo I), Hae III, and Hinf I enzymes, analysed and clustered using BioNumerics™ version 6.6 software. This sample exhibits two prevalent genotypes.

Following the grouping based on RFLP molecular profiles, the unidentified isolate was sequenced on the D1/D2 region of the 26S DNA fragment.

- 1/31 isolates analysed belong to *Wickerhamomyces anomalus*.
- 1/31 isolates analysed belong to *Candida stellata*.
- 17/31 isolates analysed belong to *Metschnikowia pulcherrima*.
- 4/31 isolates analysed belong to *Zygosaccharomyces bailii*.
- 1/31 isolates analysed belong to *Torulaspora delbrueckii*.
- 7/31 isolates analysed belong to *Hanseniaspora uvarum*.

R13P6 (Water)

Table 4.14. Data recorded on the morphological features of R13P6W (dilution 10^{-4}). Total count per millilitre derived from the count onto WLD plates. The morphology frequency is expressed as a percentage of the total count.

Morphological features (form, elevation, margin, colour, etc.)	Number per morphology	Total count (CFU/ml)	**Frequency %** (n. morph./total count)
Irregular-circular inside, dark green and lighter green inside, convex-raised, curled surface, lobate margin, shiny, creamy, white halo, green underneath	7	136	5.1%
Irregular form, convex, white and light green inside, lobate margin, shiny, creamy, white halo green underneath	5		3.7%
Circular, dark green, pulvinate, shiny, creamy, clear halo	7		5.1%
Circular, convex, dark green, opaque, irregular margin, white halo	117		86%

After the morphological description, a random sampling from the WLD plate was performed, and RFLP analysis was conducted on 20 isolates.

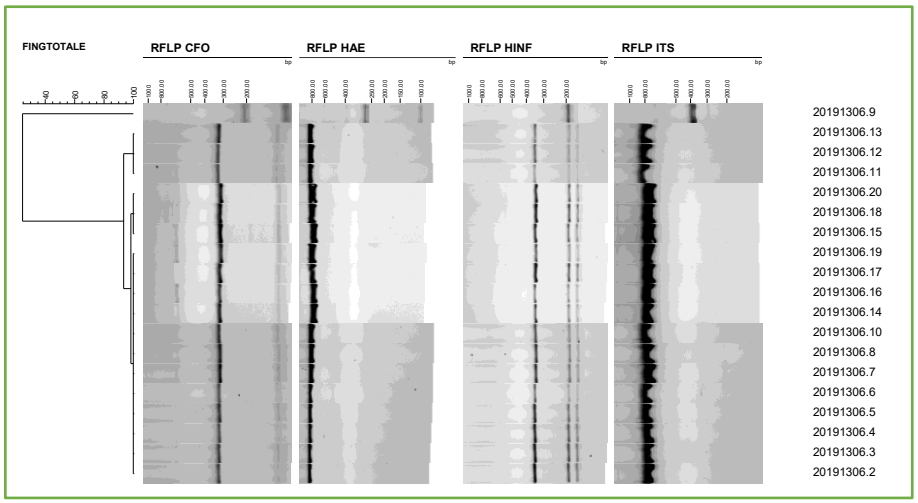

Figure 4.13. R13P6W. RFLP patterns, including ITS amplification bands and digestion profiles using Hha I (Cfo I), Hae III, and Hinf I enzymes, analysed and clustered using BioNumerics™ version 6.6 software. This sample exhibits two prevalent genotypes.

Following the grouping based on RFLP molecular profiles, the unidentified isolate was sequenced on the D1/D2 region of the 26S DNA fragment.

- 18/20 isolates analysed belong to *Hanseniaspora uvarum*.
- 1/20 isolates analysed belong to *Metschnikowia pulcherrima*.
- 1/20 isolates analysed belong to *Pichia* sp.

R13P13 (Water)

Table 4.15. Data recorded on the morphological features of R13P13W (dilution 10^{-4}). Total count per millilitre derived from the count onto WLD plates. The morphology frequency is expressed as a percentage of the total count.

Morphological features (form, elevation, margin, colour, etc.)	Number per morphology	Total count (CFU/ml)	**Frequency %** (n. morph./total count)

Circular, dark green, convex, entire margin, shiny, creamy	10	102	9.8%
Circular, light green, convex, entire margin, opaque, creamy	10		9.8%
Circular, convex, dark green inside and lighter green edge, shiny, creamy	82		80.4%

After the morphological description, a random sampling from the WLD plate was performed, and RFLP analysis was conducted on 26 isolates.

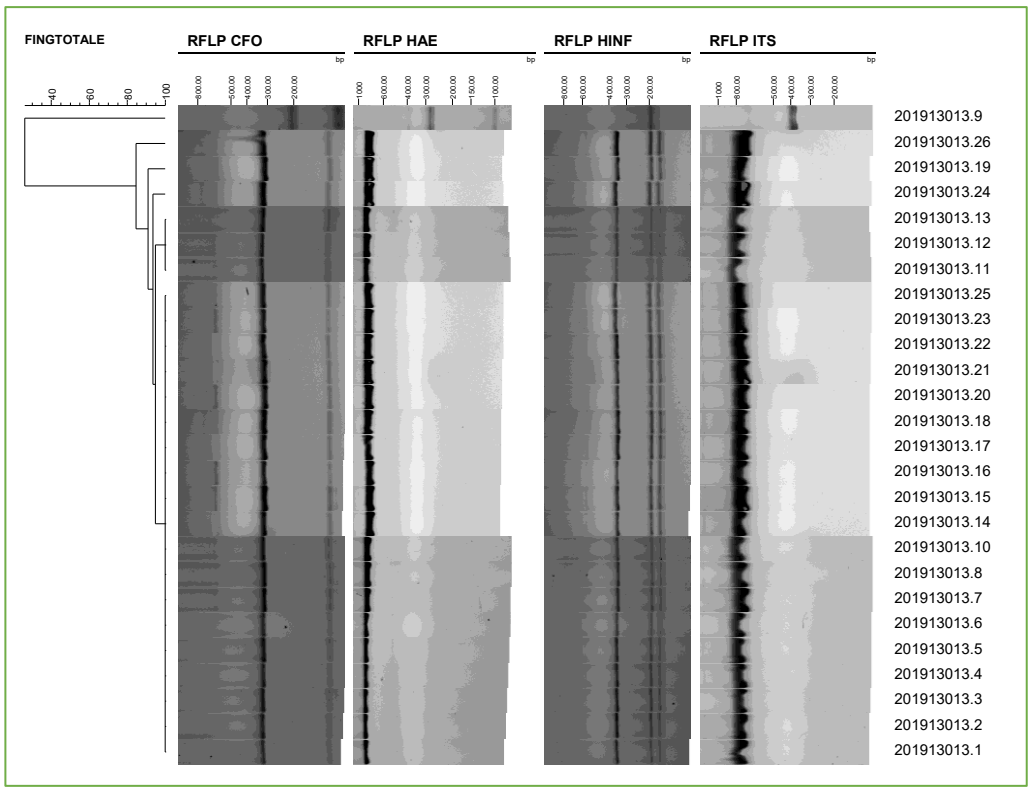

Figure 4.14. R13P13W. RFLP patterns, including ITS amplification bands and digestion profiles using Hha I (Cfo I), Hae III, and Hinf I enzymes, analysed and clustered using BioNumerics™ version 6.6 software. This sample exhibits two prevalent genotypes.

Following the grouping based on RFLP molecular profiles, the unidentified isolate was sequenced on the D1/D2 region of the 26S

DNA fragment.

- 25/26 isolates analysed belong to *Hanseniaspora uvarum*.
- 1/26 isolates analysed belong to *Metschnikowia pulcherrima*.

R13P13 (Water)

Table 4.16 Data recorded on the morphological features of R13P23 (dilution 10^{-3}). Total count per millilitre derived from the count onto WLD plates. The morphology frequency is expressed as a percentage of the total count.

Morphological features (form, elevation, margin, colour, etc.)	Number per morphology	Total count (CFU/ml)	**Frequency %** (n. morph./total count)
Irregular, light green, convex, white, and lobate margin, bullous inside, opaque, creamy	2	192	1%
Circular, light green, convex, entire margin, curled surface, opaque, creamy	23		12%
Circular, convex, dark green, shiny, creamy, slightly lobate margin	167		87%

After the morphological description, a random sampling from the WLD plate was performed, and RFLP analysis was conducted on 20 isolates.

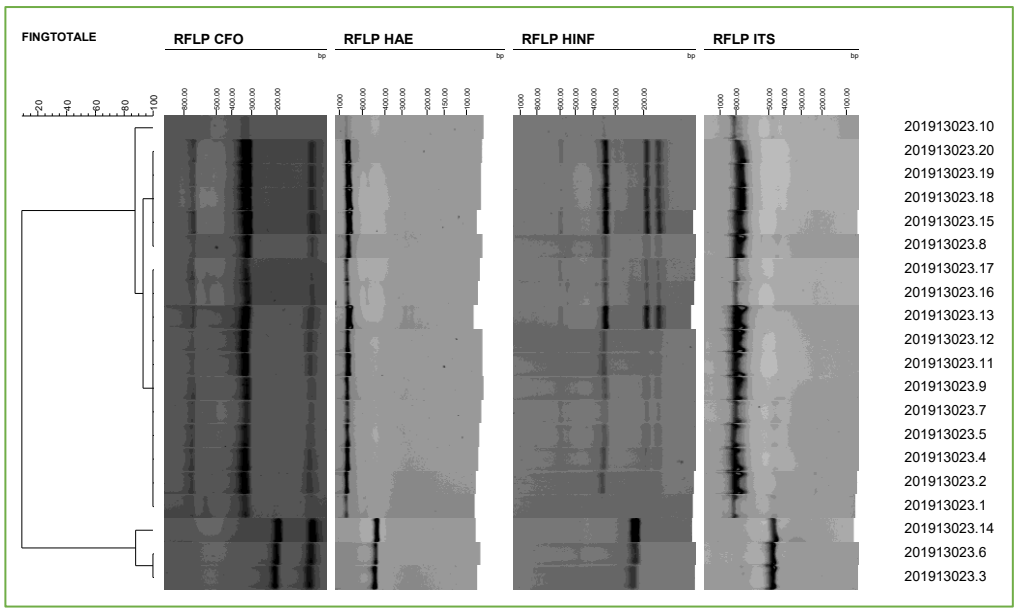

Figure 4.15. R13P13. RFLP patterns, including ITS amplification bands and digestion profiles using Hha I (Cfo I), Hae III, and Hinf I enzymes, analysed and clustered using BioNumerics™ version 6.6 software. This sample exhibits two prevalent genotypes.

Following the grouping based on RFLP molecular profiles, the unidentified isolate was sequenced on the D1/D2 region of the 26S DNA fragment.

- 17/20 isolates analysed belong to *Hanseniaspora uvarum*.
- 3/20 isolates analysed belong to *Candida stellata*.

R14P9

Table 4.17. Data recorded on the morphological features of R14P9 (dilution 10^{-4}). Total count per millilitre derived from the count onto WLD plates. The morphology frequency is expressed as a percentage of the total count.

Morphological features (form, elevation, margin, colour, etc.)	Number per morphology	Total count (CFU/ml)	**Frequency %** (n. morph./total count)
Circular, convex, dark green, shiny, creamy, entire margin	4	40	10%
Circular, dark green, convex, undulate margin, shiny, creamy, clear halo	6		15%
Circular, convex, dark green, opaque, creamy, lobate margin	30		75%

After the morphological description, a random sampling from the WLD plate was performed, and RFLP analysis was conducted on 27 isolates.

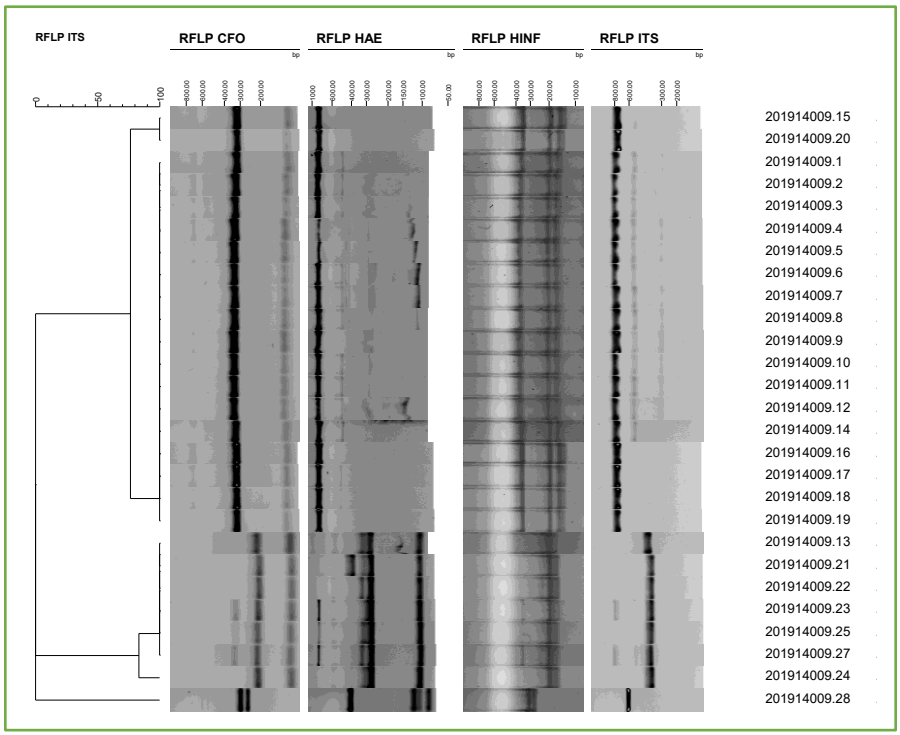

Figure 4.16. R14P9. RFLP patterns, including ITS amplification bands and digestion profiles using Hha I (Cfo I), Hae III, and Hinf I enzymes, analysed and clustered using BioNumerics™ version 6.6 software. This sample exhibits two prevalent genotypes.

Following the grouping based on RFLP molecular profiles, the unidentified isolate was sequenced on the D1/D2 region of the 26S DNA fragment.

- 19/27 isolates analysed belong to *Hanseniaspora uvarum*.
- 7/27 isolates analysed belong to *M. pulcherrima*.
- 1/27 isolates analysed belong to *Debariomyces hansenii*.

R14P17

Table 4.18. Data recorded on the morphological features of R14P17W (dilution 10^{-4}). Total count per millilitre derived from the count onto WLD plates. The morphology frequency is expressed as a percentage of the total count.

Morphological features (form, elevation, margin, colour, etc.)	Number per morphology	Total count (CFU/ml)	**Frequency %** (n. morph./total count)
Circular, convex, light green, opaque, creamy, entire margin, large halo	3	54	5.5%
Circular, green, convex, undulate margin, curled surface, opaque, creamy	3		5.5%
Circular, pulvinate, light green, opaque, creamy, entire margin	2		3.6%
Circular, dark green, undulate margin, shiny, creamy	46		85.4%

After the morphological description, a random sampling from the WLD plate was performed, and RFLP analysis was conducted on 25 isolates.

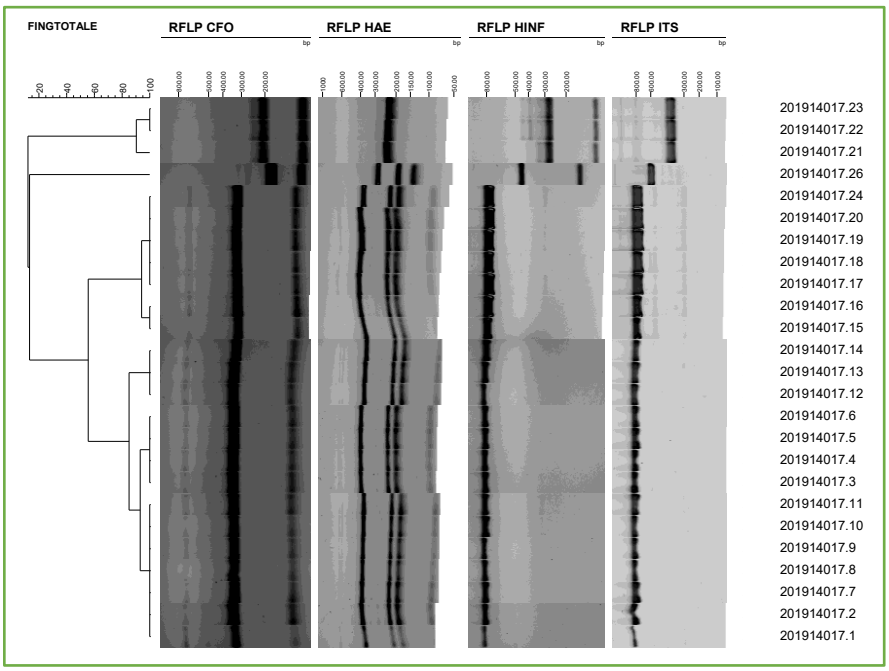

Figure 4.17 R14P17W. RFLP patterns, including ITS amplification bands and digestion profiles using Hha I (Cfo I), Hae III, and Hinf I

enzymes, analysed and clustered using BioNumerics™ version 6.6 software. This sample exhibits two prevalent genotypes.

Following the grouping based on RFLP molecular profiles, the unidentified isolate was sequenced on the D1/D2 region of the 26S DNA fragment.

- 21/25 isolates analysed belong to *Z. bisporus*.
- 3/25 isolates analysed belong to *M. pulcherrima*.
- 1/25 isolates analysed belong to *Aureobasidium pullulans.*

Colony types not identified by RFLP analysis were subjected to Sanger sequencing. The 26S sequences obtained were identified using the NCBI BLAST tool. The identified species and their respective 26S sequences are shown below.

Table 4.19. Strain identification by Sanger sequencing of the 26S region 310 Genetic Analyzer (ABI PRISM™, AB Applied Biosystems).

Isolated Strains	Assigned species by BLASTn Analysis	Identity (%)	Gene Banck accession number
R6P11-001	*Zygosaccharomyces bailii*	99.83	MH681731.1
R9P3-16	*Starmerella bacillaris*	99.76	MH681733.1
R6P11-04	*Pichia terricola*	99.82	MH892868.1
R8P1-011	*Pichia kluyveri*	99.83	MH681741
R8P1-10	*Candida californica*	99.46	MH681743.1
R5P8-12	*Aureobasidium pullulans*	99.82	MH681750.1

4.1.1 Discussion

In this descriptive part of the yeasts associated to grape skins we detected species widely described in the literature, such as *H. uvarum, M. pulcherrima, A. pullulans, Debariomyces hansenii, Zygosaccharomyces bailii, Pichia* sp., *Candida* sp. (19- 22). It is

appropriate to give space to the evaluation of biodiversity through a metagenomic approach allowing for a more objective comparison of the treatments outlined in Chapter 3. This method considers the entire yeast population, including non-cultivable species, and provides extensive information by analyzing all samples simultaneously. It helps avoid errors inherent in classic microbiological approaches, such as losing non dominant fungal species due to serial dilutions, and eliminates subjective evaluations, thereby streamlining lengthy procedures.

4.2 Fungal population on the berry skin by a metagenomic approach

4.2.1 Preliminary assessment of whole DNA

Following nucleic acid purification through a manual protocol, DNA quantification and purity assessments were conducted. As the purity values for each sample exceeded 1.8, the DNA was deemed suitable for subsequent metabarcoding analyses. (Tab. 4.19).

Table 4.19. Measure quantity and purity of whole DNA for metabarcoding analysis, by spectrophotometer.

Sample name	dsDNA Quantity (µg/ml) (3 measures)			Avarage	x 100 (µg/ml)	dsDNA Purity (260/280 Ratio)
R3P18C	24.145	24.15	24.173	24.156	2415.600	1.924
R5P8C	16.596	16.597	16.596	16.596	1659.633	1.909
R6P11C	14.341	14.354	14.374	14.356	1435.633	1.904
R7P13C	14.393	14.359	14.383	14.378	1437.833	1.945
R8P1C	123.98	123.09	122.2	123.090	12309.000	1.954
R9P3B	13.877	13.848	13.855	13.860	1386.000	1.923
R9P11B	16.167	16.164	16.137	16.156	1615.600	1.918
R10P6B	25.312	25.322	25.332	25.322	2532.200	1.916
R10P16B	21.012	21.009	20.952	20.991	2099.100	1.92
R11P7B	24.641	24.628	24.659	24.643	2464.267	1.905
R13P6W	48.992	49.001	48.976	48.990	4898.967	1.941
R13P13W	15.935	15.939	15.906	15.927	1592.667	1.844
R13P23W	101.66	101.95	101.9	101.837	10183.667	1.998
R14P9W	24.973	24.644	24.653	24.757	2475.667	1.98
R14P17W	17.898	17.934	17.901	17.911	1791.100	1.952

Seeing the Illumina Metagenomic Sequencing Library Preparation protocol, a test PCR was conducted using a hot-start, high-fidelity DNA polymerase (KAPA HIFI HS Ready Mix, KAPA BIOSYSTEMS, Cape Town, South Africa). This step aimed to confirm the quality of the purified DNA. The PCR thermal cycle specific to the ITS region was performed, and the resulting amplicons were visualized through electrophoresis in a 2.5% agarose gel. The image, post-staining with Ethidium bromide, confirmed the successful

amplification of the entire DNA using ITS1 and ITS4 primers, as illustrated in Figure 4.18.

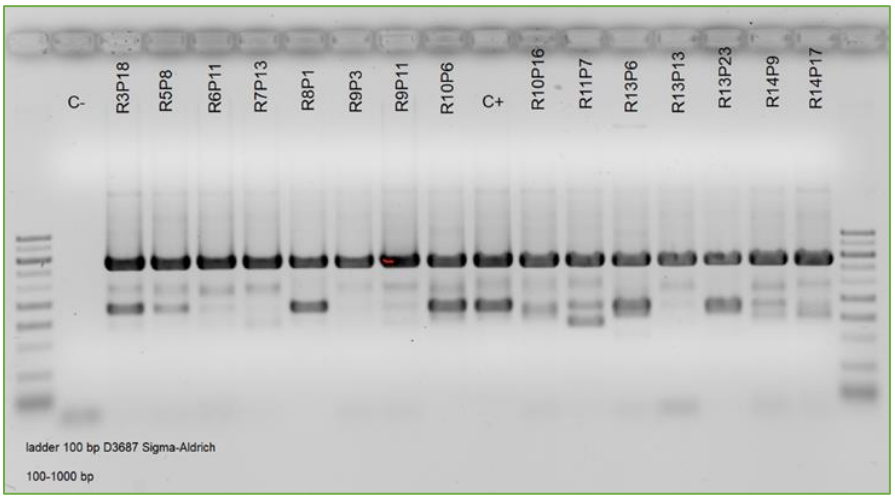

Figure 4.18. Quality control through electrophoresis of whole DNA. The resulting gel image provides a visual representation of the DNA fragments, confirming their suitability for further analysis.

Once the standard DNA checks have been successfully completed, the next step involves proceeding with the metabarcoding protocol, as outlined in the preceding chapter.

After completing the massive sequencing, the raw reads undergo a cleaning phase. The objective of this phase is to eliminate low-quality reads and sequencing artifacts, as illustrated in the figure 4.19.

The subsequent section delineates the outcomes pertaining to the metabarcoding analyses conducted through the Microbiome-Analyst online platform.

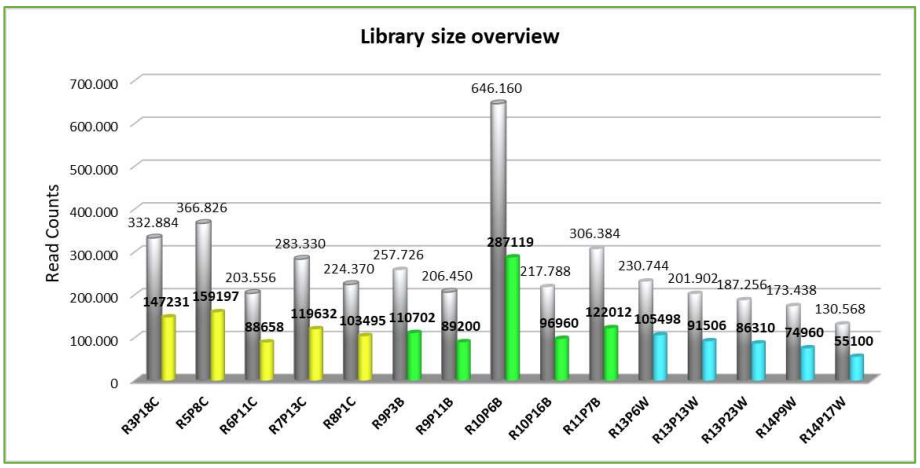

Figure 4.19. Overview of read counts before and after the data integrity check. (In grey reads count before data check; in yellow the Control, in green the Bion, in azure the Water).

4.2.2 Mycobiota characterization

A total of 3,969,382 reads were generated, with an average of 264,625 reads per sample. Following the demultiplexing process, 1,737,580 reads were utilized for subsequent analyses, averaging 115,839 reads per sample. The genomic sequences have been included into the BioProject PRJNA801453, titled "Study of the yeast microbiota of grape skin," accessible in the National Center for Biotechnology Information (NCBI) database as of January 28th, 2022. This BioProject encompasses 15 BioSamples with accession IDs ranging from SAMN25351049 to SAMN25351063. Among these samples, 1,882 features (taxa) were initially present, and after data filtering, 1,772 features remained.

The rarefaction curves (Figure 4.20) obtained from the statistical analysis of the OTUs indicate that a substantial number of fungal species were sequenced in each sample, with a minimum of 197 in R8P1C and a maximum of 403 in R10P16B. These curves suggest

excellent sequencing coverage for all processed samples, consistently exceeding 99.5% (4,5).

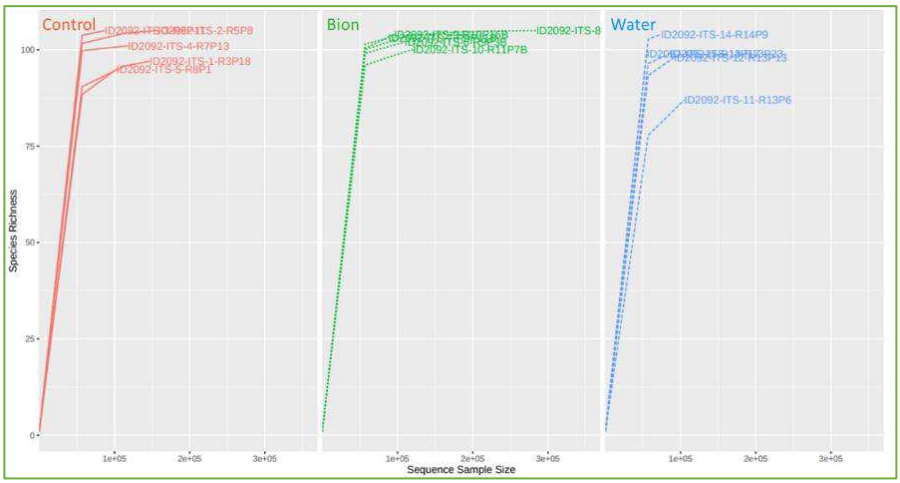

Figure 4.20. Rarefaction curves. Group Control in red; Group Bion in green; Group Water in blue; x axis: species richness or number of OTUs; y axis: sequence sample size or number of reads.

Alpha diversity

Table 4.20. Recorded data of the alpha biodiversity estimators in terms of number of observed species, Shannon's and Simpson's index, as output from Microbiome-Analyst. In bold type are highlighted the median values.

Thesis	Sample	Observed (p= 0.049894)	Shannon's Index (p= 0.73345)	Simpson's Index (p= 0.56553)
Group1 (Control)	R3P18C	65	1.14	0.558
	R5P8C	**79**	**1.41**	0.637
	R6P11C	93	1.67	0.646
	R7P13C	84	1.45	**0.606**
	R8P1C	63	1.05	0.503
Group2 (Bion)	R9P3B	**83**	1.11	0.455
	R9P11B	86	1.59	**0.618**
	R10P6B	94	1.30	0.543
	R10P16B	69	1.61	0.699
	R11P7B	75	**1.53**	0.713
Group3 (Water)	R13P6W	57	1.41	0.696
	R13P13W	51	**1.44**	**0.667**
	R13P23W	**60**	1.49	0.688
	R14P9W	83	1.51	0.604
	R14P17W	62	1.39	0.586

The assessment of three alpha diversity estimators was conducted at the species level, as depicted in Figure 4.21. The number of observed species (richness) on the grape skin showed significant differences according to the treatment (p = 0.04999). However, Shannon's diversity index did not differ significantly based on the treatment (p = 0.73345), indicating similar diversity levels. Similarly, Simpson's Index showed no significant differences between the treatments (p= 0.56553). The respectively boxplot are showed in figure 4.21.

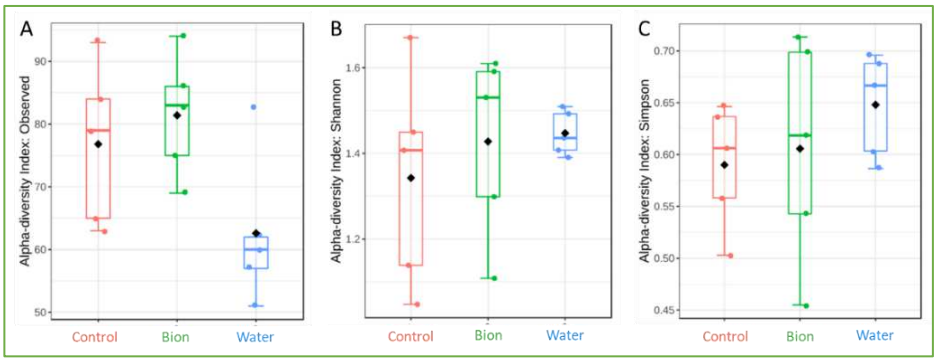

Figure 4.21. Alpha diversity analysis at species level estimated as number of species observed (p-value= 0.04999) in graphic A, as Shannon's Index (p-value= 0.73345) in graphic B, as Simpson's Index (p-value= 0.56553) in graphic C. p-value cut-off for significance is 0.05. (The black dot indicates the mean value while the inside the coloured rectangles is represented the median value. (In red, Control; in green, Bion; in blue, Water).

Beta diversity

Beta diversity (the comparison of fungal communities based on their composition) provides a measure of the dissimilarity between each sample pair. Principal Coordinates Analysis (PCoA), performed on the recorded species, indicates that the axis 1 explains 73.4% of the diversity and the axis 2 explains 12.1%. The overall

composition of the grape skin mycobiota, considered at species level, was not significantly affected by the treatments, as determined by non-parametric multivariate analysis of variance testing (PERMANOVA; $p < 0.001$).

The three data groups were not clustered according to the three different treatments, appearing collected in the same cluster as shown in Figure 4.22. Thus, the treatments characteristics did not affect the biodiversity of the fungal communities on the grape of the 15 vines considered.

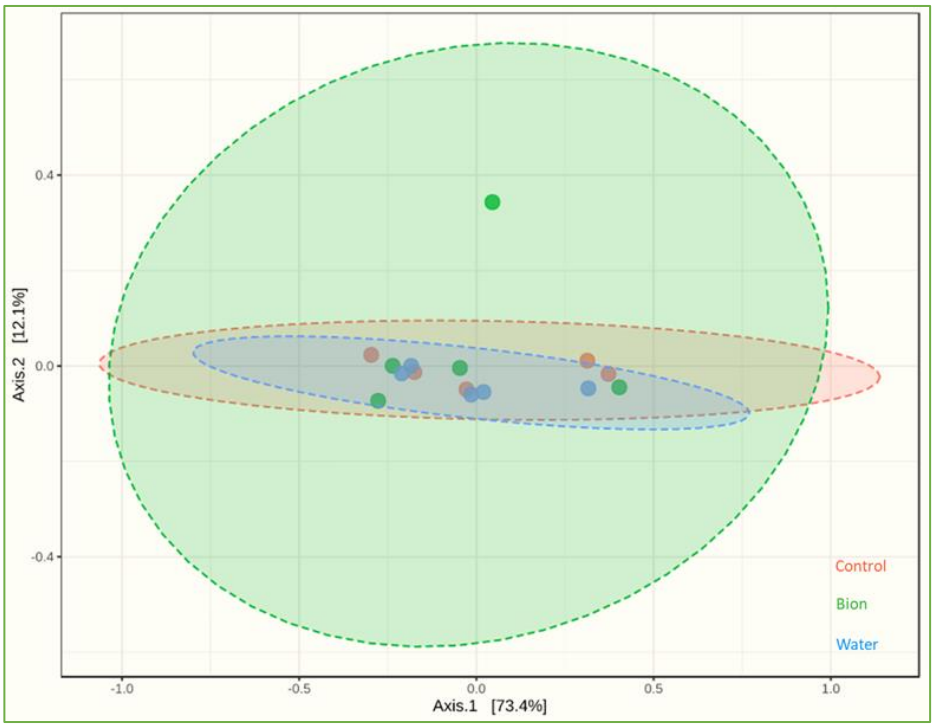

Figure 4.22. PCoA based on Bray-Curties metrics shows the dissimilarity of the fungal communities in the different samples according to the three treatments (p= 0.688). (In red Control; in green Bion; in blue Water).

Following are other descriptions of the mycobiota performed by Microbiome-Analyst tools.

Richness in terms of fungal species

A graphical view of the abundance at species level in the three different experimental conditions is showed in Figure 4.23, that consider the total counts of reads and represent the frequency of the OTUs assigned at species level.

A significant portion of the reads was assigned to *Incertae sedis* at the species level. In all analysis was reported a relevant percentage of *Incertae sedis* due to the uncertainty in these assignments. However, these reads can be categorized at a higher taxonomic level.

During the analysis of the sequencing data, a subset of reads labelled as "Not Assigned", did not match any OTUs in the reference database (UNITE2016). This indicates a lack of representation for these specific sequences in the established database.

The prevalence of *Hanseniaspora uvarum* is conspicuous across all treatments, constituting approximately 40% of the Operational Taxonomic Units (OTUs). The species distribution in the chart reflects their relative abundance, also highlighting *I. terricola* and *C. californica* as prominent yeasts during grape ripening. A substantial portion of reads, around 34% in Control, 33% in Bion, and 24% in Water, were labelled as *Incertae sedis* at the species level. Unassigned reads accounted for 20% in Control, 24% in Bion, and 14% in Water.

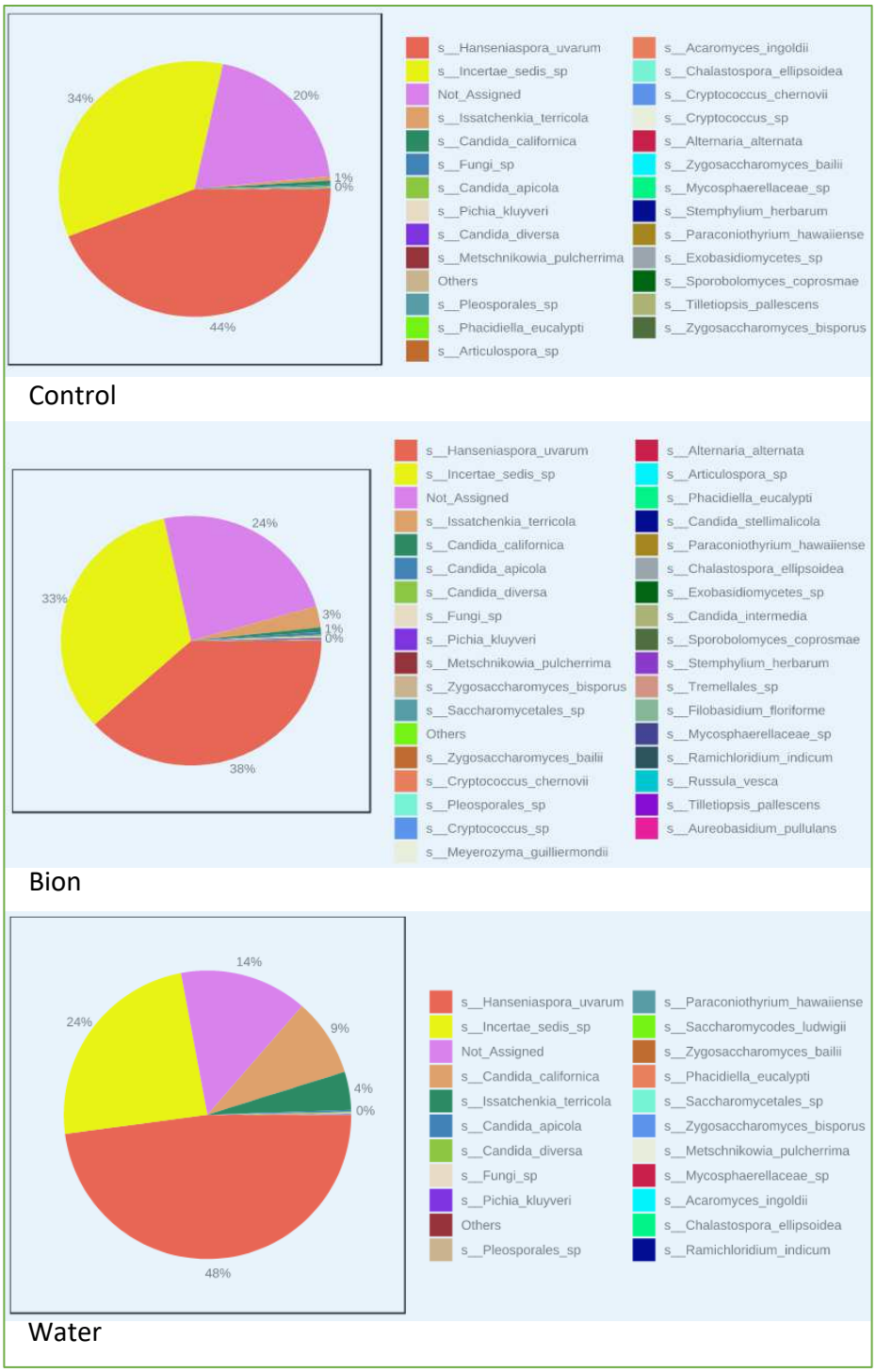

Figure 4.23. Pie-Chart of relative abundance at species level. Relative abundance in percentage of the species detected in each thesis.

Core mycobiota

The core microbiome analysis comprises the most abundant yeast species residing on the berry surface. This elaboration is shown in Figure 4.24.

H. uvarum emerged as the predominant species across all the treatments. *Issatchenkia terricola* was identified in the Bion and Water treatments, with a higher prevalence observed in the latter, while it was absent in the Control. *Candida californica* exclusively appeared in the core mycobiota of the Water treatment.

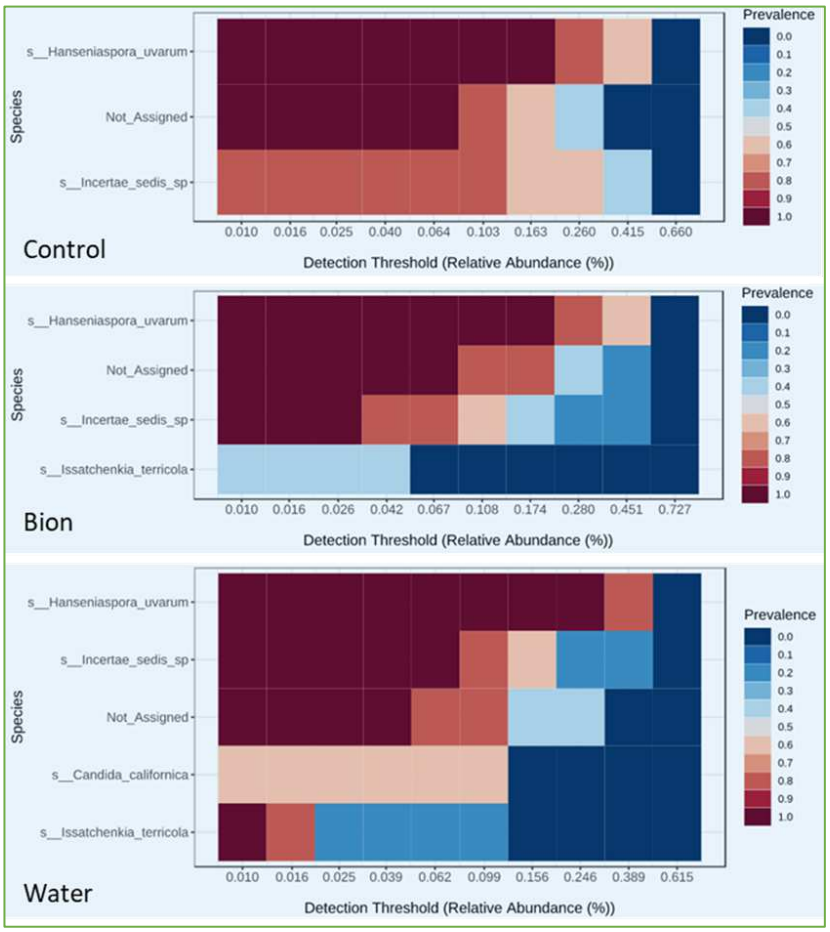

Figure 4.24. Representation of the main yeast at species level for each treatment, considering the median data from five samples for each treatment.

Heat three

The heat tree chart visually represents the abundance of species in the different treatments. It employs a hierarchical taxonomic structure to depict the differences quantitatively and statistically among fungal communities per treatment (Fig. 4.25).

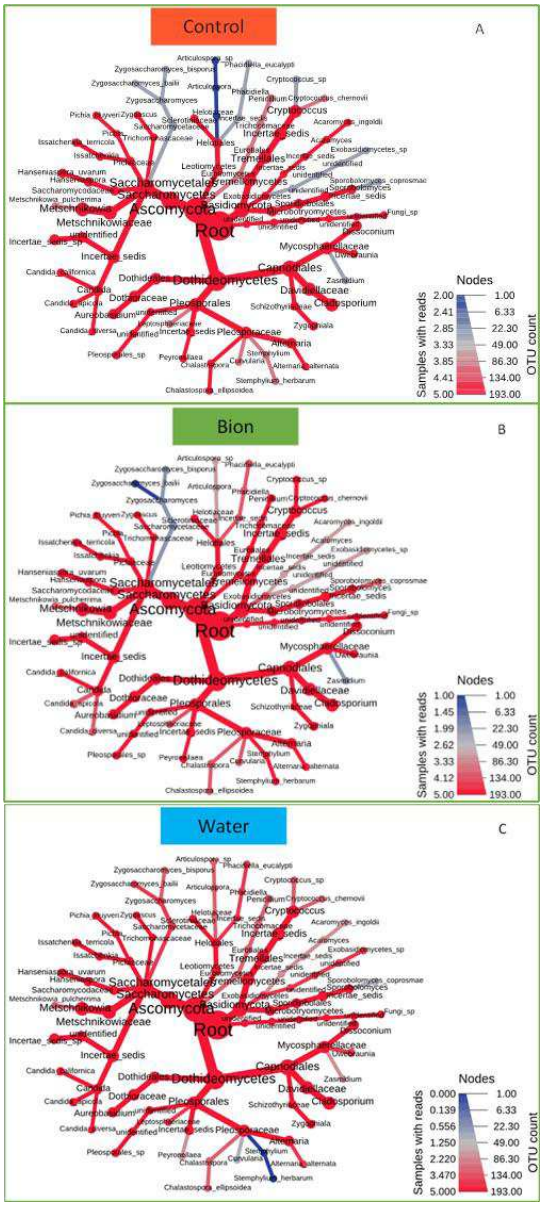

Figure 4.25. The graphical comparison of abundance at species level within each treatment.

These graphs highlight all the taxonomic categories, detailing the minority species better than the pie chart, also including those relating to pathogenic fungal species (e.g. *Alternaria alternata*, *Cladosporium* sp.).

Heatmap

The heatmap (Figure 4.26) illustrates the abundance distribution of various fungal species based on the samples. It reveals the presence of several filamentous fungi. The relative abundance of the species assigned is not uniform within each treatment, confirming that no significant differences exist among the treatments.

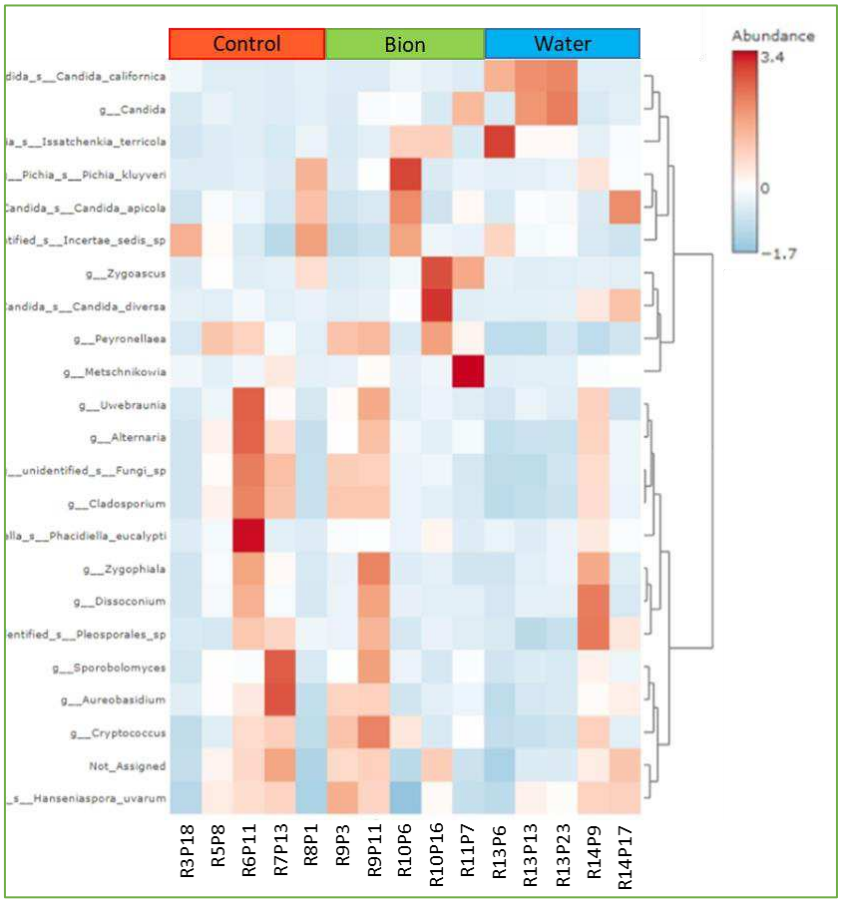

Figure 4.26. Heatmap, the graphical representation of the abundance at species and higher taxa level respect each sample

(five per treatment). The clustering reflects the distance measure using the Euclidean algorithm and the clustering algorithm using ward.D. Hierarchical clustering, performed with the hclust function in the stat package of Microbiome-Analyst.

Nevertheless, some yeast species showed a certain association with the treatments used. Particularly, the Control group exhibited a high frequency of genera such as *Peynorellaea*, *Cladosporium*, *Alternaria*, *Aureobasidium*, and unidentified fungi. These genera, known as plant pathogens, appeared prevalent in grapes treated with conventional agropharmaceuticals (IPM). Samples R3P18 and R8P1 from the Control showed similarities but displayed different species abundances compared to the other three samples (R5P8, R6P11, R7P13) located in the central portion of the Control parcel. Samples collected from row 9 (R9P3 and R9P11; Bion treatment) exhibited a fungal composition similar to R5P8, R6P11, R7P13 of the Control group. While there was a prevalence of fermenting yeasts belonging to the *Candida* genus in the other three samples of the Bion group (R9P11, R10P16, R11P7). Water samples exhibited a lower diversity of fungal species. This group showed a distinctive grouping, with row 13 samples, where a prevalence of the *Candida* genus was observed, differing from row 14, where *H. uvarum*, *Aureobasidium* sp., *Pleosporales* sp. were the prevalent fungi observed.

Correlation among species and treatments

To evaluate the advantages or disadvantages of a species based on treatment, it is helpful to refer to the following graph (Fig. 4.27).

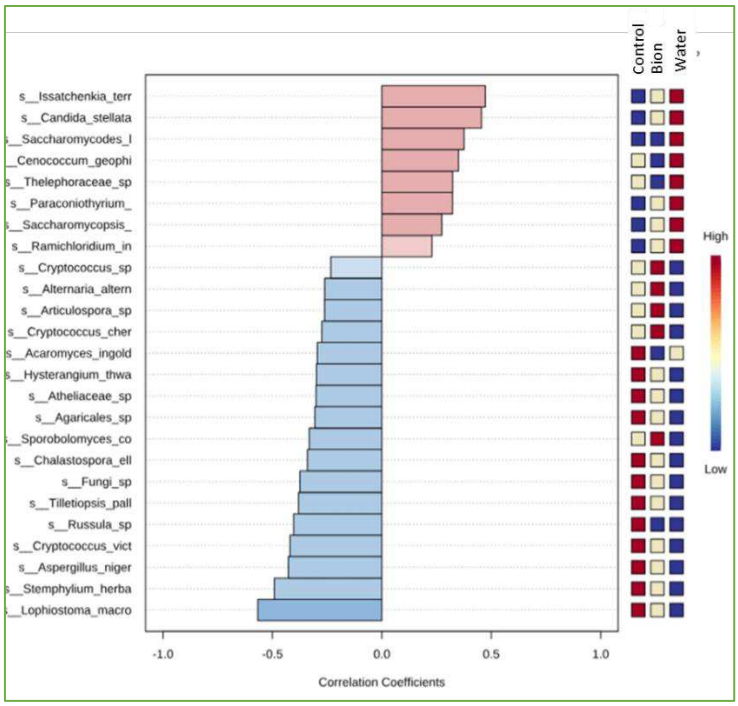

Figure 4.27. "pattern search" tool of Microbiome-Analyst Top 25 OTUs have been correlated with the three treatments.

This correlation considers the 25 OTUs at specie level more correlated with the Water treatment. It shows how positively or negatively these species correlate with the condition of water parcel. The sidebar shows their abundance in other treatments. Here is highlighted as *I. terricola*, *C. stellata*, *Saccharomycodes ludwigii* were notably prevalent in treatment Water, while they were relatively less frequent in Control (IPM unmodified). Conversely, filamentous fungi as *Lophiostoma macrostomum*, *Stemphylium herbarum*, *Aspergillus niger*, etc. appears advantaged in the Control. Species as *Cryptococcus* sp., *Articulospora* sp., *Alternaria alternata* seemed more abundant in Bion treatment.

Signature

Linear Discriminant Analysis Effect Size (LEfSe) was applied

at species level to determine the signature; it was aimed to identify the fungal species with significant differential abundance according to the treatment.

In this analysis 66 OTUs have been identified and taxonomically assigned, as reported in Table 4.21.

Table 4.21. Linear discriminant analysis at species level taking into account all five samples per treatment, reveals distinct patterns. n the visual representation, light gray indicates species less prevalent in the Bion treatment compared to the Control, with red denoting a presence less than 50%. Light green highlights species more abundant in the Bion treatment than in the Control, with purple denoting a presence more than 200%. Signature results are derived from a non-parametric factorial Kruskal-Wallis (KW) sum-rank test, with an adjusted p-value cutoff of 0.05 and an LDA score of 1.0. (* *Mycobank database https://www.mycobank.org/ to associate the species at the corresponding Phylum).*

OTUs assigned at species level	Phylum *	P value	FDR	Control	Bion	Water	LDA score	Bion / Control (%)
Hanseniaspora uvarum	*Ascomycota*	0.81058	0.90706	4,428,800.00	4,599,000.00	5,000,900,.00	5.46	103.84
Not Assigned		0.56553	0.84636	2,073,400.00	2,819,500.00	1,607,200.00	5.78	135.98
Issatchenkia terricola	*Ascomycota*	0.06522	0.56146	56,298.00	216,560.00	374,330.00	5.2	384.67
Fusarium sp	*Ascomycota*	0.57853	0.84636	35,122.00	92,297.00	26,681.00	1.53	262.79
Oidiodendron sp	*Ascomycota*	0.73129	0.87269	22,559.00	83,656.00	46.34	1.5	370.83
Aspergillus niger	*Ascomycota*	0.26624	0.74325	52,233.00	69,658.00	0.00	1.43	133.36
Rozellomycota sp	*Rozellomycota*	0.97977	0.97977	33,436.00	69,658.00	21,856.00	1.15	208.33
Saccharomycopsis crataegensis	*Ascomycota*	0.59392	0.84665	13,584.00	69,387.00	72,319.00	1.48	510.80
Tricholoma saponaceum	*Basidiomycota*	0.58109	0.84636	54,336.00	61,881.00	0.00	1.5	113.89
Bensingtonia sp	*Basidiomycota*	0.26624	0.74325	12,563.00	38,813.00	0.00	1.31	308.95
Udeniomyces pyricola	*Basidiomycota*	0.58109	0.84636	16,718.00	36,133.00	0.00	1.28	216.13
Mortierella horticola	*Zygomycota*	0.58109	0.84636	0.00	36,133.00	26,681.00	1.28	tends to ∞
Acremonium implicatum	*Ascomycota*	0.58109	0.84636	22,559.00	36,133.00	0.00	1.28	160.17
Inocybe assimilata	*Basidiomycota*	0.11732	0.56146	0.00	31,998.00	0.00	1.23	tends to ∞
Hansfordia pulvinata	*Ascomycota*	0.97977	0.97977	19,325.00	27,863.00	26,681.00	0.722	144.18
Candida diversa	*Ascomycota*	0.69073	0.86564	2,784.70	21,917.00	14,604.00	3.98	787.05
Candida apicola	*Ascomycota*	0.69073	0.86564	17,703.00	21,485.00	25,185.00	3.57	121.36

Candida stellata	*Ascomycota*	0.26624	0.74325	0.00	13,932.00	45,026.00	1.37	tends to ∞
Metschnikowia pulcherrima	*Ascomycota*	0.04903	0.56146	2,744.50	8,929.20	406.45	3.63	325.35
Pichia kluyveri	*Ascomycota*	0.56553	0.84636	4,297.40	8,020.60	3,915.90	3.31	186.64
Cryptococcus chernovii	*Basidiomycota*	0.04541	0.56146	524.73	1,089.10	139.51	2.68	207.55
Zygosaccharomyces bisporus	*Ascomycota*	0.92517	0.95859	169.14	1,010.10	285.43	2.62	597.20
Articulospora sp	*Ascomycota*	0.68113	0.86564	624.23	813.06	132.49	2.53	130.25
Cryptococcus sp	*Basidiomycota*	0.09813	0.56146	446.47	748.62	213.42	2.43	167.68
Zygosaccharomyces bailii	*Ascomycota*	0.44436	0.84636	391.04	661.75	553.30	2.13	169.23
Alternaria alternata	*Ascomycota*	0.16041	0.64427	429.50	501.99	248.13	2.11	116.88
Paraconiothyrium hawaiiense	*Ascomycota*	0.69723	0.86564	306.65	422.43	915.95	2.49	137.76
Exobasidiomycetes sp	*Basidiomycota*	0.92998	0.95859	290.07	417.58	152.33	2.13	143.96
Candida intermedia	*Ascomycota*	0.10133	0.56146	0.00	403.00	26,681.00	2.31	tends to ∞
Candida stellimalicola	*Ascomycota*	0.11732	0.56146	0.00	386.02	0.00	2.29	tends to ∞
Sporobolomyces coprosmae	*Basidiomycota*	0.16347	0.64427	310.06	379.60	23.17	2.25	122.43
Tremellales sp	*Basidiomycota*	0.30851	0.79501	47.02	261.48	77,112.00	2.03	556.10
Dissoconium sp	*Ascomycota*	0.12972	0.57943	0.00	104.55	53,362.00	1.73	tends to ∞
Saccharomycodes ludwigii	*Ascomycota*	0.03178	0.56146	0.00	0.00	540.83	2.43	-
Cenococcum geophilum	*Ascomycota*	0.22522	0.74325	49,627.00	43,099.00	105.11	1.51	86.85
Atheliaceae sp	*Basidiomycota*	0.58109	0.84636	81,505.00	41,254.00	0.00	1.62	50.62
Candida californica	*Ascomycota*	0.11418	0.56146	44,246.00	38,470.00	776,360.00	5.57	86.95
Hysterangium thwaitesii	*Basidiomycota*	0.58109	0.84636	62,815.00	32,784.00	0.00	1.51	52.19
Rhodotorula sp	*Ascomycota*	0.77203	0.89183	70,243.00	31,998.00	36,298.00	1.3	45.55
Mortierella pseudozygospora	*Zygomycota*	0.8911	0.94768	33,436.00	27,593.00	23.17	0.788	82.52
Lophiostoma macrostomum	*Ascomycota*	0.07658	0.56146	81,121.00	22,422.00	0.00	1.62	27.64
Agaricales sp	*Basidiomycota*	0.58109	0.84636	45,117.00	20,627.00	0.00	1.37	45.72
Fungi sp		0.22993	0.74325	23,879.00	20,067.00	11,400.00	3.8	84.04
Tomentella sp	*Basidiomycota*	0.54367	0.84636	22,559.00	18,067.00	49,851.00	1.23	80.09
Meyerozyma guilliermondii	*Ascomycota*	0.54367	0.84636	19,325.00	1,327.90	53,362.00	2.82	6.87
Pleosporales sp	*Ascomycota*	0.73345	0.87269	1,287.80	1,218.50	1,104.70	1.97	94.62
Saccharomycetales sp	*Ascomycota*	0.47098	0.84636	54,446.00	768.17	341.24	2.55	1.41
Phacidiella eucalypti	*Ascomycota*	0.74244	0.87269	1,370.50	591.07	565.06	2.61	43.13
Chalastospora ellipsoidea	*Ascomycota*	0.46512	0.84636	676.11	384.99	286.01	2.29	56.94
Stemphylium herbarum	*Ascomycota*	0.01732	0.56146	307.83	303.24	0.00	2.19	98.51
Ramichloridium indicum	*Ascomycota*	0.85864	0.92789	55,994.00	255.30	266.81	2.03	0.46
Mycosphaerellaceae sp	*Ascomycota*	0.82583	0.90706	357.27	230.47	318.80	1.81	64.51
Filobasidium floriforme	*Basidiomycota*	0.10958	0.56146	58,562.00	213.77	23.17	1.98	0.37
Aureobasidium pullulans	*Ascomycota*	0.82116	0.90706	124.55	183.40	122.45	1.5	147.25
Acaromyces ingoldii	*Basidiomycota*	0.45469	0.84636	842.59	168.87	286.04	2.53	20.04
Tilletiopsis pallescens	*Basidiomycota*	0.2881	0.77211	291.83	165.72	53,362.00	2.08	56.79

Ascomycota sp	*Ascomycota*	0.42625	0.84636	55,994.00	155.92	36,298.00	1.78	0.28
Cryptococcus victoriae	*Basidiomycota*	0.05683	0.56146	137.25	136.26	0.00	1.84	99.28
Russula vesca	*Basidiomycota*	0.63054	0.86217	66,872.00	132.13	26,681.00	1.73	0.20
Dothideomycetes sp	*Ascomycota*	0.42113	0.84636	50,252.00	113.04	26,681.00	1.65	0.22
Tremellomycetes sp	*Basidiomycota*	0.19862	0.73931	22,559.00	103.60	26,681.00	1.62	0.46
Devriesia pseudoamericana	*Ascomycota*	0.63054	0.86217	22,559.00	65.47	18,958.00	1.38	0.29
Russula sp	*Basidiomycota*	0.11732	0.56146	84,394.00	0.00	0.00	1.64	0
Thelephoraceae sp	*Basidiomycota*	0.26624	0.74325	16,718.00	0.00	59,468.00	1.49	0
Scleroramularia abundans	*Ascomycota*	0.58109	0.84636	16,718.00	0.00	53,362.00	1.44	0
Periconia sp	*Ascomycota*	0.58109	0.84636	45,117.00	0.00	26,681.00	1.37	0
Incertae sedis sp		0.69768	0.86564	3,335,700.00	2,231,500.00	2,178,100.00	5.76	66.90

In the signature results obtained from the data of five samples per treatment, it can be observed that some species were inhibited by the treatments. For instance, fourteen species are not detected in Water, such as *Aspergillus niger*, *Tricholoma saponaceum*, *Acremonium implicatum*, *Lophiostoma macrostomum*, *Stemphylium herbarum*. In the Bion treatment, species like *Saccharomycodes ludwigii*, *Scleroramularia abundans*, *Russula* sp, *Thelephoraceae* sp, *Periconia* sp are absent. Meanwhile, in the Control group species such as *Mortierella horticola*, *Inocybe assimilata*, *C. stellata*, *C. intermedia*, *C. stellimalicola*, *Dissoconium* sp. and *Saccharomycodes ludwigii* are not found.

Hence the treatment parameter can influence the distribution of fungal species abundances. In Table 4.21, the most relevant yeast species in the Bion treatment are outlined. Various colours indicate different species prevalence when comparing the Bion treatment with the Control. This table generated from LEfSe highlighted *Hanseniaspora uvarum* as the most represented species in all the experimental conditions. This sheet confirms that the yeast *I. terricola* (or *Pichia terricola*), *C. californica*, *Meyerozyma guilliermondii* (basionym *Pichia guilliermondii*), *C.*

stellata, *C. intermedia* are more abundant in Water treatment.

Excluding *H. uvarum*, which is prevalent in each case, a specific fungal signature is outlined comparing the abundance of the Control and Bion group. As the comparison between these groups may be relevant in the vineyard applications.

The Bion treatment is characterized by greater richness of:

- *Issatchenkia terricola* (Phylum Ascomycota)
- *Fusarium sp.* (Phylum Ascomycota)
- *Oidiodendron sp.* (Phylum Ascomycota)
- *Saccharomycopsis crataegensis* (Phylum Ascomycota)
- *Candida stellata* (Phylum Ascomycota)
- *Candida intermedia* (Phylum Ascomycota)
- *Candida stellimalicola* (Phylum Ascomycota)
- *Metschnikowia pulcherrima* (Phylum Ascomycota)
- *Zygosaccharomyces bisporus* (Phylum Ascomycota)
- *Dissoconium sp.* (Phylum Ascomycota)
- *Rozellomycota sp.* (Phylum Rozellomycota)
- *Cryptococcus chernovii* (Phylum Basidiomycota)
- *Bensingtonia sp.* (Phylum Basidiomycota)
- *Udeniomyces pyricola* (Phylum Basidiomycota)
- *Inocybe assimilata* (Phylum Basidiomycota)
- *Tremellales sp.* (Phylum Basidiomycota)
- *Mortierella horticola* (Phylum Zygomycota)

The Control is characterized by:

- *Lophiostoma macrostomum* (Phylum Ascomycota)
- *Ramichloridium indicum* (Phylum Ascomycota)
- *Saccharomycetales sp.* (Phylum Ascomycota)
- *Dothideomycetes sp.* (Phylum Ascomycota)
- *Cenococcum geophilum* (Phylum Ascomycota)
- *Candida californica* (Phylum Ascomycota)
- *Rhodotorula sp.* (Phylum Basidiomycota)
- *Atheliaceae sp.* (Phylum Basidiomycota)
- *Hysterangium thwaitesii* (Phylum Basidiomycota)
- *Russula vesca* (Phylum Basidiomycota)
- *Russula sp.* (Phylum Basidiomycota)
- *Filobasidium floriforme* (Phylum Basidiomycota)
- *Agaricales sp.* (Phylum Basidiomycota)
- *Mortierella pseudozygospora* (Phylum Zygomycota).

Using the LEfSe tool, it is possible to highlight the OTUs (species) that show a significant difference between the treatments, even if the three experimental conditions do not show significant differences between the fungal communities under study. It also allows to access the magnitude of differences between the treatments on the species in question. These species could be identified as potential biomarkers for the experimental conditions (Fig. 4.28).

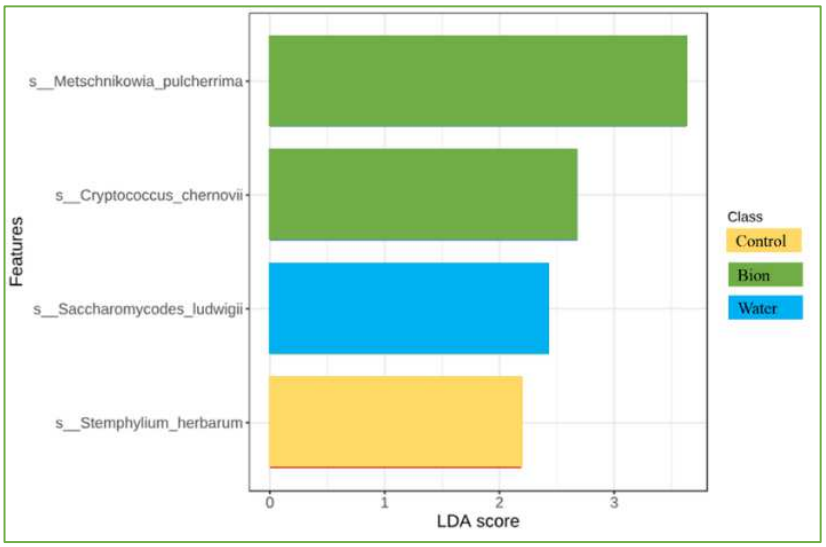

Figure 4.28. "LEfSe" tool identifies features (OTUs) with statistically significant differences and highlight the species driving the differences (α=0.05).

4.2.3 Discussion

The aim of this work was to describe the mycobiota associated with grapes from vines subjected to three different pest management conditions: Integrated Pest Management (IPM), IPM

combined with the plant biostimulant BION®50WG (Syngenta) and IPM combined with water fogging.

The results showed that the two-year treatment with BION®50WG did not reveal any significant differences in the biodiversity of the mycobiota from the three experimental conditions. Geographical location is therefore always the main determinant of the composition of the fungal community in the vineyard. Climatic conditions, seasonal pattern, pollution, soil conditions, etc. have a decisive influence on the microbial structure, as well as on the fungal microbiota balance (6,7,8). In the research of Perazzoli and co-workers (8), has been demonstrated that the phyllosphere microbiota of the grapevine was minimally affected by the treatments tested, while they differed mainly according to the topographical localisation of the grapevine (7).

The table 4.20, including the values of all indexes for each sample. The highest Shannon's Index values were observed in samples R6P11 (Control) with 1.67, R9P11 (Bion) with 1.59, and R10P16 (Bion) with 1.61. Conversely, samples R3P18 (Control) with 1.14, R8P1 (Control) with 1.05, and R9P3 (Bion) with 1.11 exhibited the lowest fungal biodiversity. The Shannon alpha diversity values in Control and Bion groups were dispersed, while in the Water treatment, they were closer to the median (Figure 4.21B). Simpson's index values were all close to 0.618, indicating a low biodiversity in each treatment (Figure 4.21C).

No more than the alpha diversity, related to the "observed" species (richness in species), was statistically significant among the samples (p-value = 0.04999). And it is noted that the water atomisation caused a reduction in the yeast biodiversity of the

grape skin probably due to the wash-out effect, as shown in the box plot in Figure 4.21 A. In fact, the lowest number of fungal species observed was found in the water samples. The highest number of fungal species observed was found in the Bion samples (Fig. 4.21 A and tab. 4.20). It is observed that the commercial product BION®50WG is formulated as water-dispersible granules, intended for use in water suspension through foliar treatment. Therefore, it is not directly comparable to the action of water alone, due to the co-formulants that may have adhesive properties. Typically, plant protection products are designed with specific chemical and physical properties that enable the active molecule to adhere to and penetrate the leaves.

The statistical analysis of diversity among the samples indicates their similarity in terms of the composition of fungal communities. The beta-diversity in all the treatments is notably regular. It can be hypothesized that the grouping of samples is independent of the treatments and is likely influenced by climatic conditions and position, as suggested by Vaudano and colleagues (9,10). This hypothesis finds support in the heatmap graphic, illustrating the fungal community composition in terms of the main species and their respective abundance.

The similarity observed in both Alpha and Beta diversity indexes is corroborated by the minimal differences in the species belonging to the identified signature, as detailed below.

The data presented as a pie chart (Figure 4.23), illustrates that the Not-Assigned OTUs constitute a substantial group in terms of relative abundance. This highlights a limitation of the metabarcoding method, as some reads lack corresponding ITS libraries database, particularly for fungi not yet cultivated or those

deemed unculturable in laboratory conditions (7,8).

The core microbiota graphs (Figure 4.24) highlight that *H. uvarum* represents the dominant species in all the treatments, particularly in the Water one. This confirms that *H. uvarum* is the most common yeast during grape ripening (11). It is demonstrated that the strains of this species are highly adapted to living on grapes, partly due to their ability to metabolize some microbial toxins (8,12).

The heatmap figure (Figure 4.26) shows a considerable uniformity among the samples R3P18 (Control), R8P1 (Control), R13P6 (Water), R13P13 (Water), which are characterised by a low yeast abundance. This is probably due to their location, close to the vineyard edge and more exposed to wind and drought effects.

In terms of the species assigned and their abundance, the bunches sampled in the middle of the Control parcel (R6P11 and R7P13) exhibit a similar composition. Sample R5P8 (Control) seems to behave as an intermediate between R3P18 (Control) and R6P11 (Control) or R7P13 (Control) in number fungal species and the respective abundance. Samples taken from row 9 (Bion) are more similar to the central samples of the Control group. This is probably due to the drift effect which conveyed the BION®50WG spray towards the lower rows (10 and 11), considering the land slop. Consequently, R9P3 (Bion) and R9P11 (Bion) show more similarity to R6P11 (Control) or R7P13 (Control) than the other three grapes harvested from Bion parcel. R10P6 (Bion), R10P16 (Bion) and R11P7 (Bion) are quite similar to each other; indeed, they only have in common a notable abundance of *Zygoascus* sp., *Candida* sp., *Pichia* sp. and the scarceness of all other species

considered in the heatmap. Looking at the Bion group, the biostimulant seems to have a slightly positive effect on biodiversity. However, *H. uvarum*, which is ubiquitous on ripening grapes according to literature, is present in low abundance in three out of five samples from the Bion group. The Water group exhibits a low fungal biodiversity, likely attributed to the washout effect of foliar irrigation involving the vine crown. The sample collected from row 13 displayed a predominance of the *Candida* genus, primarily represented by the species *C. californica*. Conversely, the samples from row 14 exhibited high abundances of *Pleosporales* sp., *Aureobasidium* sp., *H. uvarum*, and *C. diversa*.

Regarding the signature, the unique set of fungal taxa (Table 4.21) that characterise a specific environment or condition, no significant differences can be observed (13,14).

However, four OTUs showning to be significantly affected by the experimental conditions could be extrapolated from the LEfSe (Fig. 4.28).

- *Metschinkowia pulcherrima* and *Cryptococcus chernovii* are favourite by the Bion conditions.
- *Saccharomycodes ludwigii* is favourite by the humidity of water condition and appeared absent in Bion and Control group as in table Lefse.
- *Stemphylium herbarium* is favourite in Control.

This species may be considered as biomarker associated to a specific treatment.

Some species were inhibited by the treatments, as in the table of LEfSe, where the absence is annotated.

Through the ratio between Bion and Control abundance (Tab.

4.21) it is possible to appreciate that the proliferation of some yeasts, such as *Issatchenkia terricola, Saccharomycopsis crataegensis, Candida stellata, C. intermedia, C. stellimalicola, Zygosaccharomyces bisporus, Tremellales sp., Dissoconium sp.,* seams favourite by BION®50WG.

Much research has been conducted on fungal communities at the time of grape harvesting. Analysing the mycobiota of Montepulciano cv. in organic, conventional and not treated management (respectively OM, CM, NTM), Agarbati and coworkers (15) did not find significant differences among treatments, and *H. uvarum* resulted the predominant yeast in each sample. Analogous conclusion was achieved by Costantini *et al*. (11). Similarly, in our Barbera cv. samples, the frequency of *H. uvarum* was 43.96% in Control, 38.28% in Bion and 47.88% in Water (relative abundance per treatment used in pie-chart), making it dominant in the grape environment, regardless of the treatment. *H. uvarum* higher relative abundance in Water group can be explained by the erosion of 15 species due to irrigation leaching.

Costantini et al. in 2022 and Agarbati et al. in 2019 detected *Aureobasidium pullulans* (oxidative yeast-like) in all management conditions. In NMT, the highest prevalence of *A. pullulans* was recorded (50%), underlining that the absence of treatment favours its growth (11,15). Further studies showed that this microorganism was among the most commons at harvesting time of the grapevine (16). In this study *A. pullulans* was detected with low presence in each experimental condition (tab. 4.21). From the pie-chart (Fig. 4.23) it is highlighted only in the Bion group with 10% of abundance. Yeast species such as *H. uvarum*, *I. terricola*,

Meyerozyma guilliermondii, *Candida* sp., normally present on ripe grapes and in the initial stages of must fermentation (11,12,15,17), were more abundant in the water treatment. It is possible to hypothesise that they take advantage of the high humidity or of the lower presence of other species due to the foliar irrigation. Furthermore, in Water group (tab. Lefse), species such as *Aspergillus niger, Tricholoma saponaceum, Udeniomyces pyricola, Acremonium implicatum, Stemphylium herbarum* were not detectable. They could also be washed away from the grapes.

The mycobiota composition described here is similar to that reported in the De Filippis and coworkers research on the monitoring of mycobiota during the spontaneous alcoholic fermentation (18). The yeast communities in the beginning of spontaneous fermentation are comparable with the grape mycobiota. In fact, during the initial stages of fermentation, the high abundance of non-*Saccharomyces* yeasts such as *H. uvarum*, *P. kluyveri*, *C. stellata*, *M. pulcherrima*, *I. terricola* is typical of the grape skin (18).

REFERENCES

(1) Vaudano, E.; Quinterno, G.; Costantini, A.; Pulcini, L.; Pessione, E.; Garcia-Moruno, E. (2019) Yeast Distribution in Grignolino Grapes Growing 684 in a New Vineyard in Piedmont and the Technological Characterization of Indigenous Saccharomyces Spp. Strains. *Int. J. Food Microbiol*. 289, 154–161. DOI: 10.1016/j.ijfoodmicro.2018.09.016.

(2) Polizzotto, G.; Barone, E.; Ponticello, G.; Fasciana, T.; Barbera, D.; Corona, O.; Amore, G.; Giammanco, A.; Oliva, D. (2016) Isolation, identification and oenological characterization of non-Saccharomyces yeasts in a Mediterranean island. Lett. Appl. Microbiol. 63(2), pp 131-138. DOI: 10.1111/lam.12599

(3) Capece; A.; Pietrafesa, R.; Siesto, G.; Romaniello, R.; Condelli, N.; Romano, P. (2019) Selected Indigenous *Saccharomyces cerevisiae* Strains as Profitable Strategy to Preserve Typical Traits of Primitivo Wine. Fermentation. 5, no. 4: 87. DOI: 10.3390/fermentation5040087

(4) Yunan, D.; Xianliang, Q.; Xiaochen, W. Study on Cation Exchange Capacity of Agricultural Soils. IOP Conf. Ser. Mater. Sci. Eng. 2018, 392, 042039, doi:10.1088/1757-899X/392/4/042039

(5) Edgar, R.C. Accuracy of Microbial Community Diversity Estimated by Closed- and Open-Reference OTUs. PeerJ 2017, 5, e3889, 719 doi:10.7717/peerj.3889 720 67.

(6) Bokulich, N.A.; Thorngate, J.H.; Richardson, P.M.; Mills, D.A.

PNAS Plus: From the Cover: Microbial Biogeography of Wine Grapes Is Conditioned by Cultivar, Vintage, and Climate. Proc. Natl. Acad. Sci. USA 2014, 111, E139–E148.

(7) Stone, B.W.G.; Jackson, C.R. Seasonal Patterns Contribute More Towards Phyllosphere Bacterial Community Structure than Short-Term Perturbations. Microb. Ecol. 2021, 81, 146–156.

(8) Perazzolli, M.; Antonielli, L.; Storari, M.; Puopolo, G.; Pancher, M.; Giovannini, O.; Pindo, M.; Pertot, I. Resilience of the Natural Phyllosphere Microbiota of the Grapevine to Chemical and Biological Pesticides. Appl. Environ. Microbiol. 2014, 80, 3585–3596.

(9) Ramirez, K.S.; Snoek, L.B.; Koorem, K.; Geisen, S.; Bloem, L.J.; ten Hooven, F.; Kostenko, O.; Krigas, N.; Manrubia, M.; Cakovi´c, D.; et al. Range-Expansion Effects on the Belowground Plant Microbiome. Nat. Ecol. Evol. 2019, 3, 604–611.

(10) Vaudano, E.; Quinterno, G.; Costantini, A.; Pulcini, L.; Pessione, E.; Garcia-Moruno, E. Yeast Distribution in Grignolino Grapes Growing in a New Vineyard in Piedmont and the Technological Characterization of Indigenous Saccharomyces spp. Strains. Int. J. Food Microbiol. 2019, 289, 154–161.

(11) Costantini, A.; Vaudano, E.; Pulcini, L.; Boatti, L.; Gamalero, E.; Garcia-Moruno, E. (2022) Yeast Biodiversity in Vineyard during Grape Ripening: Comparison between Culture

Dependent and NGS Analysis. *Processes*. 10, 901.

(12) Gómez-Albarrán, C.; Melguizo, C.; Patiño, B.; Vázquez, C.; Gil-Serna, J. Diversity of Mycobiota in Spanish Grape Berries and Selection of *Hanseniaspora uvarum* U1 to Prevent Mycotoxin Contamination. Toxins 2021, 13, 649.

(13) Bona, E.; Massa, N.; Toumatia, O.; Novello, G.; Cesaro, P.; Todeschini, V.; Boatti, L.; Mignone, F.; Titouah, H.; Zitouni, A.; et al. (2021) Climatic Zone and Soil Properties Determine the Biodiversity of the Soil Bacterial Communities Associated to Native Plants from Desert Areas of North-Central Algeria. Microorganisms. 9, 1359.

(14) Segata, N.; Izard, J.; Waldron, L.; *et al.* (2011) Metagenomic biomarker discovery and explanation. *Genome Biol* **12**, R60. DOI: 10.1186/gb-2011-12-6-r60

(15) Agarbati, A.; Canonico, L.; Mancabelli, L.; Milani, C.; Ventura, M.; Ciani, M.; Comitini, F. (2019) The Influence of Fungicide Treatments on Mycobiota of Grapes and Its Evolution during Fermentation Evaluated by Metagenomic and Culture-Dependent Methods. Microorganisms. 7, 114

(16) Setati, M.E.; Jacobson, D.; Andong, U.-C.; Bauer, F. (2012) The Vineyard Yeast Microbiome, a Mixed Model Microbial Map. PLoS ONE. 7, e52609.

(17) Comitini, F.; Ciani, M. (2008) Influence of fungicide treatments on the occurrence of yeast flora associated with wine grapes. Ann. Microbiol. 58, 489–493.

(18) De Filippis, F.; La Storia, A.; Blaiotta, G. (2017) Monitoring the Mycobiota during Greco Di Tufo and Aglianico Wine Fermentation by 18S RRNA Gene Sequencing. Food Microbiol. 63, 117–122.

(19) Rosini, G., Federici, F. & Martini, A. (1982) Yeast flora of grape berries during ripening. Microb Ecol 8, 83–89. DOI: 10.1007/BF02011464

(20) Renouf, V., Claisse, O. and Lonvaud-funel, A. (2005), Understanding the microbial ecosystem on the grape berry surface through numeration and identification of yeast and bacteria. Australian Journal of Grape and Wine Research, 11: 316-327. DOI: 10.1111/j.1755-0238.2005.tb00031.x

(21) Fleet, G., Prakitchaiwattana, C., Beh, A., Heard, G. (2002) The yeast ecology of wine grapes. In: Ciani, M. (Ed.), Biodiversity and Biotechnology of Wine Yeasts. Research Signpost, Kerala, India, pp. 1–17.

(22) Barata, A.; Malfeito-Ferreira, M.; Loureiro, V. (2012) The microbial ecology of wine grape berries, Int. J. of Food Microbiology, Volume 153, I 3, pp 243-259. DOI: 10.1016/j.ijfoodmicro.2011.11.025.

(23) Hoffmann, A.; Posirca, A.-R.; Lewin, S.; Verch, G.; Büttner, C.; Müller, M.E.H. Environmental Filtering Drives Fungal Phyllo-sphere 721 Community in Regional Agricultural Landscapes. Plants 2023, 12, 507. doi: 10.3390/plants12030507

Chapter V

Exploring the yeast at the end of the spontaneous alcoholic fermentation

5.1 Spontaneous alcoholic fermentation

Considering that due to the very low concentration of *Saccharomyces cerevisiae* DNA respect to the whole DNA of the mycobiota, this species was undetectable by NGS technique and metabarcoding. Similarly, because of the rare presence of this species in vineyard, after the serial dilution, through ARDRA method applied on the species isolated from the berries skin, *cerevisiae* shown non-existent. Just by the way of spontaneous fermentation, that represents an enrichment broth for *Saccharomyces* sp. and other fermentative yeasts, their presence could assess.

In this section I'm going to describe the effect of the experimental vineyard conditions on the fermentation process, evaluating the dominant indigenous strains, especially *Saccharomyces cerevisiae*, at the end of the spontaneous alcoholic fermentation (AF) of five grape sampled per thesis. Fifteen micro-fermentations were prepared as described in chapter 3 (Fig.5.1).

Figure 5.1. Fifteen spontaneous micro-fermentation corresponding to fifteen grapes collected from the experimental vineyard according to the three treatments.

The trend of the fermenting must during the spontaneous process was monitored. The fermentations were followed recording the weight loss and were considered completed at constant weight (Fig. 5.2) even if the sugar was not finished. The spontaneous process lasted about 2 months.

On the fifteen natural wines the alcohol content was implemented to know the effectiveness of the spontaneous fermentation and predict the presence of *S. cerevisiae* in the sampled bunches.

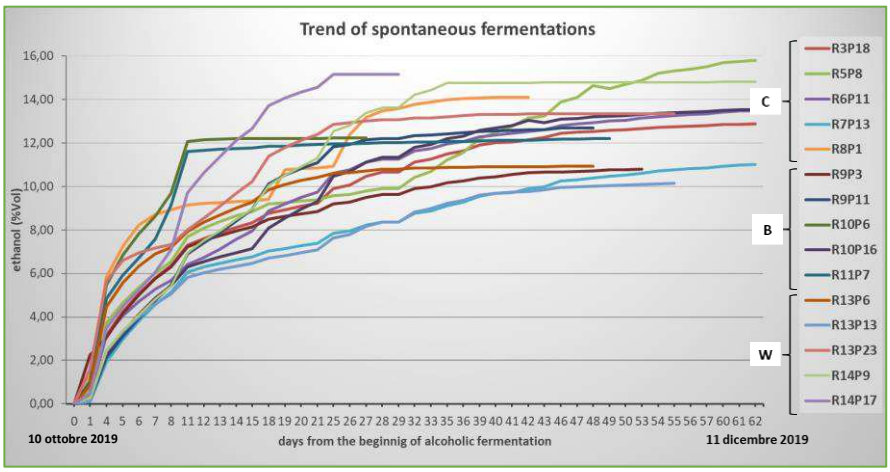

Figure 5.2. Fermentation trend: Monitoring of AF by the registration of the daily weight loss. Due to the absence of a culture starter is possible verify as the fermentation trend is very variable, according to the microflora present on the grapes.

At the end of AF chemical and microbiological protocols was carried out. The basic chemical analysis was performed to demonstrate the true ethanol production and the quantitation of dry extract was performed to evaluate the residual sugar.

While the microbiological analysis, concerning in the identification at strain level of *S. cerevisiae* through microsatellite analysis or at species level of vinery yeast through ARDRA was

applied.

5.1.1 Chemical analysis at the end of the Alcoholic fermentation

Both the alcohol content and the dry extract was evaluated by DMA 5000 Anton Paar Density Meter (Anton Paar GmbH – Graz, Austria) for each sample.

After the evaluation of the wine density, the distillation of 100 ml was performed, and the alcohol density was completed. Each value was recorded to estimate the alcohol ratio and the total dry matter (Tab. 5.1). All the four parameters represent the estimation of the sugar consumption by the yeast.

Table 5.1. The values of alcohol percentage were returned directly by the instrument such as the wine density and the distillate. While the total dry matter was obtained from the conversion tables.

Sample (Row/Plant)	Wine $D_{20/20}$	Alcohol (% vol)	Alcohol $D_{20/20}$	Total Dry Matter (g/l)
R3P18C	1,007742	12,41	0,983646	62,4
R5P8C	0,995794	15,98	0,979653	41,6
R6P11C	1,007657	12,91	0,983076	63,7
R7P13C	1,029808	9,99	0,986490	112,4
R8P1C	0,993592	13,92	0,981940	30,0
R9P3B	1,027559	9,93	0,98657	104
R9P11B	1,013056	11,69	0,984488	74,1
R10P6B	0,9942305	11,91	0,984222	25,8
R10P16B	1,007196	12,94	0,983038	62,6
R11P7B	0,994413	11,07	0,985212	23,7
R13P6W	0,998072	9,60	0,986962	28,7
R13P13W	1,021925	9,77	0,986759	91,0
R13P23W	0,993684	13,55	0,982352	29,2
R14P9W	0,994037	14,76	0,980992	33,6

R14P17W	0,990848	15,32	0,980374	27,1

To obtain the dry extract value we had to apply a calculation that involve the density:

$$d_r = d_v - d_a + 1.000$$

$$d_r = 1.00180^* (r_v - r_a) + 1.000$$

where:

r_v = density of the wine at 20°C (corrected for volatile acidity

r_a = density at 20°C of the water alcohol mixture of the same alcoholic strength as the wine for a temperature of 20°C.

* The coefficient 1.0018 corrects the density for the volatile acidity, it is approximated to 1 when r_v is below 1,05, which is often the case.

Looking for the d_r results in the tables conversion we found the total dry matter. The higher alcohol content in the distillate match with the lower total dry matter value (Fig 5.3). Also, the density of the wine greater than 1 was mean that the concentration of glucose and fructose was still consistent, higher than 2 g/l.

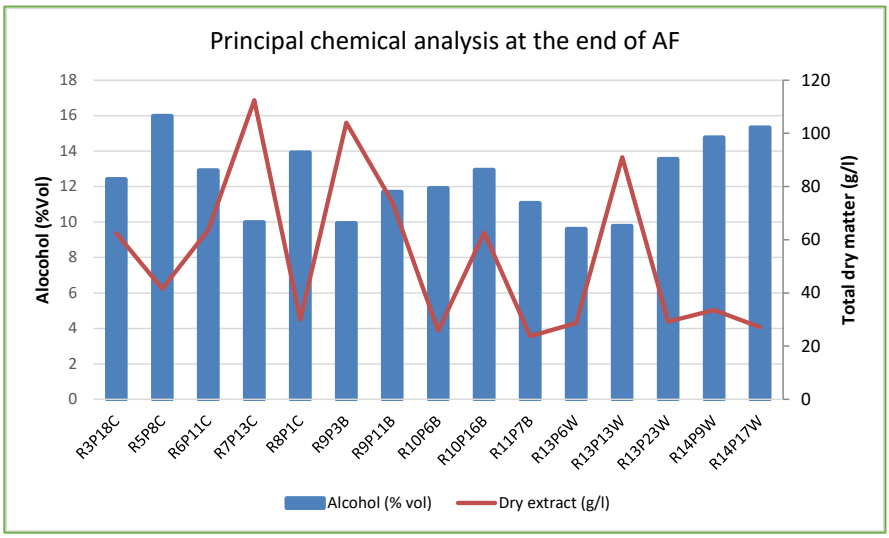

Figure 5.3. Graphic representation of both the alcohol content and the total dry matter in comparison.

The more informative chemical parameters to assess the fermentation process were alcohol content and total dry matter or dry extract that were applied for the statistical analysis in this step using the program XL-STAT.

For alcohol and dry extract parameters the descriptive statistics data was calculated and shown in tab. 5.2:

Table 5.2. The statistical descriptive parameters of alcohol percentage and dry extract were shown below.

Alcohol (%V/V)					
Category	Observations	Minimum	Maximum	Mean	Standard deviation
Control	5	9,99	15,98	13,04	2,19
Bion	5	9,93	12,94	11,51	1,11
Water	5	9,60	15,32	12,60	2,74
Dried extract (g/l)					
Category	Observations	Minimum	Maximum	Mean	Standard deviation
Control	5	30	112,4	62,02	31,56
Bion	5	23,7	104,0	58,0	33,95
Water	5	27,1	91	41,92	27,54

In order to evaluate if the three different treatments could show distinct and significative differences in the spontaneous fermentation the ANOVA, by Fisher's test, was done and demonstrate that there were no statistical differences among the thesis (Tab 5.3).

Table 5.3. ANOVA, Analysis of variance results, using Fisher's F test and considering a confidence interval of 95%, an α value threshold of 5%. For all category the F test was less than F critical therefore the difference between the samples was non-significant.

ANOVA total (2; 12 DF) Fisher's F test	**F test**	**critical F (α=0,05)**	**Pr > Diff (%) ***	**Significant**

Alcohol content (%Vol)	0,692	3,89	51,9	NO
Total dry matter (g/l)	0,585	3,89	57,2	NO

A Tukey's test through a pairwise comparison was performed and shown non-significant differences between the theses (tab 5.4).

*Table 5.4. ANOVA between the groups in comparison pairwise using Tukey's test and considering a confidence interval of 95%. The standardized difference resulted less than the critical values therefore the data tends to be much similar and the difference between the theses was non-significant (*Risk to conclude that the null hypothesis is wrong). Tukey's critical d= 3,773 (k=3; DF= 12).*

Alcohol content (%Vol)					
Contrast	Difference	Standardized difference	Critical value	Pr > Diff	Significant
Control vs Water	1,534	1,143	2,668	0,507	NO
Control vs Bion	0,442	0,329	2,668	0,942	NO
Bion vs Water	1,092	0,814	2,668	0,702	NO
Total dry matter (g/l)					
Contrast	Difference	Standardized difference	Critical value	Pr > Diff	Significant
Control vs Water	20,100	1,021	2,668	0,578	NO
Control vs Bion	3,980	0,202	2,668	0,978	NO
Bion vs Water	16,120	0,819	2,668	0,699	NO

5.1.2 Microbiological analysis at the end of the Alcoholic fermentation

This part of the research was focused on the culturable yeasts isolated at the end of AF on WLD media after an incubation for 72 h at 25°C (Fig. 5.4). The fifteen fermentations corresponding to the fifteen grapes collected for mycobiota analysis had the same

denomination by adding “EF”, for “end of fermentation”. The description and the total count of the colonies in the representative dilutions was completed (fig. frequency, tab.5.5) (1).

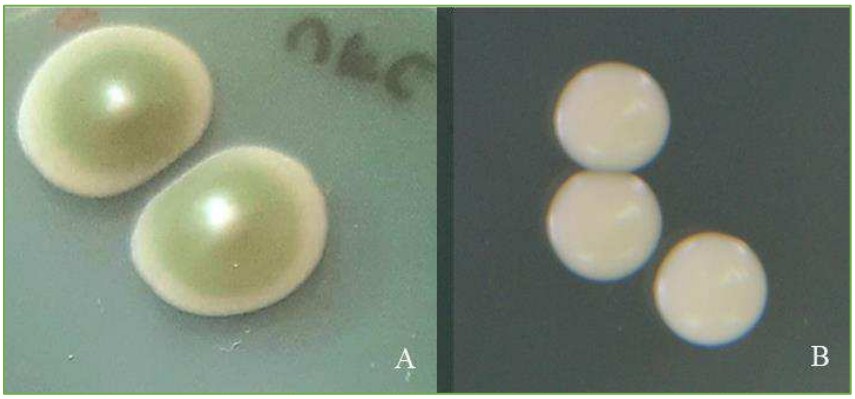

Figure 5.4. Some wine yeast morphologies. A: Saccharomyces cerevisiae colonies fully growth (wine R6P11EF); B: Zigosaccharomyces bisporus (wine R13P6EF).

Two dominant morphologies were found (Fig. 5.5):

- GREEN: rounded shape, smooth edge, opaque, creamy consistency, shape profile umbonate, green in the centre of the colony and clear in the periphery.
- CREAM: rounded shape, regular edge, opaque (sometimes shiny), shape profile convex, creamy consistency, cream colour.

A molecular identification according to Vaudano and Garcia-Moruno (2008) was accomplished. This protocol allows to discriminate *S. cerevisiae* through the detection of 100-500 bp length fragments after amplification. On the contrary, no amplifications or amplicons bigger than 500 bp indicate that the DNA is from other species (2,3).

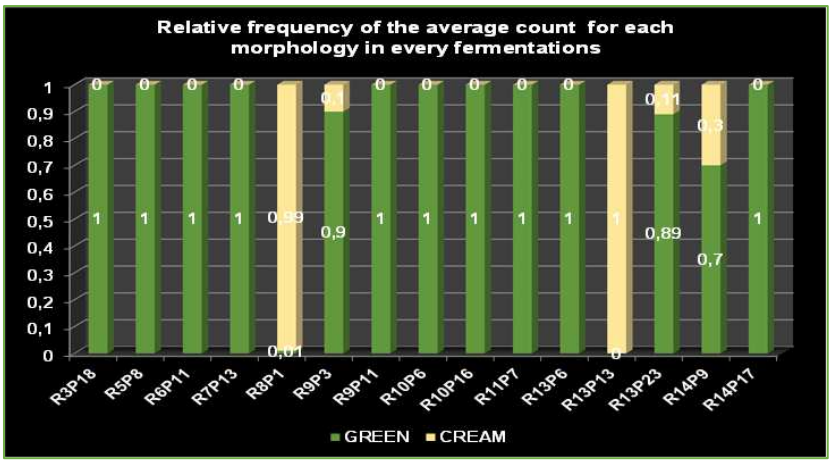

Figure 5.5. Histogram of the relative frequencies of yeast morphologies at the end of AF. The frequency was obtained by the mean count of three repetitions per fermentation.

Through microsatellite multiplex PCR the occurrence of different strains (genotype) within the species *S. cerevisiae* can be assessed, as shown in figure 5.6-5.10. Through the identification of various strain of *S. cerevisiae* at the end of the spontaneous fermentation it is directly evaluate that in R3P18, R5P8, R6P11, R8P1, R10P6, R11P7, R13P23, R14P9 and R14P17 processes was driven by the *S. cerevisiae* species.

Since the isolate at the end of AF of R7P13, R9P3, R9P11, R10P16, R13P6 and R13P13 gave unreadable microsatellite profiles after multiplex PCR with hypervariable microsatellites, their non-*Saccharomyces* identity was estimated.

Table 5.5. of the two morphologies per spontaneous fermentation in three repetitions made at the end of alcoholic fermentation.

Sample name	Dilution	Repetition	Count per morphology	Colour
R3P18	10^{-2}	I	80	green
				cream
		II	60	green
				cream
		III	94	green
				cream
R5P8	10^{-2}	I	470	green
				cream
		II	470	green
				cream
		III	502	green
				cream
R6P11	10^{-3}	I	640	green
				cream
		II	624	green
				cream
		III	604	green
				cream
R7P13	10^{-3}	I	276	green
				cream
		II	280	green
				cream
		III	280	green
				cream
R8P1	10^{-3}	I	1600	green
				cream
		II	2000	green
				cream
		III	1880	green
				cream
R9P3	10^{-3}	I	1684	green
				cream
		II	1780	green
				cream
		III	1760	green
				cream
R9P11	10^{-1}	I	20	green
				cream
		II	22	green
				cream
		III	26	green
				cream

R10P6	10^{3}	I	192	green
				cream
		II	172	green
				cream
		III	180	green
				cream
R10P16	10^{3}	I	674	green
				cream
		II	640	green
				cream
		III	652	green
				cream
R11P7	10^{2}	I	594	green
				cream
		II	520	green
				cream
		III	572	green
				cream
R13P6	10^{2}	I	202	green
				cream
		II	176	green
				cream
		III	194	green
				cream
R13P13	10^{3}	I	234	green
				cream
		II	224	green
				cream
		III	236	green
				cream
R13P23	10^{3}	I	352	green
				cream
		II	356	green
				cream
		III	342	green
				cream
R14P9	10^{5}	I	144	green
				cream
		II	142	green
				cream
		III	150	green
				cream
R14P17	10^{4}	I	406	green
				cream
		II	392	green
				cream
		III	396	green
				cream

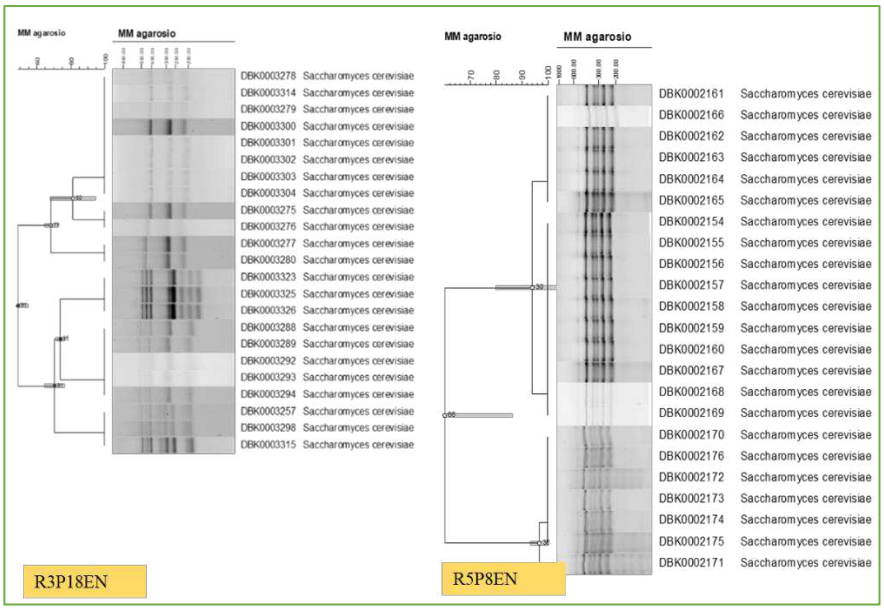

Figure 5.6. Cluster of S. cerevisiae genotypes characterised by three hypervariable microsatellite loci from the spontaneous fermentation R3P18EN (Control) and R5P8EN (Control).

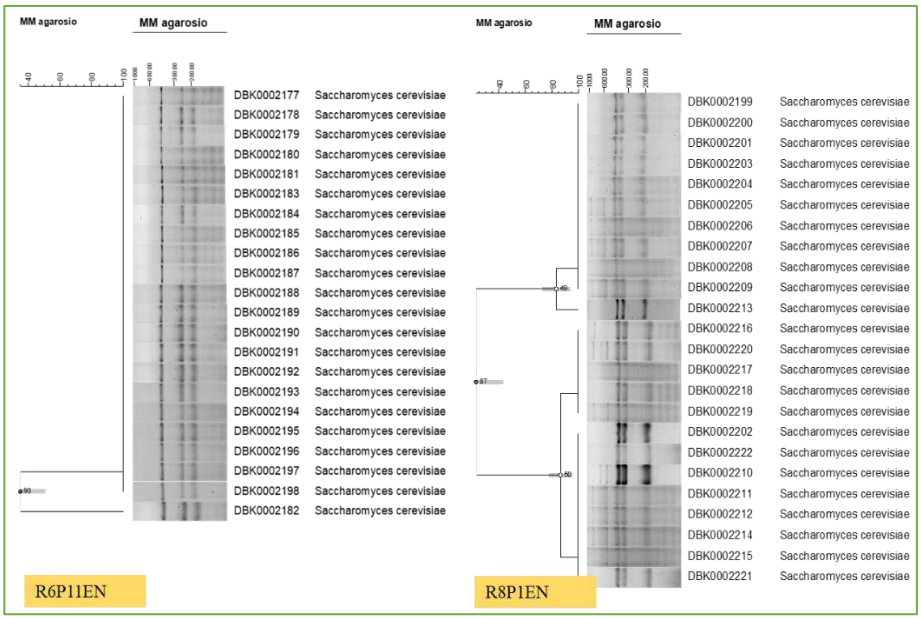

Figure 5.7. Cluster of S. cerevisiae genotypes characterised by three hypervariable microsatellite loci from the spontaneous fermentation R6P11EN (Control) and R8P1EN (Control).

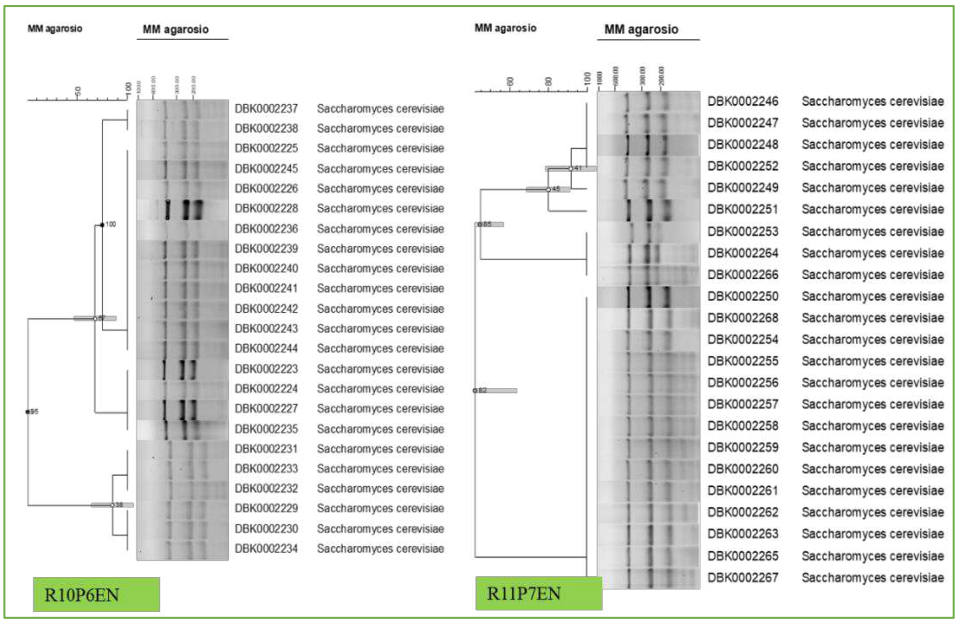

Figure 5.8. Cluster of S. cerevisiae genotypes characterised by three hypervariable microsatellite loci from the spontaneous fermentation R10P6EN (Bion) and R11P7EN (Bion).

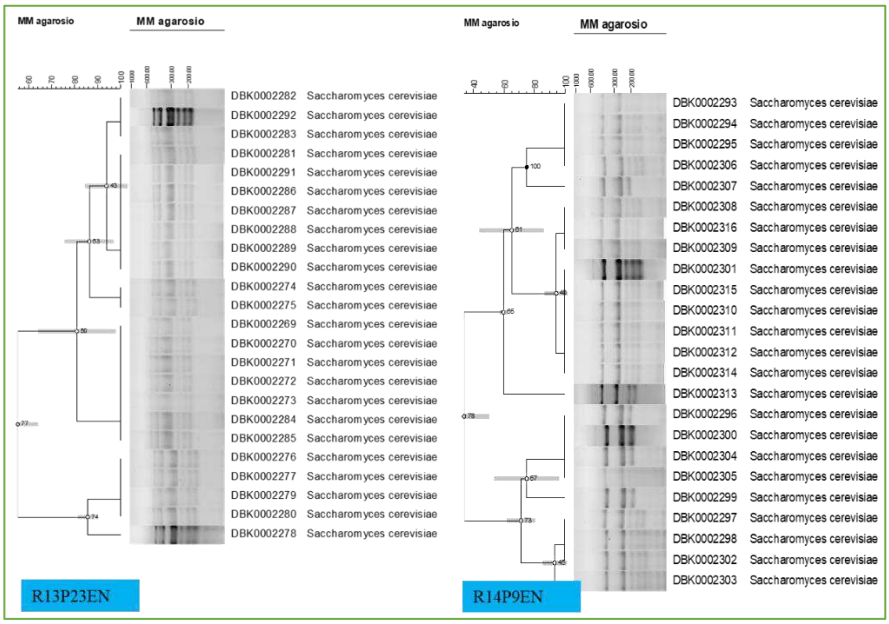

Figure 5.9. Cluster of S. cerevisiae genotypes characterised by three hypervariable microsatellite loci from the spontaneous fermentation R13P23EN (Water) and R14P9EN (Water).

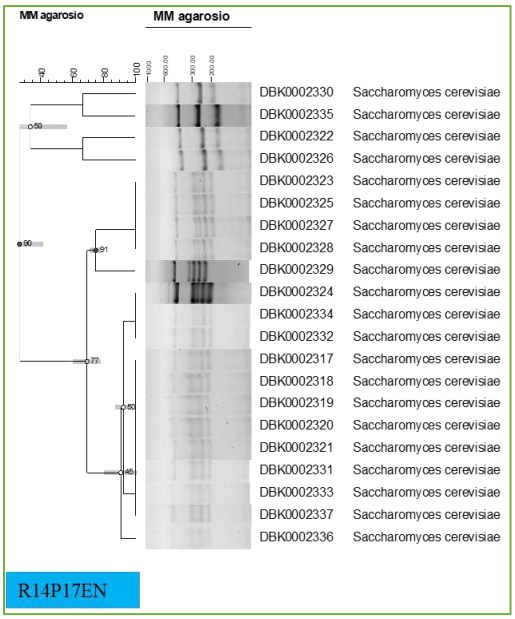

Figure 5.10. Cluster of S. cerevisiae genotypes characterised by three hypervariable microsatellite loci from the spontaneous fermentation and R14P17EN (Water).

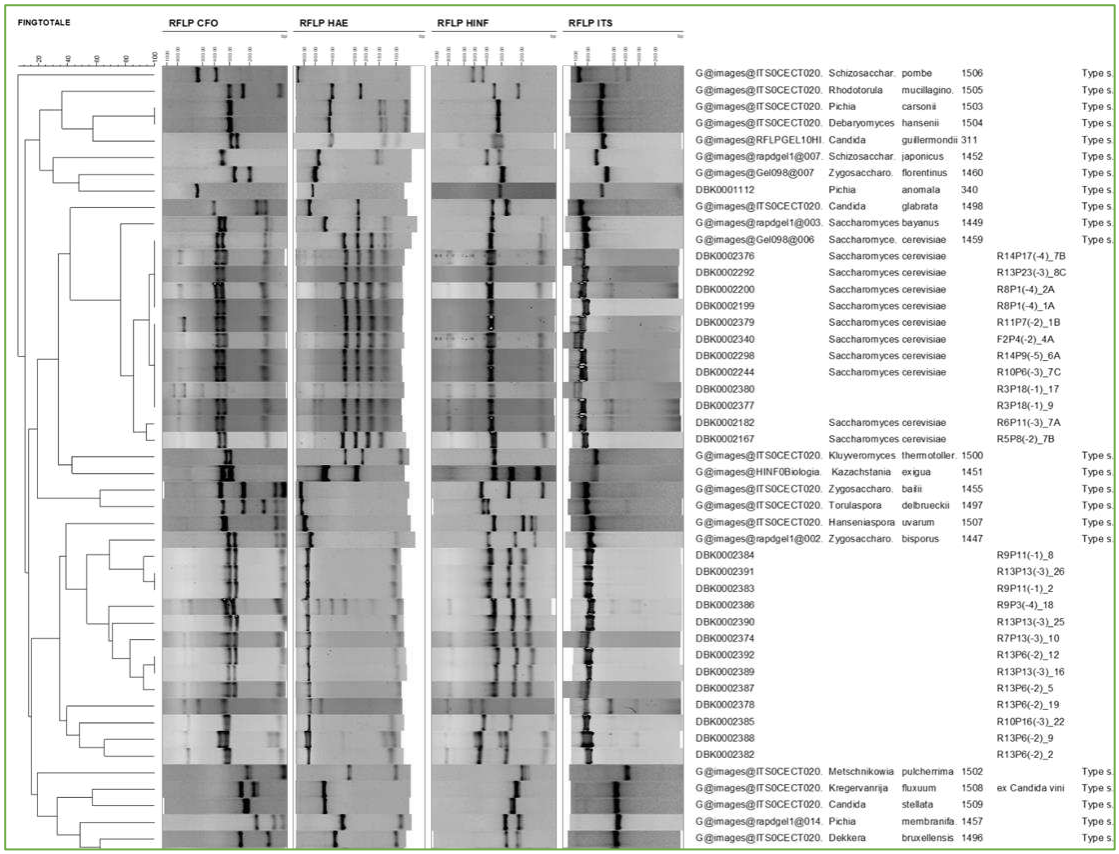

Figure 5.11. Comparison analysis among the RFLP band profile of wine yeast under study and some type strains in the CREA-VE collection, used to assess the identification at species level.

The non-*Saccharomyces* species were identified through RFLP method (4). The Analysis Comparison performed by Bionumerics™ was used to assess the identification at species level (Fig. 5.11). In these wines the fermentation was mainly driven by *Zigosaccharomyces bisporus*.

In conclusion, *S. cerevisiae* was identified in:

- Control must with four wines to five (R3P18EN, R5P8EN, R6P11EN, R8P1EN).
- Bion must with two wines to five (R10P6EN, R11P7EN).
- Water must with three wines to five (R13P23EN, R14P9EN, R14P17EN)

In general, fourteen to fifteen fermentations were carried out by *S. cerevisiae* and six to fifteen by *Z. bisporus*.

5.1.3 Discussion

This section of the thesis was focused on evaluating of possible influence of the vineyard treatments on the spontaneous alcoholic fermentation. The monitoring of the process showed that the trend was positive and there was no stop in the fermentation.

From the chemical quantification of ethanol and total dry matter, carried out two months after the beginning of the AF, it is assessed which wine was produce by *S. cerevisiae* or not. In fact, an ethanol content of less than 10% is an indication of the presence of non-*Saccharomyces* in the fermenting wine (5,6,7).

Therefore, based on the results of the molecular analyses, it can be concluded that in fermentations with ethanol concentrations reaching 12-15%, the fermentation of fermentable sugars was completed by *S. cerevisiae*. On the other hand, in vinification that

ceased with ethanol concentrations below 10%, accompanied by total dry matter values exceeding 40 g/l, the predominant yeast was *Z. bisporus*.

In literature are described yeast such as *Z. bailii*, *Wickerhamomyces anomalus*, *Hansensiaspora uvarum*, *Saccharomycodes ludwigii*, *Kluyveromyces thermotolerans*, (5), *Kloeckera apiculata*, *Candida stellata* and *Metschnikowia pulcherrima* (7), among the most abundant in spontaneous fermentation. However, Denisa *et al*. (2020) reported the presence of *Z. bisporus* in Port Wine fermented spontaneously (8).

Zygosaccharomyces sp. was detected in wine, both during and at the end of alcoholic fermentation and are associated with flavour defects (9).

In the contest of this testing, it is not found any relationship between the three experimental conditions in the vineyard (Control, Bion, Water) and the yeast species detected at the end of wine fermentation. Thus, the treatments did not select the wine yeast.

REFERENCES

(1) Vaudano, E.; Quinterno, G.; Costantini, A.; Pulcini, L.; Pessione, E.; Garcia-Moruno, E. (2019) Yeast Distribution in Grignolino Grapes Growing 684 in a New Vineyard in Piedmont and the Technological Characterization of Indigenous *Saccharomyces* Spp. Strains. Int. J. Food Microbiol. 289, 154–161. DOI: 10.1016/j.ijfoodmicro.2018.09.016.

(2) Legras, J.-L.; Ruh, O.; Merdinoglu, D.; Karst, F. (2005) Selection of hypervariable microsatellite loci for the characterization of *Saccharomyces cerevisiae* strains. International Journal of Food Microbiology, 102(1): 73-83. DOI: 10.1016/j.ijfoodmicro.2004.12.007

(3) Vaudano, E., E. Garcia-Moruno (2008) "Discrimination of *Saccharomyces cerevisiae* wine strains using microsatellite multiplex PCR and band pattern analysis", Food Microbiology 25: 56–64 doi:10.1016/j.fm.2007.08.001

(4) Esteve-Zarzoso, B., C. Belloch, F. Uruburu, A. Querol, (1999) "Identification of yeasts by RFLP analysis of the 5.8S rRNA gene and the two ribosomal internal transcribed spacers", International Journal od Systematic Bacteriology, 49, 329-337. doi:10.1099/00207713-49-1-329

(5) Capece, A., Pietrafesa, R. & Romano, P. (2011) Experimental approach for target selection of wild wine yeasts from spontaneous fermentation of "Inzolia" grapes. World J Microbiol Biotechnol 27, 2775–2783. DOI: 10.1007/s11274-011-0753-z

(6) Pinto C, Pinho D, Cardoso R, Custódio V, Fernandes J, Sousa S, Pinheiro M, Egas C and Gomes AC (2015) Wine fermentation microbiome: a landscape from different Portuguese wine appellations. Front. Microbiol. 6:905. DOI: 10.3389/fmicb.2015.00905

(7) Combina, M., Elía, A., Mercado, L., Catania, C., Ganga, A., & Martinez, C. (2005). Dynamics of indigenous yeast populations during spontaneous fermentation of wines from Mendoza, Argentina. International journal of food microbiology, 99(3), 237-243. DOI: 10.1016/j.ijfoodmicro.2004.08.017

(8) Denisa, M.; Sousa, S.; Coimbra, C.; Rogerson, F. S.; and Simões, J. (2020) "Identification and Characterization of Non-*Saccharomyces* Species Isolated from Port Wine Spontaneous Fermentations" Foods 9, no. 2: 120. DOI: 10.3390/foods9020120

(9) Pretorius, I. S., Van Der Westhuizen, T. J. & Augustyn, O. P. H. 1999. Yeast biodiversity in vineyards and wineries and its importance to the South African wine industry. a review. South African Journal of Enology & Viticulture, 20(2):61-70, doi:10.21548/20-2-2234

Chapter VI
Conclusion

6. Conclusion

Gathering all the information presented in the previous chapters, I described the following observations, focusing primarily on the metagenomic results.

The aim of this study was to evaluate the possible shifts in the fungal communities living on grapevine bunches due to the application of the biostimulant BION®50WG. Vineyards under Integrated Pest Management (IPM) were subjected to three experimental conditions: IPM, IPM + BION®50WG and IPM + foliar water fogging. Particular attention was paid to the yeast fraction, which is the main actor in the early stages of the vinification process. Three different approaches were used to characterise the fungal communities to obtain a complete picture of the yeast composition.

The metabarcoding approach were applied to compare the mycobiota on grapes according to each treatment. Alpha diversities were analysed through Shannon and Simpson indexes an in terms of richness. The statistical analysis shown no significant differences among the treatments. Only the alpha diversity of the observed species shows a significant statistical difference due to the lower number of species detectable in the Water treatment. Considering the beta diversity reported as PCoA, no statitical differences among the three groups of samples were observed. The heatmap also highlights the lower abundance of several species in Water compared to the other two groups. The LEfSe table shows that the yeasts seem inhibited in the Control group, whereas the filamentous fungi are fewer or absent in the Bion and Water treatments. Species as *Aspergillus niger* (mycotoxin producer), *Tricholoma saponaceum*,

Bensingtonia sp, *Udeniomyces pyricola*, *Acremonium implicatum* (endophytic in grapevine), *Atheliaceae* sp, *Hysterangium thwaitesii*, *Lophiostoma macrostomum* (saprophytic and plurivorous fungus), *Agaricales* sp. and *Stemphylium herbarum* (plant pathogen) are absent in Water group, instead are recorded in Bion and Control ones.

The vineyard was managed by using agrochemical against the vine parasites (IPM unites all experimental conditions); thus, the major fungal parasites are not detected in the three treatments. Since from the LEfSe table *Letiomycetes* ad *Oomycetes* Class are not reported. So, *Oidium tuckeri*, *Botritis cinerea* and *Plasmopara viticola* were contained, in fact there were no symptoms of the diseases in the vineyard.

The Control was characterized by a lower abundance of yeasts, while the Bion treatment seems preserving them.

The identification at species level through RFLP technique of the culturable yeast demonstrated that this fraction of fungi corresponds to the usual species detectable on the grape coming from vineyards where integrated pest control is conducted. So, the use of BION® 50WG generate no effect on the wine yeasts on the berry skin.

Finally, at the end of spontaneous alcoholic fermentation, no anomalies were found in terms of fermentation trend and yeast species examined, since in most spontaneous fermentations the dominance of *S. cerevisiae* was found. However, in six fermentations out of fifteen the prevalence of the wine yeast *Zigosaccharomyces bisporus* was detected. This non-Saccharomyces yeast cannot be directly associated with a specific treatment.

In conclusion, according to these results, the three different treatments do not significantly affect the fungal microbiota at the ripening time. Moreover, the use of the phytostimulant

BION®50WG on grapevine do not significantly affect the composition of fungal communities resident on the mature berries surface. Thus, concerning the wine yeast communities, ASM don't substantially modify their composition on the grapes, from this point of view, it can be used in addition to the IPM or in Integrated vine management. Considering the trial on spontaneous alcoholic fermentation, it is plausible assuming that BION®50WG will not cause problems in winemaking, probably commercial *S. cerevisiae* should not be blocked in driven fermentation.

However, in order to confirm the hypothesis, tests should be carried out with selected *S. cerevisiae* using grapes treated with BION®50WG.

Further studies must be conducted to evaluate the correlation between microbial biodiversity and the use of new product like phytostimulant, fertilizer or biocontrol agents, that will be more used in the future for their environmental sustainability. It would be advisable to carry out tests in a controlled environment so as not to have the climatic variables, which tend to alter treatments.

In the project perspective, certain aspects remain unexplored, such as assessing the technological characteristics of the selected indigenous *S. cerevisiae*. Additionally, to fully conclude the study, the assessment of both chemical parameters of oenological interest and aromatic compounds in the grape and wine should be performed. This final step would be to associate the wine style with the *Saccharomyces* yeast and the must, establishing specific aromatic compounds to estimate the microbial contribution to the "terroir".

For a comprehensive evaluation of "terroir", it is

recommended to conduct a wine tasting with a panel of experts. The wine should be produced from grapes that have been treated differently according to three experimental conditions. The results of sensory analysis should be collected, statistically processed, and represented graphically.

Therefore, it would be advisable to evaluate the effect of the BION® 50WG on plant and yeast metabolism, in order to verify the possible onset of aromatic defects that could be derivate from Acibenzolar S-Methyl.

List of publications

1. Pulcini, L.; Bona, E.; Vaudano, E.T.; Tsolakis, C.; Garcia-Moruno, E.; Costantini A. and Gamalero, E. The Impact of a Commercial Biostimulant on the Grape Mycobiota of *Vitis vinifera* cv. Barbera. Microorganisms; 2023; 11:1873. DOI: 10.3390/microorganisms11081873

2. Costantini A.; E. Vaudano; L. Pulcini; L. Boatti; E. Gamalero; Garcia-Moruno, E. Yeast Biodiversity in Vineyard during Grape Ripening: Comparison between Culture Dependent and NGS Analysis. Processes; 2022;10: DOI: 10.3390/pr10050901

3. Pulcini L., Gamalero E., Costantini A., Vaudano E.T., Tsolakis C., Garcia-Moruno E. An overview on *Saccharomyces cerevisiae* indigenous strains selection methods. In *Grapes and Wine*, Editor Prof. Antonio Morata, 1st ed. IntechOpen. 2021 ISBN 978-1-83969-642-8 http://dx.doi.org/10.5772/intechopen.99095

4. Costantini A., Cravero M.C., Panero L., Bonello F. Vaudano E., Pulcini L., Garcia-Moruno E. Wine Fermentation Performance of Indigenous *Saccharomyces cerevisiae* and *Saccharomyces paradoxus* Strains Isolated in a Piedmont Vineyard. Beverages 2021, 7, 30. https://doi.org/10.3390/beverages7020030

Poster and conference proceeding

1. Pulcini L.; Costantini A.; Bona E.; Gamalero E.; Tsolakis C.; Vaudano E. T.; Garcia-Moruno E. (2022) A look at the yeast community on grapes treated with a biostimulant, using Next Generation Sequencing technique; Poster_2022-2674; Section 2.1 Validation of omics methods with reference methods and the collection-management of big data in oenology; 43° World Congress of Vine and Wine, held in Ensenada, Mexico 31 Oct. - 4 Nov. 2022.

2. Cravero M.C.; Costantini A.; Panero L.; Bonello F.; Vaudano E.; Pulcini L.; Garcia Moruno E. (2022) "Indigenous *Saccharomyces cerevisiae* and *Saccharomyces paradoxus* strains isolated in a requalified Piedmont vineyard" 979-12-80673-04-6 Symposium Gastronomy at The Crossroad Of Ecological Transition and Social Justice, held in Turin, Italy, 23-25/09/2022

Acknowledgements

La prima persona che voglio ringraziare è la Prof.ssa Elisa Gamalero, che si è resa disponibile durante questo lungo percorso, e che mi ha dato la possibilità di rendermi più consapevole del mio potenziale, spronandomi a cimentarmi in lavori che mi sembravano irrealizzabili.

Al coordinatore del programma del Dottorato di ricerca, Prof. Gian Cesare Tron, un particolare ringraziamento per avermi concesso la proroga e per la sua squisita comprensione.

La Prof.ssa Elisa Bona è stata fondamentale per l'analisi del mycobiota; quindi, la ringrazio per questo importante insegnamento.

Uno speciale ringraziamento va alla Dott.ssa Antonella Costantini, mia tutor interna al CREA, che ha saputo intervenire nelle criticità tecniche che mi si sono presentate, nonostante i suoi pressanti impegni lavorativi.
Fondamentale è stata la completa disponibilità dei miei colleghi del CREA-VE di Asti, Dott. Christos Tsolakis, Dott. Enrico Vaudano ed Dott.ssa Emilia Garcia Moruno, che pur avendomi avvisata che alla mia età questa strada non sarebbe stato una passeggiata, hanno saputo supportarmi sia nel percorso del dottorato di ricerca che nella vita lavorativa. Grazie a tutti!

Un grazie va anche alla Dott.ssa Antonella Bosso e alla Dott.ssa Loretta Panero che erano coinvolte nel progetto "Elicitori di resistenza a supporto della difesa dalla Flavescenza dorata della vite" coordinato dal CNR-IPSP, che interessava anche il vigneto sperimentale del CREA-VE, e senza il quale il mio lavoro non avrebbe avuto esistenza.

Grazie al Direttore, Dott. Riccardo Velasco, che seppur sorpreso dalla mia iniziativa non mi ha ostacolata.

Infine, devo ringraziare immensamente il mio compagno Graziano, mia madre e mio padre per la infinita pazienza che hanno dovuto impiegare in questi quattro anni. Sono riusciti nell'ardua impresa di sostituirmi in tante funzioni legate alla famiglia, a sopportare i miei umori e a farmi sentire serena nonostante il peso che ho fatto sopportare loro.
Soprattutto ringrazio i miei bambini che mi hanno sopportato, e che inconsapevolmente, mi hanno fatto superare dei momenti di crisi con il loro amore, i loro abbracci e i loro sorrisi.